

DIMENSIONAL CHANGES IN HARDENED GAGE STEELS

By

Benjamin Lewis Averbach

M.Met.Eng., Rensselaer Polytechnic Institute, 1942

Submitted in Partial Fulfillment of the

Requirements for the Degree of

DOCTOR OF SCIENCE

at the

Massachusetts Institute of Technology

1947

Signature of Author  
Department of Metallurgy  
September 5, 1947

Signature of Professor  
in Charge of Research

Signature of Chairman  
Department Committee on  
Graduate Students

TABLE OF CONTENTS

---

	<u>Page</u>
List of Figures	ii
List of Tables	vii
Acknowledgments	
I Introduction	1
II Precision Length Measurements	6
III Quenching Dilatometer Measurements	23
IV The Quantitative Determination of Retained Austenite.	31
A. The Problem	31
B. Quantitative Analysis by X-ray	35
C. Experimental Procedure for Retained Austenite	39
D. Extinction and Absorption Effects	51
E. Results of Austenite Determinations	59
F. Effect of Tempering on Austenite Determinations	66
V The Decomposition of Martensite	70
VI The Isothermal Decomposition of Retained Austenite	92
VII Conclusions	106
VIII References	109
Abstract	viii
IX Biographical Note	x

LIST OF FIGURES

---

	<u>Page</u>
Figure 1. Method of aligning rod specimen in comparator for precision length measurement, showing gage block arrangement for adjusting total length to 4.120 inches.	7
Figure 2. Relative changes in length on aging of a ball-bearing steel austenitized at 1550° F (845° C) for 30 minutes and quenched into oil at 68° F (20° C).	9
Figure 3. Relative changes in length on aging of a ball-bearing steel austenitized at 1550° F (845° C) for 30 minutes, quenched into oil at 68° F, and refrigerated immediately in liquid nitrogen at -321° F (-195° C) for one hour.	12
Figure 4. Relative changes in length on aging of a ball-bearing steel austenitized at 1550° F (845° C) for 30 minutes, quenched into oil at 125° F (50° C), and air-cooled to room temperature.	14
Figure 5. Relative changes in length on aging of a ball-bearing steel austenitized at 1550° F (845° C) for 30 minutes, quenched into oil at 250° F (120° C), and air-cooled to room temperature.	15

	<u>Page</u>
Figure 6. Relative changes in length on aging of a ball-bearing steel austenitized at 1550° F (845° C) for 30 minutes, quenched into molten salt at 450° F (230° C), and air-cooled to room temperature.	16
Figure 7. Relative changes in length on aging of a plain carbon tool steel austenitized at 1450° F (790° C) for 30 minutes and quenched into water at 68° F (20° C).	17
Figure 8. Relative changes in length on aging of a plain carbon tool steel austenitized at 1450° F (790° C) for 30 minutes, quenched into water at 68° F (20° C), and refrigerated immediately in liquid nitrogen at -321° F (-195° C) for one hour.	19
Figure 9. Relative changes in length on aging of a plain carbon tool steel austenitized at 1450° F (790° C) for 30 minutes, quenched into water at 125° F (50° C), and air-cooled to room temperature.	20
Figure 10. Relative changes in length on aging a plain carbon steel austenitized at 1450° F (790° C) for 30 minutes and quenched into iced brine at 23° F (-5° C).	21

	<u>Page</u>
Figure 11. Quenching dilatometer apparatus showing arrangement of the equipment and a close-up of the specimen. The dial gage and timer are turned 90° from their normal position	24
Figure 12. Quenching dilatometer record showing relative change in length and temperature as functions of time for a ball-bearing steel, austenitized at 1550° F (845° C) and quenched into oil at 68° F (20° C).	28
Figure 13. Quenching dilatometer record showing relative change in length and temperature as functions of time for a plain carbon steel, austenitized at 1450° F (790° C) and quenched into water at 68° F (20° C).	29
Figure 14. Variation of absorption correction with diffraction angle for a flat sample.	38
Figure 15. Arrangement of diffraction camera to obtain monochromatic radiation on a flat sample.	41
Figure 16. X-ray diffraction patterns obtained with CoK <sub>α</sub> monochromatic radiation showing austenite and martensite lines.	43
Figure 17. Microphotometer traces of diffraction patterns shown in Figure 16.	44

	<u>Page</u>
Figure 18.	49
The variation of $V \cdot A(\theta)$ with diffraction angle obtained for K steel (1.07 carbon) austenitized at $1450^{\circ}$ F ( $790^{\circ}$ C) and quenched into water. The lower points are calculated from the austenite lines and the constant ratio needed to bring the lower points on to the upper curve gives the volume ratio of martensite to austenite.	
Figure 19.	54
Diffraction of x-rays by a given grain in a mass of crystallites. (After Brindley <sup>(19)</sup> ).	
Figure 20.	73
Relative changes in length on aging 100 percent martensite of a ball-bearing steel austenitized for 30 minutes at $1550^{\circ}$ F ( $845^{\circ}$ C) and quenched into oil.	
Figure 21.	74
Relative changes in length on aging 100 percent martensite of a plain carbon tool steel austenitized for 30 minutes at $1450^{\circ}$ F ( $790^{\circ}$ C) and quenched into water.	
Figure 22.	88
Rate equation for martensite decomposition in a plain carbon tool steel at temperatures from $32$ to $300^{\circ}$ F ( $0$ to $150^{\circ}$ C).	
Figure 23.	89
Activation equations for rate constants of martensite decomposition in a plain carbon tool steel.	

	<u>Page</u>
Figure 24. Isothermal decomposition of austenite at 68° F (20° C) for a ball-bearing steel.	96
Figure 25. Isothermal decomposition of austenite at 68° F (20° C) for a plain carbon tool steel.	97
Figure 26. Effect of aging on the decomposition of austenite for the ball-bearing steel. The initial reaction at 68° F (20° C) is the decomposition of austenite into martensite, and the later reaction, which occurs after prolonged times at 250 and 300° F (120 and 150° C), is the decomposition of austenite into bainite.	103
Figure 27. Effect of aging on the decomposition of austenite for the plain carbon steel. The initial reaction at 68° F (20° C) is the decomposition of austenite into martensite and the later reaction, which occurs after prolonged times at 250 and 300° F (120 and 150° C), is the decomposition of austenite into bainite.	104

LIST OF TABLES

---

	<u>Page</u>
I. Analyses of Steels	3
II. X-ray Constants for Austenite and Martensite Lines	46
III. Integrated Intensities for Austenite Determination	48
IV. Effect of Room Temperature Aging on Retained Austenite Contents	52
V. The Microabsorption Effect	56
VI. Retained Austenite Contents (K steel)	60
VII. Retained Austenite Contents (T steel)	61
VIII. Comparison of X-ray Determination vs. Lineal analysis	63
IX. Effect of Quenching Conditions on Retained Austenite Content	64
X. Effect of Tempering on Austenite Determinations	68
XI. Effect of Tempering on Hardness (T steel)	77
XII. Effect of Tempering on Hardness (K steel)	78
XIII. Constants of Rate Equation for Martensite Decomposition	86
XIV. Isothermal Decomposition of Austenite at 68° F	95
XV. Decomposition of Austenite on Tempering (T steel)	99
XVI. Decomposition of Austenite on Tempering (K steel)	100
XVII. Relative Change in Length Caused by Decomposition of 1 percent of Austenite at Various Temperatures.	102



ABSTRACT

---

The reaction rate of martensite decomposition and the mechanism by which retained austenite transforms isothermally have been studied by means of precision length measurements, quenching dilatometer observations and quantitative x-ray analyses developed specifically to measure small amounts of retained austenite in quenched steels. These studies have shown that it is practically impossible to eliminate all of the retained austenite by a continuation of the quench even to liquid nitrogen temperatures, and that retarding the rate of cooling through the martensite region increases the quantity of retained austenite.

The solubility of carbon in martensite at the end of the first stage of isothermal tempering increases slightly as the tempering temperature increases up to 300° F (150° C), and the end of the first stage is marked by retardation in the rate of carbon rejection from the martensite lattice. Martensite decomposition, which occurs by means of a process of nucleation and growth of a transition precipitate, is believed to be accelerated by the stresses present in the martensite lattice and may be represented by the rate equation:

$$-\frac{dc}{dt} = K(T) \cdot \frac{c}{tS(T)}$$

where  $c$  = concentration of carbon remaining in solution at time,  $t$ .

$K(T)$  and  $S(T)$  = constants depending only on temperature.

The heat of activation of the rate coefficient  $K(T)$  has been determined as approximately 8300 cal/mol. This may be regarded as a measure of the activation energy of carbon diffusion in martensite, and is about one-half of the value calculated by Polder for carbon diffusion in ferrite. This reduction in potential barrier is probably caused by the high stress level in martensite.

The austenite-martensite reaction does not stop completely when the cooling stops, but 3 or 4 percent more of austenite may transform isothermally into martensite at room temperature. This isothermal transformation proceeds rather rapidly during the first 1.5 hours after the quench, but it continues at a diminishing rate for several months. As retained austenite is tempered at higher temperatures, the decomposition of austenite into bainite becomes evident after prolonged aging times at 250 and 300° F (120 and 150° C), but this bainite decomposition (i.e. the second stage of tempering) is quite distinguishable from the earlier isothermal decomposition into martensite.

## ACKNOWLEDGMENT

The author would like to express his appreciation to Professor Morris Cohen, who gave generously of his time to help solve the experimental and theoretical problems which arose in the course of the investigation, and to Professor B. E. Warren of the Physics Department for his valuable aid in the development of the x-ray method used in this study.

A fellowship grant from the Sheffield Foundation made this work possible and is also gratefully acknowledged.

## I. INTRODUCTION

---

Many observations have been made on the dimensional instability of hardened steels. This instability is particularly troublesome in master gage blocks which are normally required with a calibration to the nearest millionth of an inch, and as a result, many authors<sup>(1-6)</sup> have investigated these irreversible changes in length which occur on room temperature aging. Although most of these studies have been qualitative in that they evaluated a specific heat treatment used in the manufacture of commercial gage blocks, Scott<sup>(7)</sup> seems to have been among the first to recognize the correlation between dimensional instability and the structural changes which take place on tempering. He correctly deduced that expansions on aging were caused by the decomposition of retained austenite and that contractions were caused by the tempering of martensite at room temperature. To manufacture a stable gage block of hardened steel, it has been necessary, intentionally or otherwise, to either balance these opposing reactions or to minimize them with a rather involved series of proprietary tempering and "seasoning" treatments.

Since Scott's investigation, considerable progress has been made in the understanding of the austenite-martensite reaction, and these concepts have been reviewed and summarized recently<sup>(8),(9)</sup>. Rather extensive information has also been obtained on the tempering

---

(1) Numbers refer to references at the end of the paper.

process (10), (11), (12), (13), (14), (15), and with the more precise methods of measurement now available it seemed fruitful to reconsider the dimensional changes in hardened steels by studying the early stages of tempering on the basis of phase reactions occurring in metastable structures. It also seemed desirable to reconsider the austenite-martensite reaction to determine if this reaction ceases completely as cooling is stopped, or if the decomposition of austenite observed at room temperature is not, in effect merely a continuous trailing-off of the main austenite-martensite reaction. From an investigation of the kinetics of these isothermal decompositions it might, in addition, be possible to gain some approach to the mechanics of these reactions.

In the discussion which follows, dimensional behavior is considered only with reference to the changes which occur as a result of phase transformations, and it does not include the "movement" which takes place during heat treatment or the distortion which may result from stress relief. In practice, satisfactory gages must not only be dimensionally stable but must also have high hardness and good wear resistance. For this reason, combinations of steels and heat treatments were chosen to give fully hard martensitic structures with an excess of carbides. This corresponds to the normal commercial practice, and measurements were made on specimens large enough to compare directly with commonly used gages. Two representative steels, a plain carbon tool steel (K steel) and a chromium ball-bearing steel (T steel) were investigated and their compositions are listed in Table I.

TABLE I

Analyses of Steels

---

	Weight Percent						
<u>Steel</u>	<u>C</u>	<u>Si</u>	<u>Mn</u>	<u>S</u>	<u>P</u>	<u>Cr</u>	<u>V</u>
K	1.07	0.23	0.25	0.014	0.011	-	-
T	1.00	0.35	0.37	-	-	1.56	0.21

Early in the investigation it was shown that steels in the annealed and spheroidized condition were stable, and no changes in length greater than one part in a million were observed on aging at room temperature. Such steels are, however, too soft to be used as gages. Hardened steels, on the other hand, are far from stable. They contain internal stresses as well as a large percentage of martensite which is unstable and shows a marked tendency to decompose even at room temperature. In addition, hardened steels may contain up to 30 percent of retained austenite which is also far from equilibrium and which might, therefore, be expected to break down easily on aging. Undissolved carbides seem to play no direct part in dimensional stability, although they are valuable in imparting wear resistance.

If the dimensional changes resulting from the transformation of the unstable phases in the direction of their equilibrium structures are considered, it is evident that two large opposing reactions can occur. For example, in the plain carbon steel after a water quench from 1450° F (790° C) it will be shown later that there is present about 9 percent retained austenite, 2.6 percent undissolved carbides, and 88.4 percent martensite. From lattice parameter and specific volume measurements<sup>(10)</sup> it can be shown that if freshly formed martensite were to decompose into ferrite and cementite, a linear contraction of

$5300 \times 10^{-6}$  in/in\* would occur. Gages made from this steel are seldom tempered above  $300^{\circ}$  F ( $150^{\circ}$  C), and about 30 percent of this total contraction could take place during such tempering. This corresponds to almost the completion of the first stage of tempering, but there is still a large potential contraction available to cause dimensional instability. At the same time, if we assume that the 9 percent of retained austenite can transform into martensite, a linear expansion of  $1260 \times 10^{-6}$  in/in would occur\*\*. Since little of this austenite is removed by tempering up to  $300^{\circ}$  F ( $150^{\circ}$  C) for short times, considerable potential growth could be caused by the decomposition of this retained austenite, and the net effect could be either a contraction or an expansion depending on the relative magnitudes and rates of the opposing transformations. By studying these net changes in dimension, this investigation attempted to separate the martensite decomposition from the austenite transformation and to observe the kinetics of each process by itself.

---

\*This figure is  $6000 \times 10^{-6}$  in/in for 100 percent martensite containing 1 percent carbon and it also assumes that the following relationship is valid:

$$3\frac{\Delta L}{L} = \frac{\Delta V}{V}$$

\*\*This corresponds to  $140 \times 10^{-6}$  in/in for one percent of austenite transformation into martensite at room temperature.



## II. PRECISION LENGTH MEASUREMENTS

---

To investigate minute changes in length, specimens  $3/8$  inch in diameter by  $4.000 \pm 0.001$  inch long with the ends accurately ground to the contour of a 4 inch diameter sphere were used. Length determinations were made by fastening these specimens to a jig to keep them vertical, as shown in Figure 1, and then measuring them in a Sheffield Visual Gage Comparator with a magnification of 5000X. This gage compares the length of the sample with a standard gage block independently calibrated to the nearest millionth of an inch, and is able to determine deviations from this standard with an accuracy of 5 microinches. For a 4 inch sample, this corresponds to a relative accuracy of about 1.5 microinches per inch. The standard gage blocks are nominally 4.120 inches long, and the difference in length between the sample and standard was made up by inserting small gage blocks as depicted in Figure 1. This arrangement permits measurements to be made on a wide variation of sample lengths with the same standard, despite the limited range of the instrument, and contributes greatly to the ease of measurement and to the internal consistency of the data. The spherical ends prevent errors that might result from slight tilting of the specimen from vertical.

The machined and ground rod specimens were first austenitized for 30 minutes in a lead pot controlled to  $+5^{\circ}$  F ( $+3^{\circ}$  C) and quenched. Some of these specimens were subcooled immediately after the

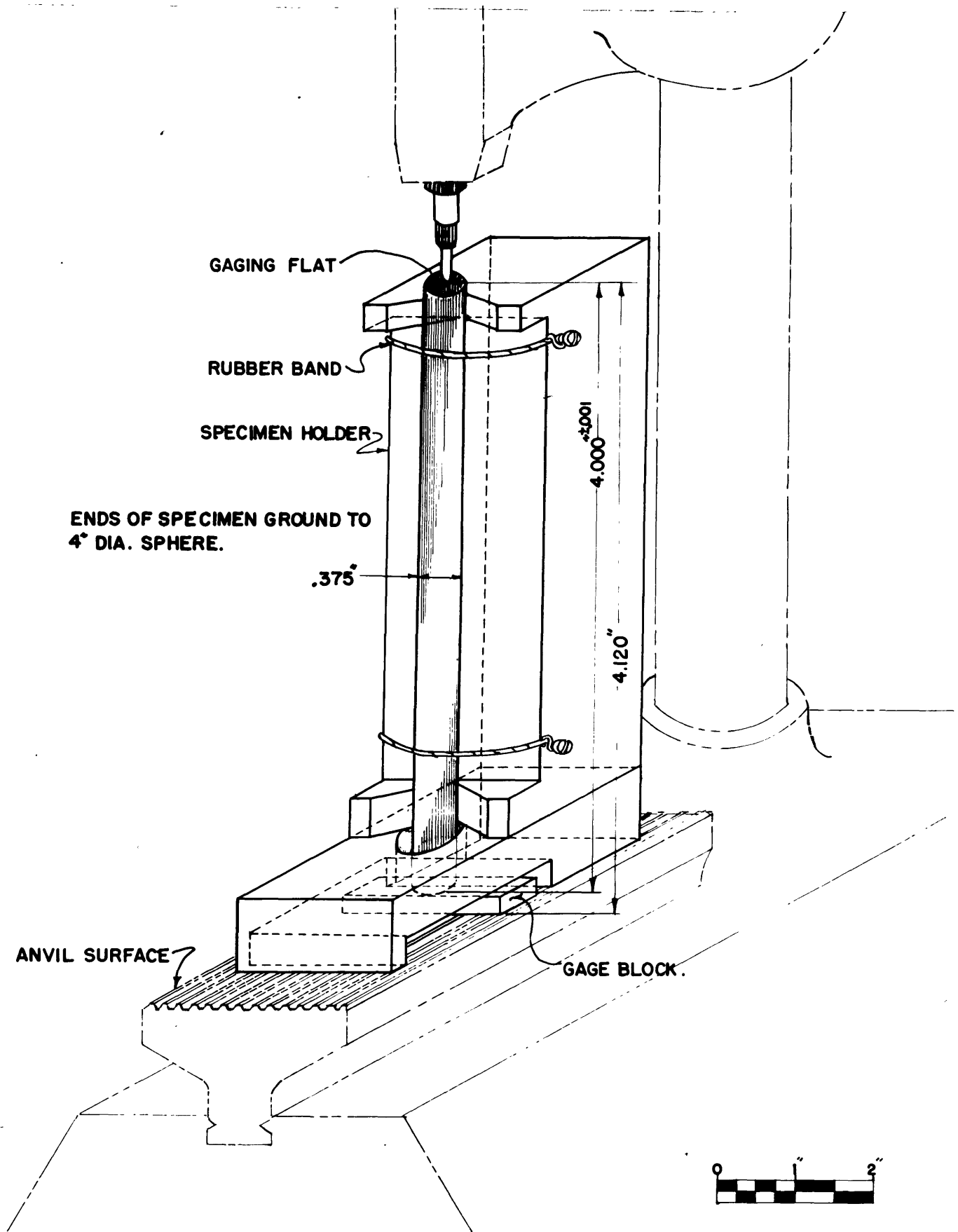


Figure 1. Method of aligning rod specimen in comparator for precision length measurement, showing gage block arrangement for adjusting total length to 4.120 inches.

quench in a closed brass tube surrounded by liquid nitrogen ( $-321^{\circ}$  F,  $-195^{\circ}$  C). Any scale accumulation was removed with emery paper in a lathe running at slow speed, and the specimens were degreased and allowed to remain for an hour on a large surface plate in the measuring room which was maintained at  $68 \pm 1^{\circ}$  F ( $20 \pm 0.5^{\circ}$  C). A length measurement was then made. Following this, the specimens were aged in oil baths maintained at 100, 150, 200, 250 and  $300^{\circ}$  F  $\pm 2^{\circ}$  F (40, 65, 95, 120 and  $150 \pm 1^{\circ}$  C), in air at  $68^{\circ}$  F ( $20^{\circ}$  C) and in an ice bath at  $32^{\circ}$  F ( $0^{\circ}$  C). Length determinations were repeated at suitable intervals for periods exceeding 200 days.

The type of data obtained from such a determination is shown in Figure 2. A series of specimens of the ball-bearing steel (T steel) was austenitized at  $1550^{\circ}$  F ( $845^{\circ}$  C) quenched into oil at room temperature and aged at the temperatures mentioned previously. Their changes in length were recorded as they aged, but for each determination it was necessary to bring the specimens to room temperature, allow them to come to thermal equilibrium for one hour, and to then make the length measurement at  $68^{\circ}$  F ( $20^{\circ}$  C). The changes caused by the time at room temperature and by the cooling to or from the measuring temperature were assumed to be negligible. Figure 2 shows the relative changes of length as a function of time at aging temperature and it should be noted that the elapsed time is plotted in hours on a logarithmic scale. Time is taken as beginning at 90 minutes after the completion of the last heat treating operation, since 90 minutes were required to clean the specimens and bring them to

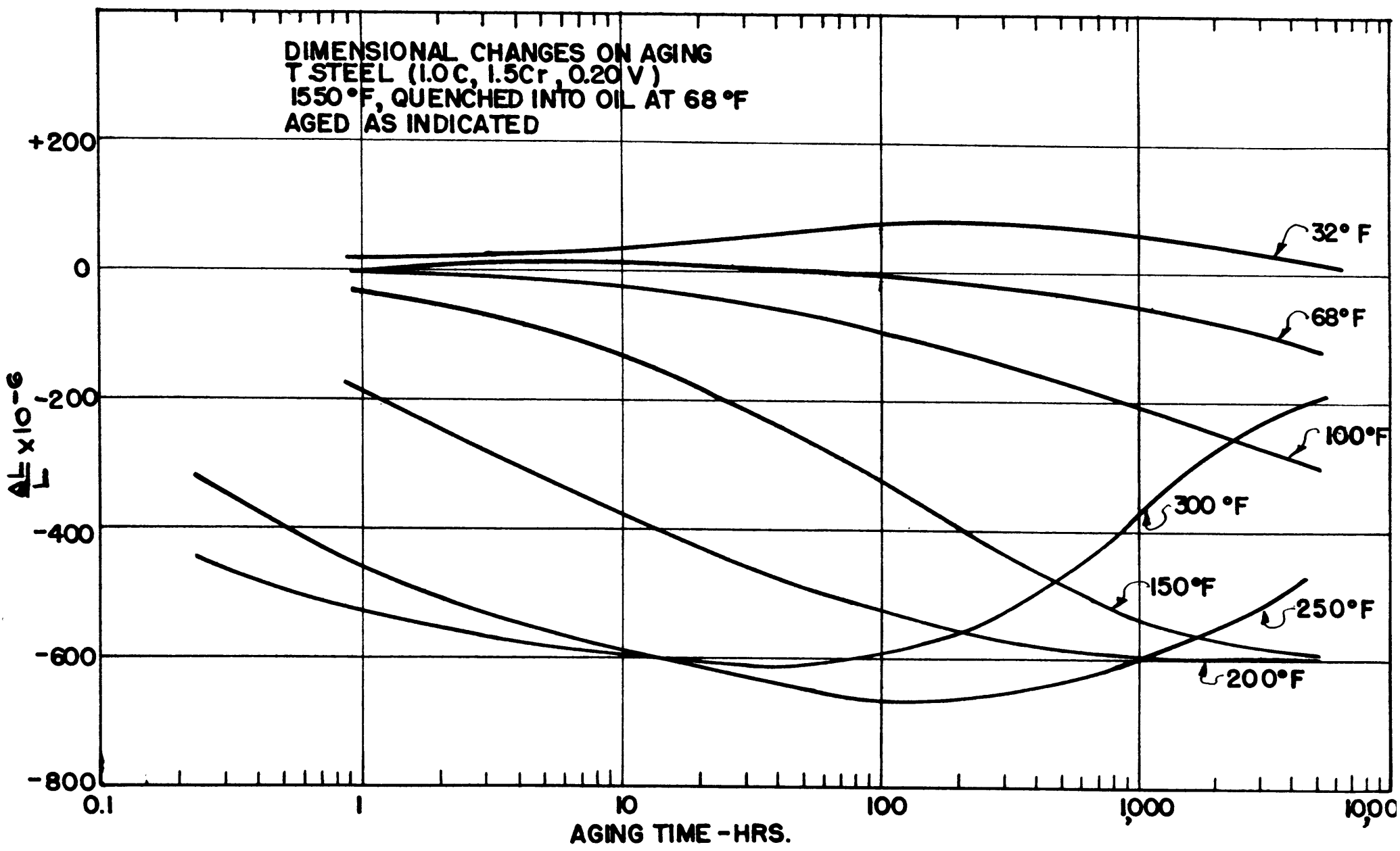


Figure 2. Relative changes in length on aging of a ball-bearing steel austenitized at 1550° F (845° C) for 30 minutes and quenched into oil at 68° F (20° C).

thermal equilibrium after heat treatment before any length measurements could be made. Accordingly, the relative changes in length are all calculated from this point. The first reading as plotted is elapsed time after this reference point, and any changes during the first 90 minutes after the quench apply as a constant correction to all of these determinations.

The relative changes in length, plotted as  $\frac{\Delta L}{L} \times 10^{-6}$  in/in are the averages of at least two specimens treated simultaneously. As aging proceeded, at least 20 length measurements were made on each specimen within the first thousand hours, but the individual points are not plotted, to avoid confusion. The readings were reproducible with an accuracy of  $\pm 2 \times 10^{-6}$  or 10 percent whichever is the greater. This error did not usually arise from the measurement itself, but from the inherent difficulties in reproducing quenching conditions precisely for each set of specimens. The structural reactions under investigation however, caused length changes which were large compared to this error. No corrections were made for the temperature coefficient of expansion since both the specimens and the standards had approximately the same coefficient, and the specimens were left on the plate long enough to come to the same temperature as the standard.

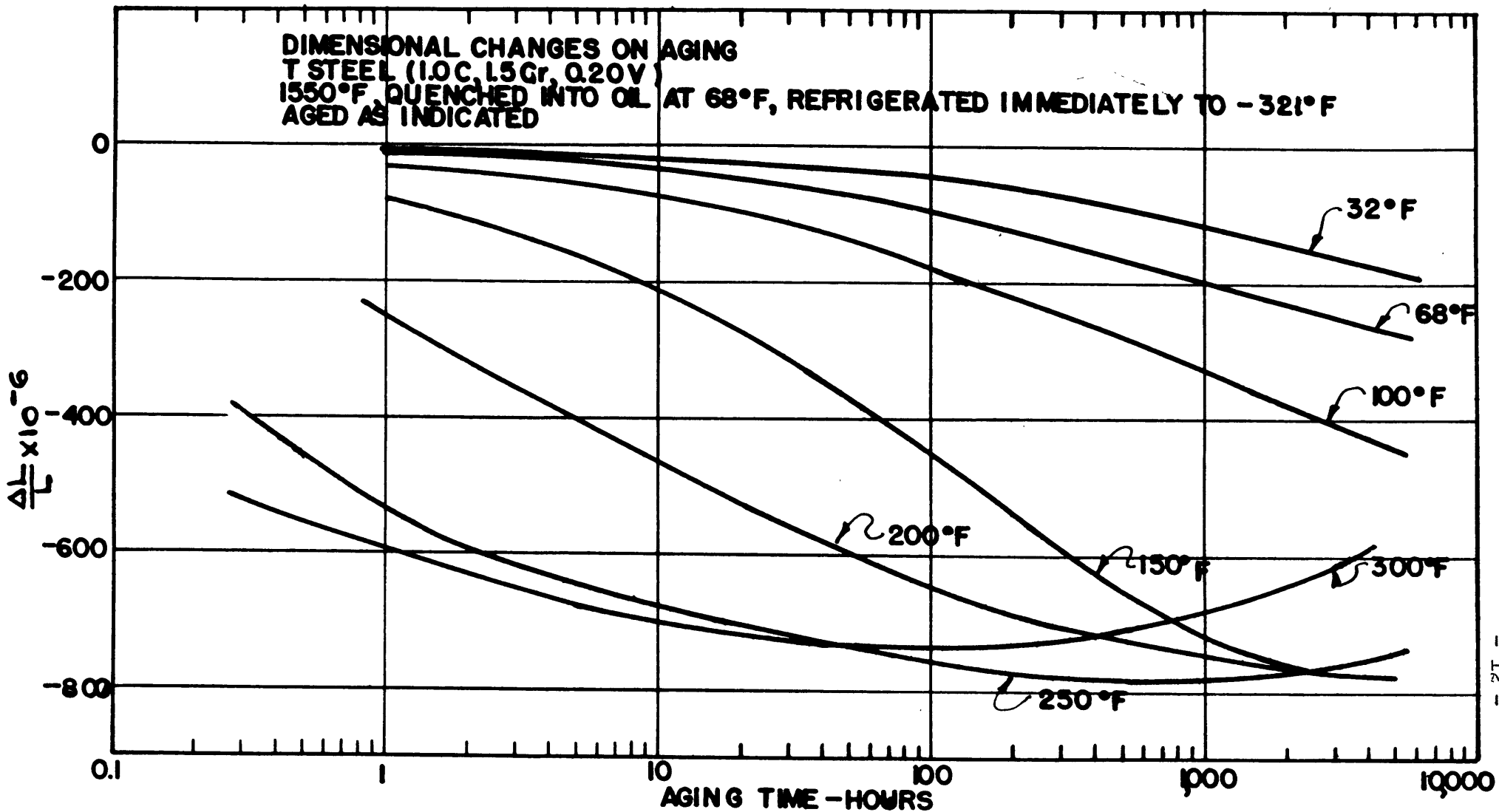
The data in Figure 2 show a maximum growth at 32° F (0° C) which disappears as the aging temperature increases, and at 250 and 300° F (120 and 150° C) a relatively large expansion at prolonged aging times is apparent as the retained austenite decomposes into bainite

during the second stage of tempering<sup>(11)</sup>. It is difficult to explain the earlier maxima at 32 and 68° F (0 and 20° C) on this basis, and qualitatively it is apparent that an isothermal decomposition of austenite must precede the bainite formation.

Figure 3 shows the dimensional behavior on aging of a similar set of specimens which had been refrigerated immediately after the quench to -321° F with liquid nitrogen. Earlier investigators<sup>(16)</sup>,<sup>(17)</sup>,<sup>(18)</sup> believed that this subcooling treatment would transform all of the retained austenite into martensite, and, indeed, the early maxima of Figure 2 did disappear for the subcooled specimens. On aging at 250 and 350° F (120 and 150° C), however, decomposition of retained austenite into bainite was still observed, but on a reduced scale. Apparently the refrigerated specimens contained significant quantities of retained austenite although in smaller amounts than the non-refrigerated specimens. The presence of austenite in these subcooled specimens was later verified and measured by an independent method. The data in Figures 2 and 3 may be considered, therefore, as being derived from two mixtures of austenite and martensite of the same chemical composition, but with different quantities of each constituent.

In commercial heat treating practice it is not uncommon to interrupt the quench at temperatures above room temperature and to then allow the work to air cool through the remainder of the martensite range. The interrupting temperature may be even above the

Figure 3. Relative changes in length on aging of a ball-bearing steel austenitized at 1550° F (845° C) for 30 minutes, quenched into oil at 68° F, and refrigerated immediately in liquid nitrogen at -321° F (-195° C) for one hour.



$M_s^*$  point, as in martempering, but the effects of such treatments on the retained austenite content and on the stability of the austenite have not previously been investigated. Figure 4 shows the dimensional behavior of the ball-bearing steel specimens quenched into oil at 125° F (50° C), held for five minutes in the quenching bath to allow it to come to thermal equilibrium, and then cooled in air to room temperature. Similarly, specimens were quenched into oil at 250° F (120° C) and molten salt at 450° F (230° C), held in the hot quenching bath for five minutes, and allowed to air-cool to room temperature. The dimensional changes on aging for these cases are shown in Figures 5 and 6. From hardness values it was evident that little or no pearlite had formed during the quench so that the dimensional behavior in Figures 4, 5 and 6 can also be taken as due to various mixtures of martensite and retained austenite. The  $M_s$  point for this steel was measured on very small specimens (1/16 inch thick x 1/4 inch diameter) by the hot-quenching method of Greninger and Troiano<sup>(19)</sup> and found to be 415° F (215° C) so that the data of Figure 6 represent the behavior of martempered specimens.

An analogous series of treatments were performed on the plain carbon steel (K steel). Figure 7 shows the dimensional behavior of this steel after quenching into water from 1450° F (790° C), and here it is also evident that considerable quantities of retained austenite decomposed into bainite at the higher aging

---

\* $M_s$  is the temperature at which martensite formation begins.



Figure 4. Relative changes in length on aging of a ball-bearing steel austenitized at 1550° F (845° C) for 30 minutes, quenched into oil at 125° F (50° C), and air-cooled to room temperature.

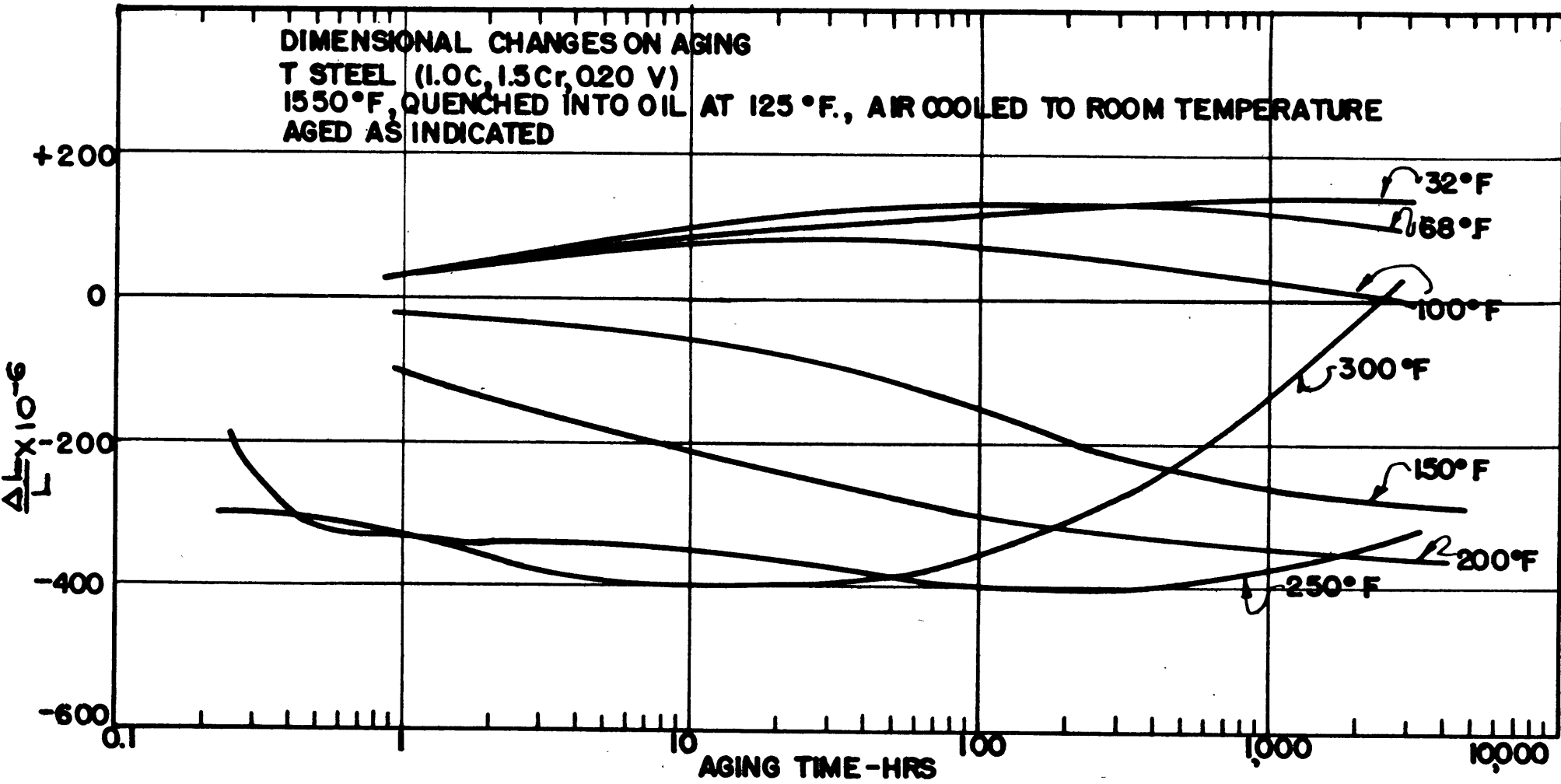


Figure 5. Relative changes in length on aging of a ball-bearing steel austenitized at 1550° F (845° C) for 30 minutes, quenched into oil at 250° F (120° C), and air-cooled to room temperature.

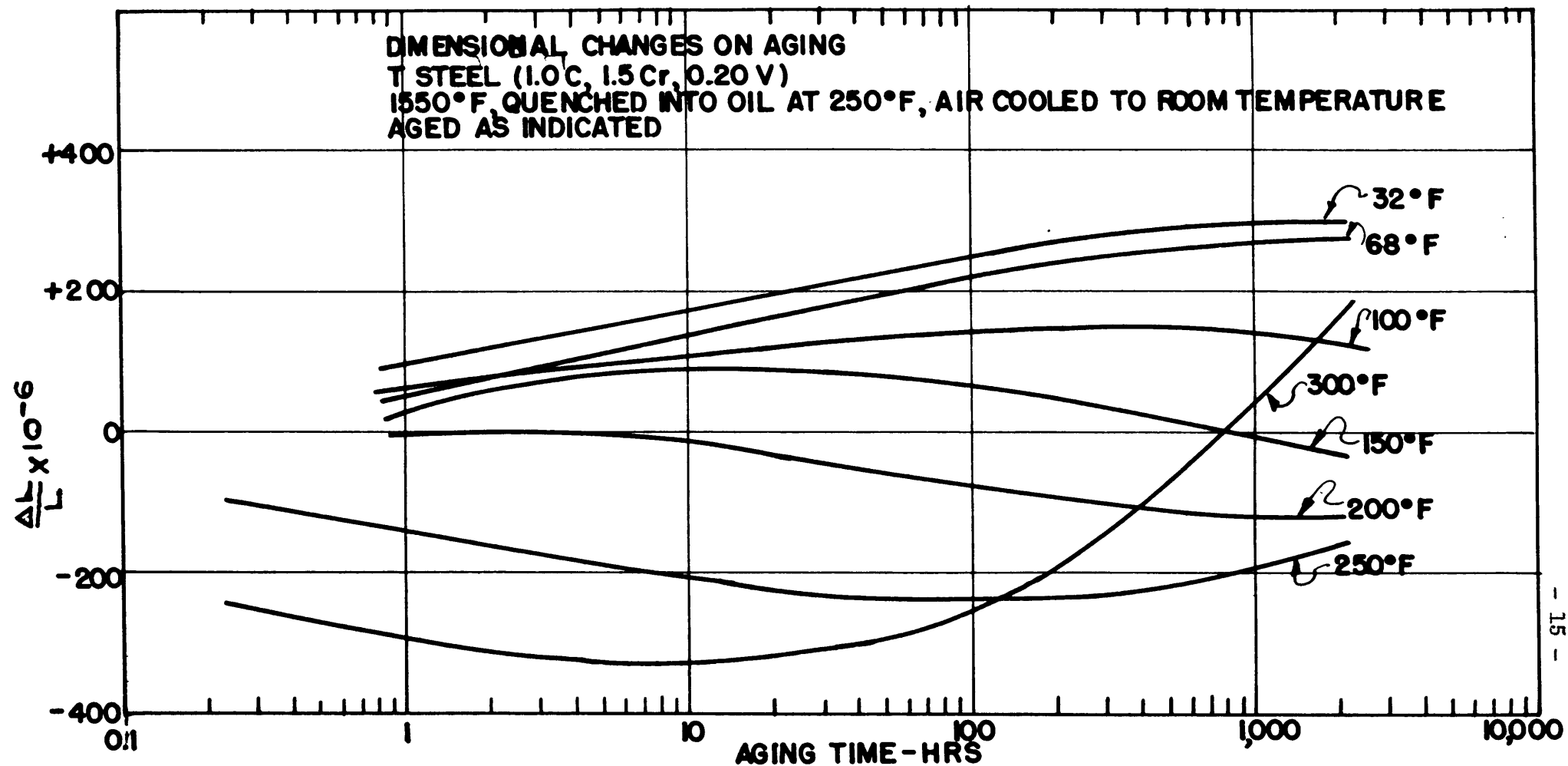


Figure 6. Relative changes in length on aging of a ball-bearing steel austenitized at 1550° F (845° C) for 30 minutes, quenched into molten salt at 450° F (230° C), and air-cooled to room temperature.

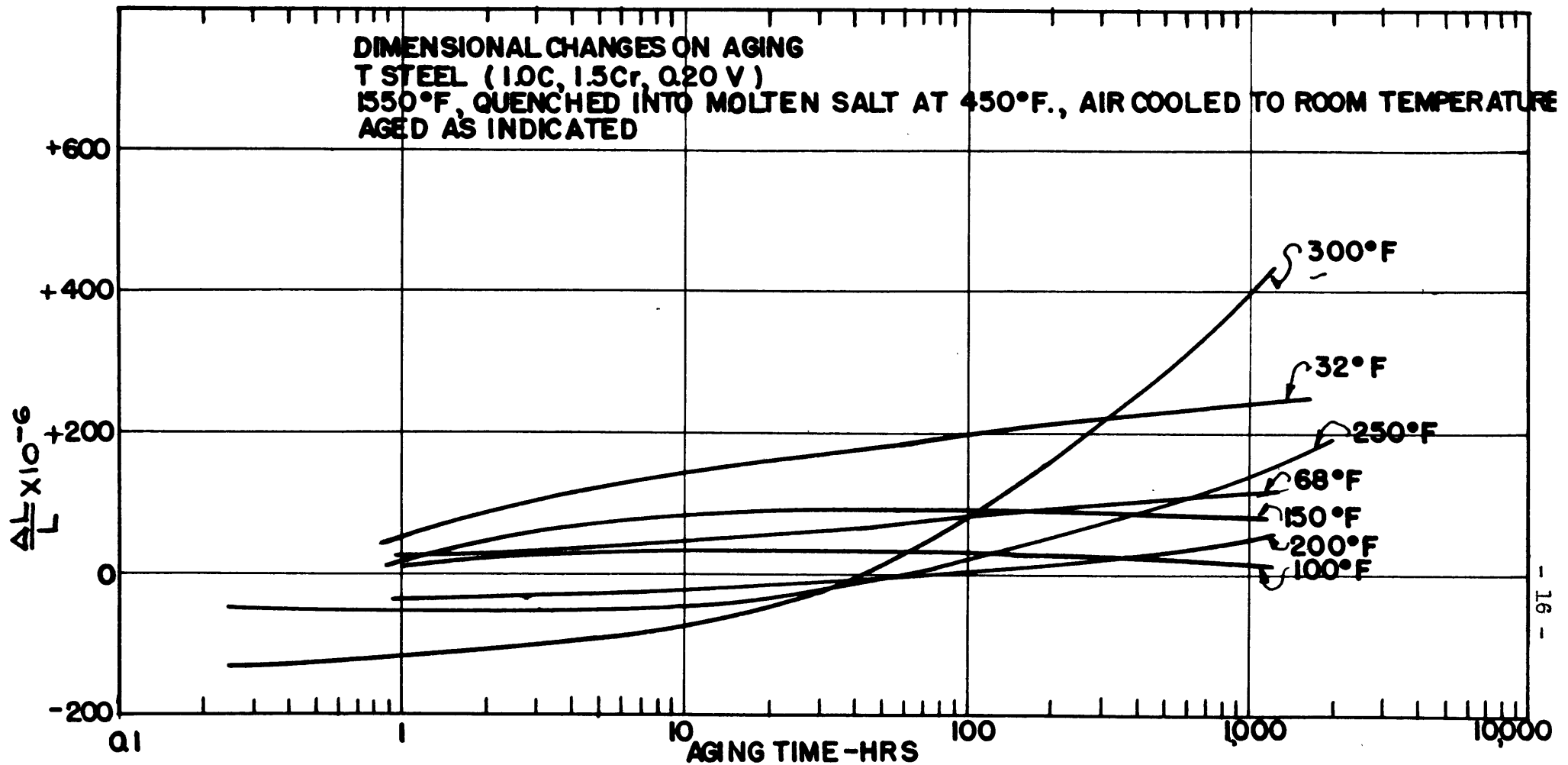
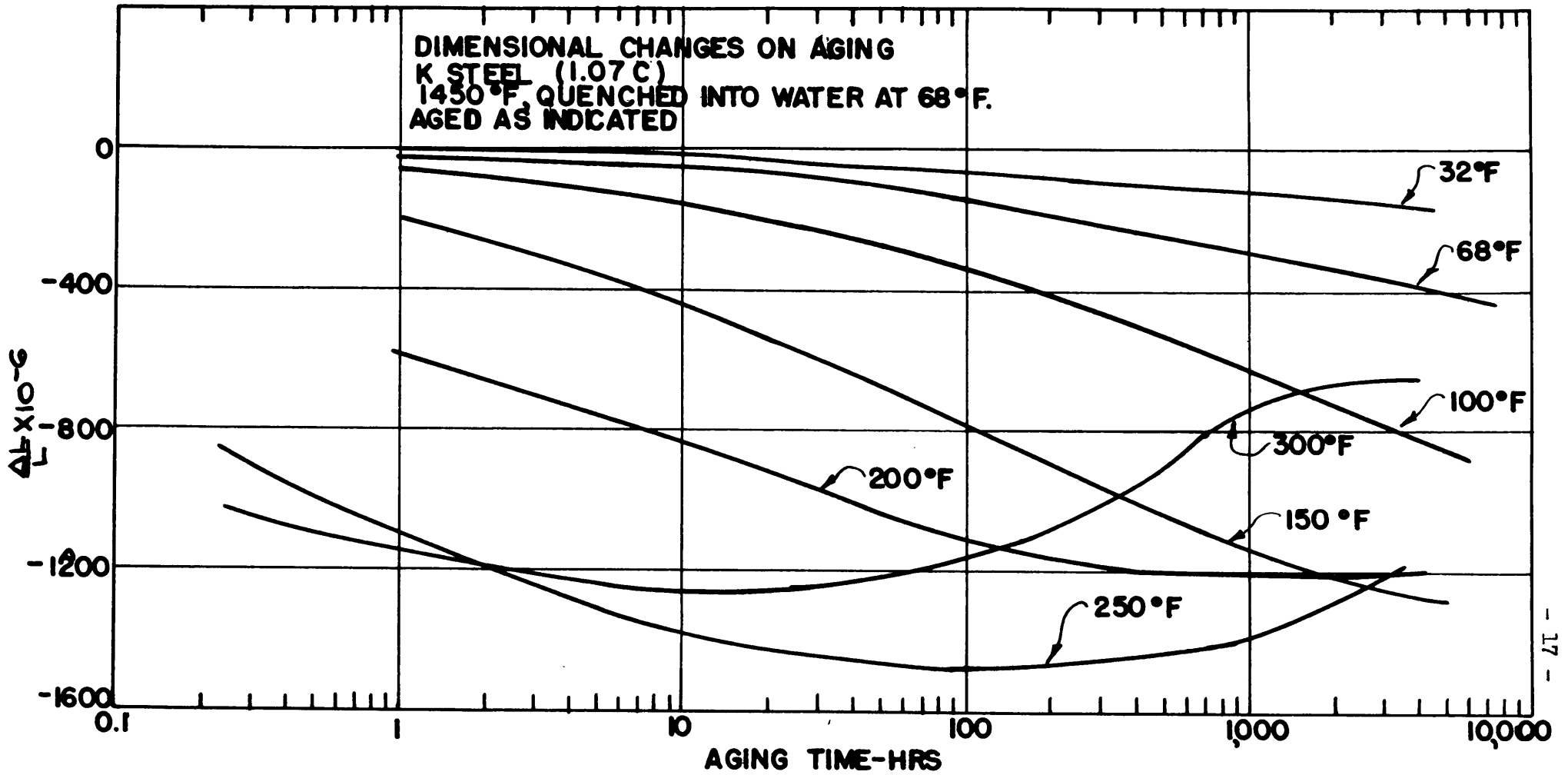


Figure 7. Relative changes in length on aging of a plain carbon tool steel austenitized at 1450° F (790° C) for 30 minutes and quenched into water at 68° F (20° C).



temperatures. The slight early maxima which were present in the low alloy steel are not apparent here. However, specimens which were quenched and immediately refrigerated to  $-321^{\circ}$  F ( $-195^{\circ}$  C) and then aged, Figure 8, shrank correspondingly faster so that there must have been some obscured expansion due to the early decomposition of the retained austenite.

Because of its relatively lower hardenability, the plain carbon steel could not be quenched into very warm baths and still remain fully martensitic for the specimen sizes used here. It was possible, however, to obtain fully hard samples on quenching into water at  $125^{\circ}$  F ( $50^{\circ}$  C), and Figure 9 shows that even this slight increase in interrupting temperature produced a marked change in dimensional behavior. Pronounced early maxima were present and it is apparent that this steel is very sensitive to quenching conditions. An iced brine quench at  $23^{\circ}$  F ( $-5^{\circ}$  C) was also used for this steel since this quench is considerably more drastic than the water quench, and these results are plotted in Figure 10. The  $M_s$  point for this steel was determined by the Greninger and Troiano technique and found to be  $400^{\circ}$  F ( $205^{\circ}$  C).

All of the specimens used in this investigation were obtained from rod stock in the spheroidized-annealed condition. The effect of fibre direction had been investigated previously<sup>(18)</sup> by cutting specimens from a plate of ball-bearing steel parallel and transverse to the rolling direction and subjecting them to various duplicate heat treatments. No significant differences

Figure 8. Relative changes in length on aging of a plain carbon tool steel austenitized at 1450° F (790° C) for 30 minutes, quenched into water at 68° F (20° C), and refrigerated immediately in liquid nitrogen at -321° F (-195° C) for one hour.

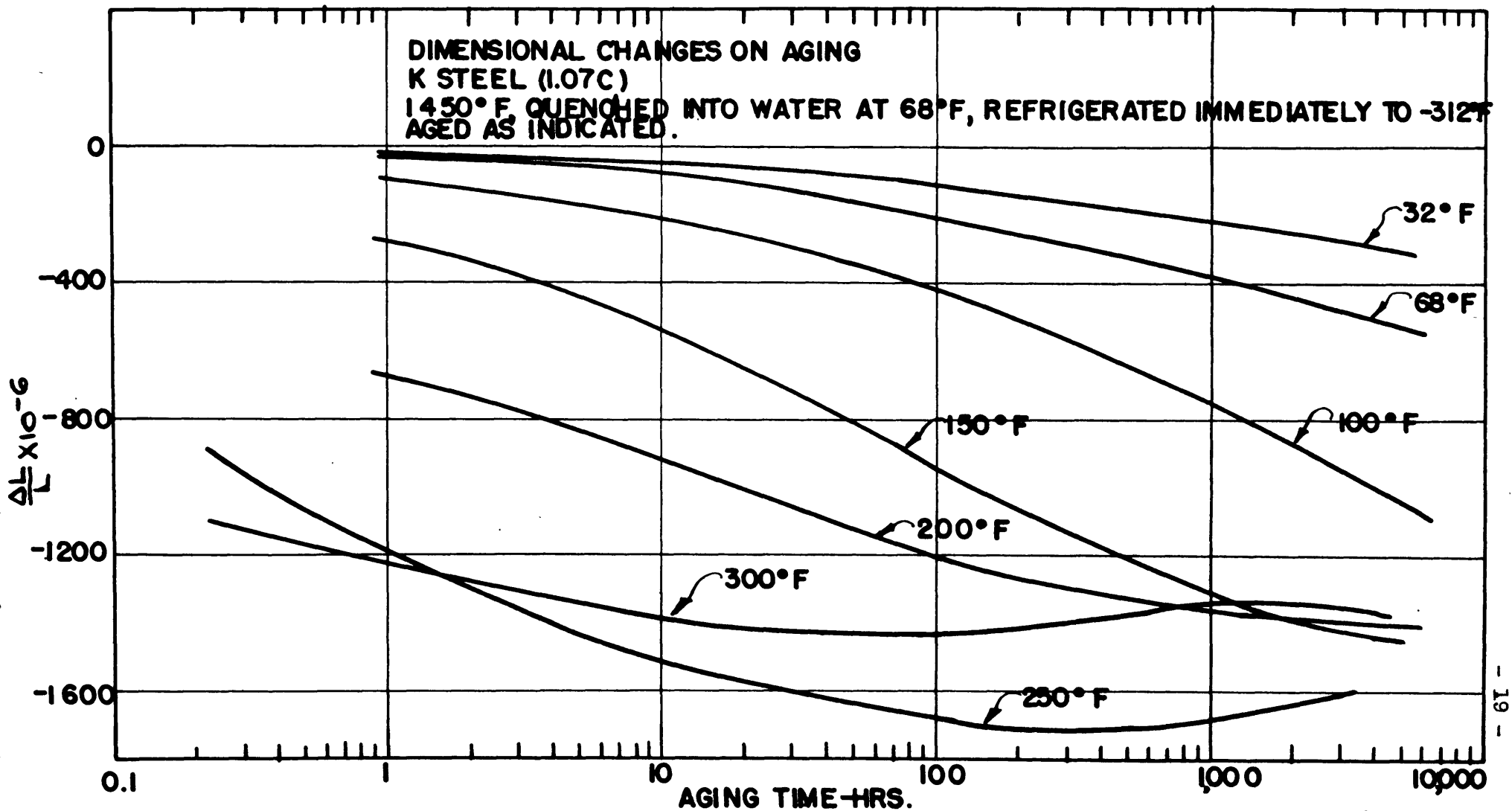


Figure 9. Relative changes in length on aging of a plain carbon tool steel austenitized at 1450° F (790° C) for 30 minutes, quenched into water at 125° F (50° C), and air-cooled to room temperature.

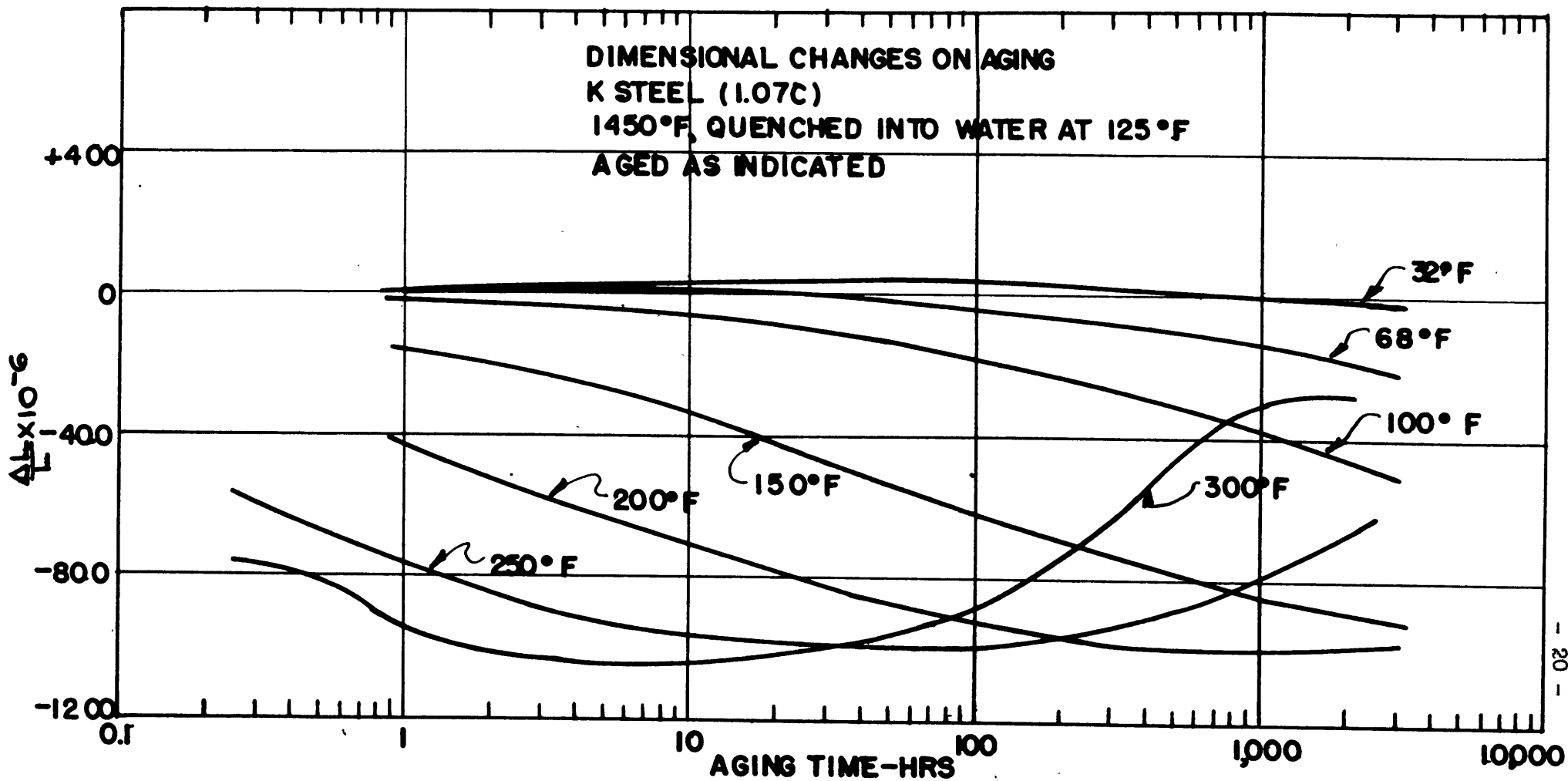
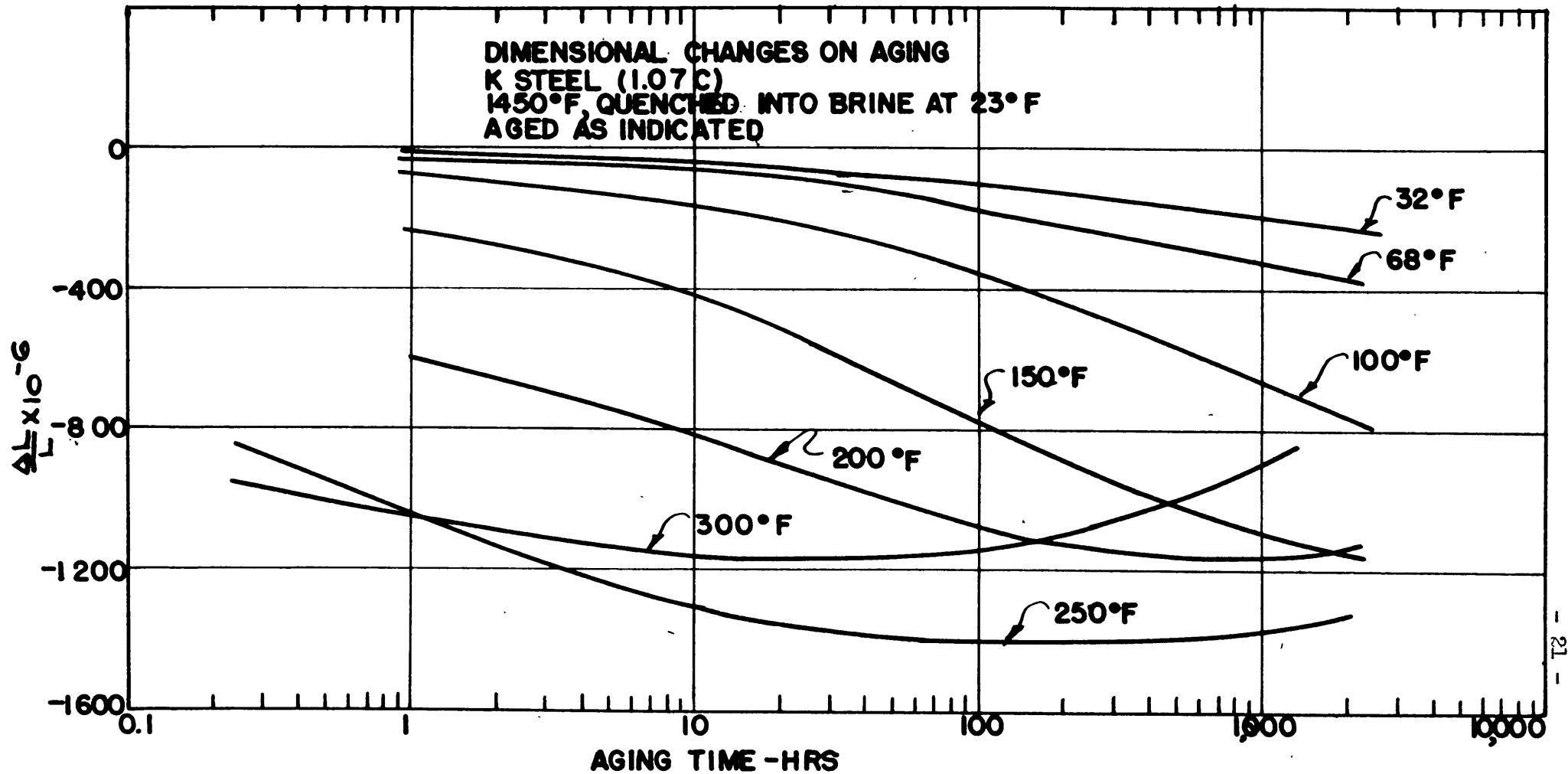


Figure 10. Relative changes in length on aging a plain carbon steel austenitized at 1450° F (790° C) for 30 minutes and quenched into iced brine at 23° F (-5° C).





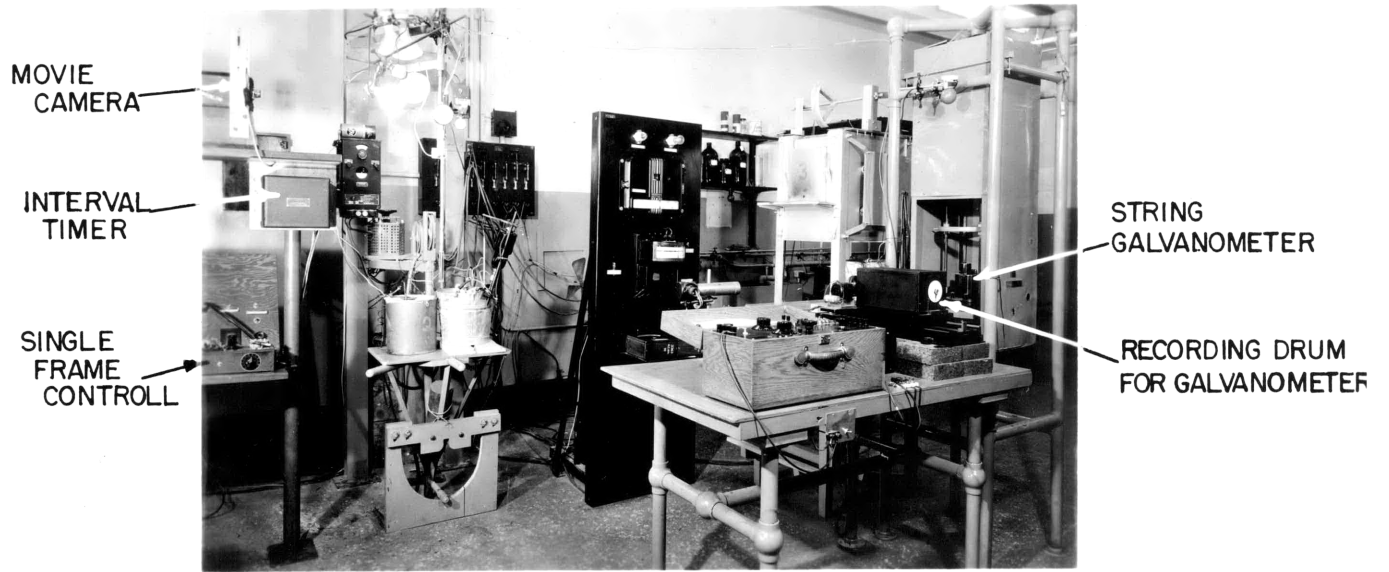
in dimensional behavior were found on aging and it has been assumed, therefore, that the length changes measured in this investigation reflect true volume changes due to phase transformations. This procedure is a much more sensitive test of directionality than either direct specific volume determinations or simultaneous measurements of length and diameter of a given specimen.

### III. QUENCHING DILATOMETER MEASUREMENTS

---

Because of the observed instability of the dimensional specimens during the 90 minute interval between the quench and the first measurement, it was suspected that rather large changes took place during this period. A quenching dilatometer was constructed, therefore, to study this interval immediately after the quench. The dilatometer was essentially that of Flinn, Cook, and Fellows<sup>(20)</sup> except that it was modified to take a thermocouple and a specimen 4 inches long by 3/8 inch diameter. This specimen was supported at its lower end by an outer quartz tube cut away to admit free access of the quenching fluid, and was held by spring compression at the upper end against a smaller quartz tube which actuated the dial gage. The arrangement is shown in Figure 11.

For a dilatometer run, the specimen was set into the quartz holder, and austenitized in the small lead pot set on the moving table. To quench, the lead pot was lowered away from the specimen and the quenching bath brought up around it, by swinging the counterweighted table through a U-shaped course described by the guide shown in Figure 11. During the quench the dial gage and timer remained in the same position and were photographed by a motion picture camera running at 16 frames per second but with shutter speed advanced to one-eightieth of a second to stop the motion of the dial. The quenching bath was equipped with a high speed electric stirrer, a cooling coil, and an immersion heater



MOVIE  
CAMERA

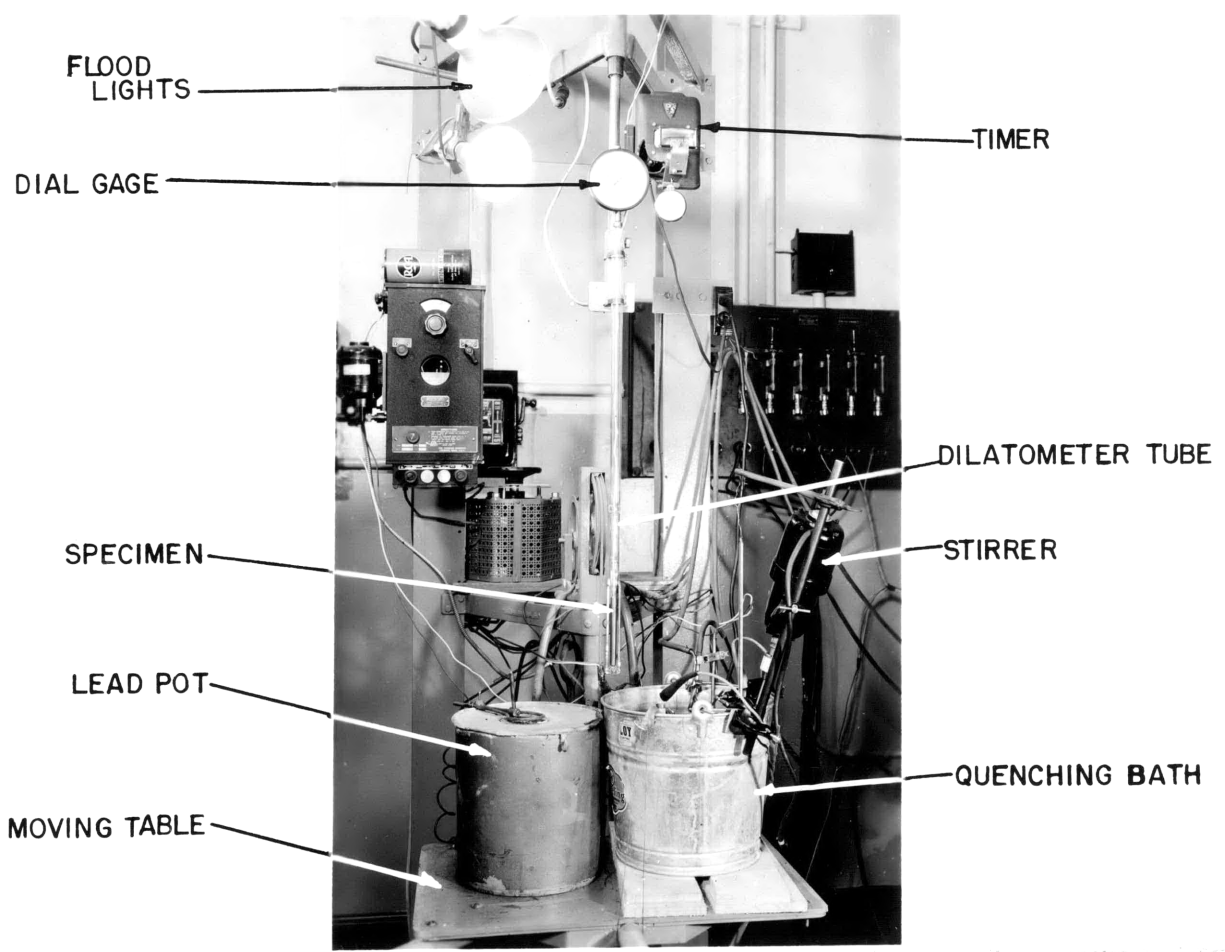
INTERVAL  
TIMER

SINGLE  
FRAME  
CONTROLL

STRING  
GALVANOMETER

RECORDING DRUM  
FOR GALVANOMETER

GUIDE FOR TABLE



FLOOD  
LIGHTS

DIAL GAGE

SPECIMEN

LEAD POT

MOVING TABLE

TIMER

DILATOMETER TUBE

STIRRER

QUENCHING BATH

Figure 11. Quenching dilatometer apparatus showing arrangement of the equipment and a close-up of the specimen. The dial gage and timer are turned 90° from their normal position

controlled by a potentiometer controller, so that a wide variety of quenching conditions were possible. A vibrator was attached to the quartz tube holder, and flood lights were provided to light the dial sufficiently to be photographed.

For these experiments it was of utmost importance to determine when the specimen had reached room temperature. A hole  $1/2$  inch deep and  $1/16$  inch in diameter was drilled into the top of each dilatometer specimen and a 28 gage chromel-alumel thermocouple inserted until it made metallic contact. This thermocouple was threaded back through the inner quartz tube of the dilatometer to a string galvanometer with a 0.007 second period which was used by Greninger<sup>(21)</sup>, and which was capable of following quenching rates up to  $10,000^{\circ}$  F per second. This galvanometer produced a trace on photographic paper attached to a revolving drum and provided, therefore, a record of temperature and time. The galvanometer deflections were calibrated in terms of temperature by measuring the austenitizing temperature with a separate portable potentiometer and recording the high trace on the revolving drum. A low trace was recorded at zero millivolts, and it was demonstrated that the temperature was a linear function of the deflection. This calibration was performed on each record. The quenching rates for the fairly massive samples used here were comparatively slow and it was an easy matter to match up corresponding records of length, temperature, and time.

In practice, the specimen was quenched with the flood lights on, the buzzer operating, the stirrer working vigorously, and the

camera running free. At the same time, the string galvanometer was recording on the revolving drum. After the main motion of the dial gage had subsided and the specimen had reached room temperature, an automatic timer was introduced, and this would in proper sequence, turn on the lights, operate the vibrator, activate an electronic circuit designed to trip the shutter for a single frame, and turn off the lights at predetermined intervals for the next 24 hours. On runs where the quenching bath was above room temperature, the specimen tended to approach the ambient rather slowly and the temperature readings were taken directly on the potentiometer. An electric fan was also used to accelerate the air-cooling of these specimens.

Considerable experimental difficulties were encountered in operating the quenching dilatometer. The specimen was quite heavy and the quartz breakage frequent. Because of the thermal shock, specimens could not be quenched into iced brine, and molten salt baths could also not be used because of the solidification of the salt about the specimen and quartz during the subsequent air cooling. In order to quench to 450° F (230° C) it was necessary to use a hot oil bath, but hardness readings as well as cooling curves demonstrated that there was little difference between salt and oil at this temperature under these conditions. Some difficulty was also encountered with oil at 450° F (230° C) because of a gummy carbon residue which formed as the hot specimen was quenched into the hot oil. Lead oxide in the austenitizing bath attacked the

quartz and caused it to deteriorate rapidly, but this was alleviated somewhat by deoxidizing the lead bath with an oil-soaked brick prior to each run. Finally, the quenching fluid tended to enter between the specimen and inner quartz rod and to flood the thermocouple. This was prevented by using a thin tight-fitting sleeve of stainless steel at the top of the specimen. The sleeve is not shown in Figure 11. After repeated trials, duplicate runs were obtained for each of the quenching conditions studied here with the exception of the iced brine quench, and since the dilatometer specimen size and quenching conditions duplicated rather closely the situation for the dimensional specimens, it was possible to unambiguously project the length changes from the dilatometer specimen to the dimensional data.

The results for a ball-bearing steel specimen (T steel) quenched from 1550° F (845° C) into oil at 68° F (20° C) are shown in Figure 12, and the corresponding results for a specimen of plain carbon steel (K steel) water quenched from 1450° F (790° C) are shown in Figure 13. The onset of the martensite reaction is indicated approximately by the sharp minima in the length curves since the austenite-martensite reaction is attended with a rather large increase in volume. The temperature readings at these minima are several hundred degrees higher than the  $M_s$  points measured by the Greninger and Troiano method, and it is evident that the thermal gradients in the dilatometer specimens were so high that the thermocouple was reading consistently too high. Although this discrepancy might be quite large during the quench, it would tend to become less as room

Figure 12. Quenching dilatometer record showing relative change in length and temperature as functions of time for a ball-bearing steel, austenitized at 1550° F (845° C) and quenched into oil at 68° F (20° C).

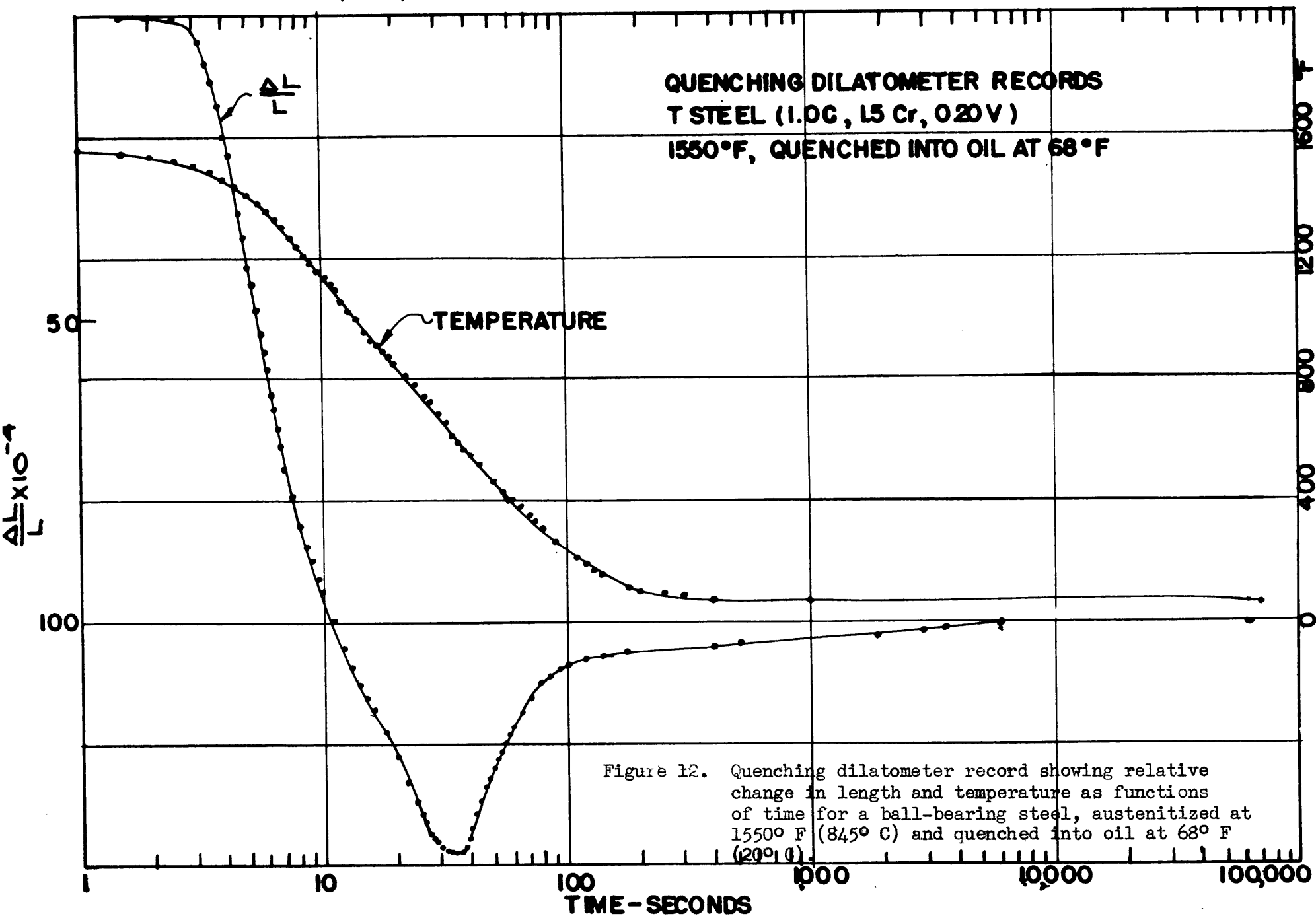
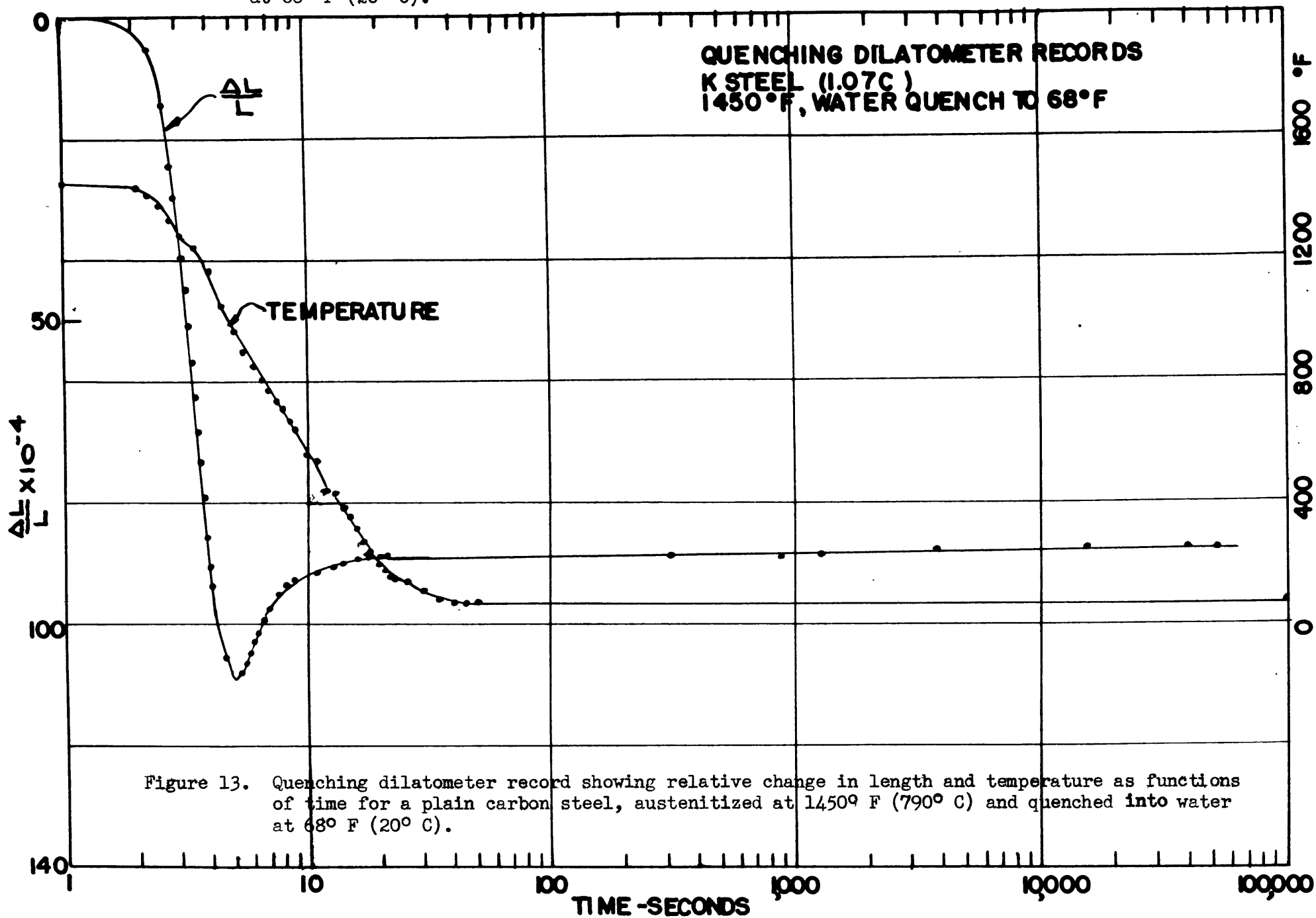


Figure 12. Quenching dilatometer record showing relative change in length and temperature as functions of time for a ball-bearing steel, austenitized at 1550° F (845° C) and quenched into oil at 68° F (20° C).

Figure 13. Quenching dilatometer record showing relative change in length and temperature as functions of time for a plain carbon steel, austenitized at 1450° F (790° C) and quenched into water at 68° F (20° C).





temperature were approached, and in any event, it would err on the conservative side in estimating when the entire sample had come to room temperature. Even on the compressed scale of Figures 12 and 13 it is seen that some expansion took place after the sample had reached room temperature, and what is equally important, that this expansion was continuous with that caused by the martensite reaction on cooling. Similar results were obtained for each of the quenching conditions studied.

#### IV. THE QUANTITATIVE DETERMINATION OF RETAINED AUSTENITE

---

##### A. The Problem

Before the reactions which hardened steels undergo on subsequent heat treatment could be considered in anything but qualitative fashion, it was necessary to make some kind of quantitative analysis for each of the reacting constituents. Martensite and retained austenite are the important reactants in the normally hardened tool steels considered here, although undissolved carbides must be considered as a diluent if they are present in measurable quantities. Once this analysis had been made, it was more precise to follow transformation reactions by observing changes in length, but this latter method could only determine differences in the amount of retained austenite, and an independent method was necessary to establish the absolute amounts of either austenite or martensite.

In certain instances the microscope has been used to determine the percentage of retained austenite. The quenched sample is tempered to darken the martensite, and then polished and etched in the usual fashion. A point counting method, which measures the percentage of the etched area which appears as austenite, or the lineal analysis of Howard and Cohen<sup>(9)</sup> which measures the percentage of a line drawn across an etched surface which is intercepted by austenite grains, has then been used to make the determination quantitative. All such microscopic methods, however, depend on the etch

itself being quantitative. On fairly coarse structures, larger than ASTM grain size No. 6, if a reasonably large percentage of retained austenite is present, i.e. larger than 15 percent, and if the austenite is not too finely divided, there is probably little smearing of the etch, and a lineal analysis or a point count is probably quite accurate. If the structure is difficult to resolve, however, the retained austenite may be completely obliterated under the microscope or it may appear disproportionately low as the lines of demarcation become difficult to distinguish. For example, a plain carbon tool steel (1.07 C - K steel) quenched from 1450° F (790° C) shows only martensite and undissolved carbides under the microscope, yet as will be shown later, such a sample contains almost 10 percent of retained austenite.

X-ray methods have been most successful in filling in the region under 15 percent retained austenite where the microscopic methods usually fail. Although austenite and martensite in the same steel may be identical chemically, their crystal structures and lattice parameters differ, and the intensity of an austenite diffraction line is some function of the percentage of retained austenite in the sample. In the method of Gardner, Antia and Cohen<sup>(22)</sup> this principle was applied by exposing the sample simultaneously with a standard aluminum foil in a Phragmen camera. The ratio of the peak blackening of the (200) austenite line to that of the (200) aluminum line as determined from a microphotometer trace was taken as proportional to the austenite content.

To calibrate this method, however, it was necessary to determine this ratio as a function of austenite content by one of the microscopic methods. At high austenite contents this calibration was probably quite accurate and it resulted in a straight line which apparently passed through the origin. Close to the point where the austenite began to disappear, however, the accuracy was probably quite low, and it is questionable if the straight line should have been continued from the last calibration point through the origin. Fletcher's modification<sup>(16)</sup> consisted of tempering the sample at 300° F (150° C) to collapse the martensite (110-101) doublet and of using the (111) austenite line which is considerably more sensitive than the (200) line.

In addition to the uncertainty in the microscopic calibration there is an inherent theoretical error in extending the calibration line as a straight line through the origin. The peak intensity of a diffraction line is not a quantity which can be calculated theoretically because it is influenced very greatly by the physical condition of the diffracting crystal. As the austenite transforms, the particle size of the retained austenite becomes smaller, and soon after it reaches the point where it can no longer be resolved under the microscope, line broadening begins to occur in the austenite diffraction lines. The peak intensities are thus lowered with a corresponding increase in line width. Retained austenite crystallites are also apt to be considerably distorted since the transformation product has a greater specific volume than the austenite

from which it forms. Such distortion also reduces the peak intensities appreciably, and these two factors together could easily reduce the peak intensities by 50 percent. However, only the intensity distribution is affected in these cases; the total diffracted energy remains the same. Other factors such as errors in photometry and uncertainty in "instrumental" broadening affect the peak intensity and the shape of the line but again have comparatively little effect on the integrated intensity, which is proportional to the energy of the diffraction line. These factors cannot be eliminated by an external calibration since the austenite is no longer visible in these regions, and they would tend to make the determination indicate less austenite than was actually present.

It is in this low austenite region that most normally hardened steels fall, and the isothermal decomposition data presented previously indicated that many interesting effects occur even with small amounts of retained austenite. These data also showed that more austenite was present in normally quenched steels than had previously been suspected, and another method of austenite determination, which would be independent of a microscopic calibration was sought.

B. Quantitative Analysis by X-rays

An x-ray method based on the measurement of diffracted energy can also be developed for determining the percentage composition of multi-phase alloys. If, for example, a mixture of martensite and austenite is irradiated with x-rays, each type of crystal will diffract in accordance with the Bragg law.

$$(1) \quad n\lambda = 2d \sin \theta$$

where  $n$  = order of the spectrum  
 $\lambda$  = wavelength in kX units  
 $d$  = interplanar spacing in kX units  
 $\theta$  = diffraction angle

To consider the energy in each of these diffraction lines it is necessary to measure the integrated intensity, i.e. the area under the intensity vs.  $\theta$  curve. This energy can be calculated on a theoretical basis, however, and for a powder sample consisting of very small crystals the integrated intensity in ergs/sec per unit length of a diffraction line for a particular substance,  $\propto$ , is given by:

$$(2) \quad P'_x = K_s I_0 V_x S^2 e^{-2M} m \text{ (L.P.) } A(\theta)$$

where 
$$K_s = \frac{N_x^2 \lambda^3 e^4}{32\pi E_0 m^2 c^4}$$

- and
- $P'_\alpha$  = power per unit length of diffraction line in erg/sec for a particular diffraction line of substance  $\alpha$
  - $N_\alpha$  = number of atoms per  $\text{cm}^3$
  - $\lambda$  = wavelength in cm.
  - $e$  = electronic charge in e.s.u.
  - $R_0$  = camera radius in cm.
  - $m_e$  = electronic mass in grams
  - $c$  = velocity of light in cm/sec.
  - $I_0$  = intensity of plane incident wave in  $\text{erg/cm}^2$  - sec.
  - $V_\alpha$  = volume in  $\text{cm}^3$  of substance,  $\alpha$ , irradiated
  - $S_\alpha$  = structure factor per atom
  - $e^{-2M}$  = Debye-Waller temperature factor
  - $m$  = multiplicity of diffracting plane
  - L.P. = Lorenz and polarization factor
  - $A(\theta)$  = sample absorption factor

Collecting all the constants which would apply for a given camera and exposure, this equation may be rearranged to:

$$(3) \quad P'_\alpha = \text{const} \cdot N_\alpha^2 F^2 e^{-2M} m (\text{L.P.}) V_\alpha A(\theta) = \text{const} \cdot R \cdot V_\alpha A(\theta)$$

- where
- $N_0$  = number of unit cells per unit volume =  $\frac{1}{v_\alpha}$
  - $v_\alpha$  = volume of unit cell of substance  $\alpha$
  - $F$  = structure factor per unit cell

If martensite is taken as the substance  $\alpha$ , then a similar equation may be written for each diffraction line of austenite, substance  $\gamma$ , where  $N_0$ ,  $F$ ,  $m$ , (L.P.),  $V_\gamma$  and  $A(\theta)$  each have different values. For each line, therefore, the coefficient  $R$  contains the factors which may be readily calculated from tabulated values, the volume irradiated is the unknown to be determined, and the absorption correction depends on the geometry of the sample. For a flat sample set at a grazing angle,  $\phi$ , the absorption correction has been given by Taylor<sup>(25)</sup> as:

$$(4) \quad A(\theta) = \frac{a(\sin \phi)}{\bar{\mu}} \cdot \frac{\sin(2\theta - \phi)}{\sin(2\theta - \phi) + \sin \phi} = \frac{a}{\bar{\mu}} A'(\theta)$$

where  $a$  = area of specimen irradiated

$\bar{\mu}$  = average linear absorption coefficient for the entire specimen.

Since "a" and " $\bar{\mu}$ " are constants for a given exposure, the factor  $A'(\theta)$  varies only with  $\theta$  in a smooth curve such as the one plotted in Figure 14 for the case where  $\phi = 60^\circ$ . It is noticeable that the absorption decreases rapidly as the back reflection direction is approached.

To determine the volume percentage of  $\alpha$  and  $\gamma$ , the diffraction lines of substance  $\alpha$  are microphotometered and the integrated intensity per unit length of line determined in arbitrary units. Division of these observed intensities by the appropriate values of  $R$  will leave the product  $V_\alpha \cdot A(\theta)$ , and since  $V_\alpha$  is a



### ABSORPTION CORRECTION FOR FLAT SAMPLE

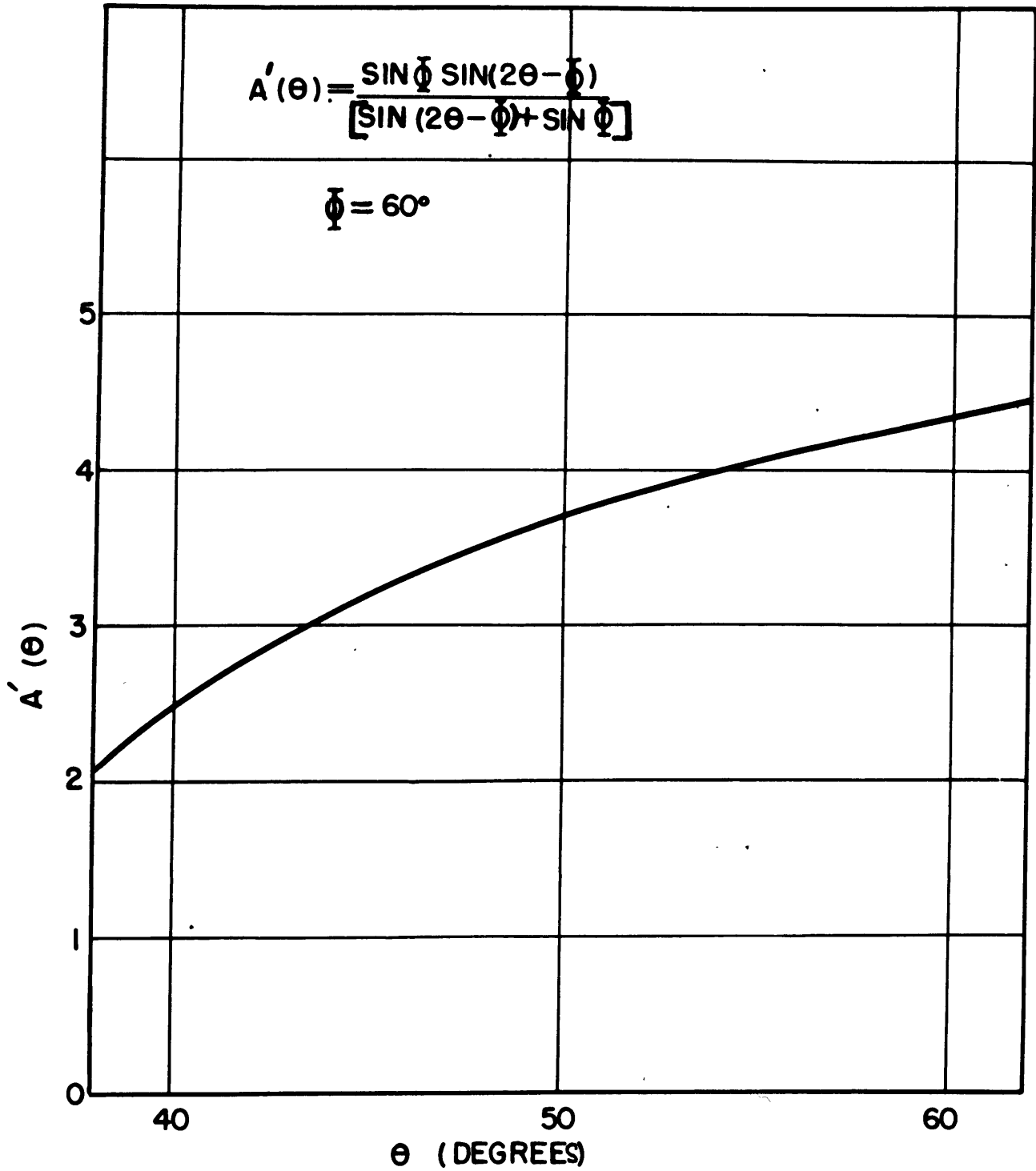


Figure 14. Variation of absorption correction with diffraction angle for a flat sample.

constant for all of the diffraction lines from substance  $\alpha$ , a plot of  $V_{\alpha} \cdot A(\theta)$  vs.  $\theta$  should have the same general shape as the curve in Figure 14. If the sample contains a different percentage of  $\alpha$  than of  $\gamma$ , a similar procedure will yield another curve for  $V_{\gamma} \cdot A(\theta)$  which should also have the same shape as the one in Figure 14. Since  $A'(\theta)$  is the same for both diffracting substances, the difference in the curves for  $\alpha$  and  $\gamma$  is due only to the fact that  $V_{\alpha}$  is different than  $V_{\gamma}$ . The constant ratio by which the ordinates of the  $\gamma$  curve must be multiplied to place them on the  $\alpha$  curve is thus equal to the volume ratio of  $\frac{\alpha}{\gamma}$ . If no other diffracting medium is present in the sample, the volume percentage of each constituent may then be calculated from the additional fact that  $\alpha + \gamma = 100$ .

### G. Experimental Procedure for Retained Austenite

The procedure may be illustrated by describing the determination of retained austenite in the K steel (1.07 carbon) austenitized at 1450° F (790° C) for 30 minutes and quenched into water at room temperature. The sample was a cylinder 3/8 inch diameter by 5/8 inch long (0.95 x 1.6 cm) heat treated in a lead pot and quenched into agitated water. After heat treatment, about 1/8 inch was removed from the flat surface on a wet grinder with precautions taken not to temper the specimen. A standard metallographic polish and etch with 1 percent nital was then used and the sample was examined for evidences of tempering and flow. Pitting

of the undissolved carbides was also avoided since the diluting effect of these carbides was considered in a subsequent calculation.

The specimen was then mounted in a Debye camera so arranged that the grazing angle,  $\phi$ , with a flat cross-section was  $60^\circ$ . This grazing angle was chosen since it was small enough to allow the (200) martensite line to diffract, and large enough to prevent excessive line broadening because of the obliqueness of the irradiated surface. A flat sample was used because of the ease of duplicating the surface preparation and because it was possible to remove sufficient metal from the surface to make certain that no edge effects were involved. A plane surface is also an efficient diffracting shape and exposure times were considerably lower than for a wedge or a thin rod. Monochromatic  $\text{CoK}\alpha$  radiation was obtained by the diffraction of cobalt radiation from the (200) face of a rock salt crystal mounted directly on the camera in front of the collimating system. Although both the half and third wavelengths were also present they did not interfere with the determination since only the relatively weak lines were used. Monochromatic radiation was used to cut down the background intensity so that the very weak lines for low percentages of austenite would be visible, and the camera was also evacuated to reduce air scattering. The camera arrangement is shown in Figure 15. Segregated areas in the specimen were avoided, and because of the fine grain size (ASTM No. 9) obtained from this particular heat treatment no sample oscillation was necessary to obtain smooth uniform diffraction lines. Exposure

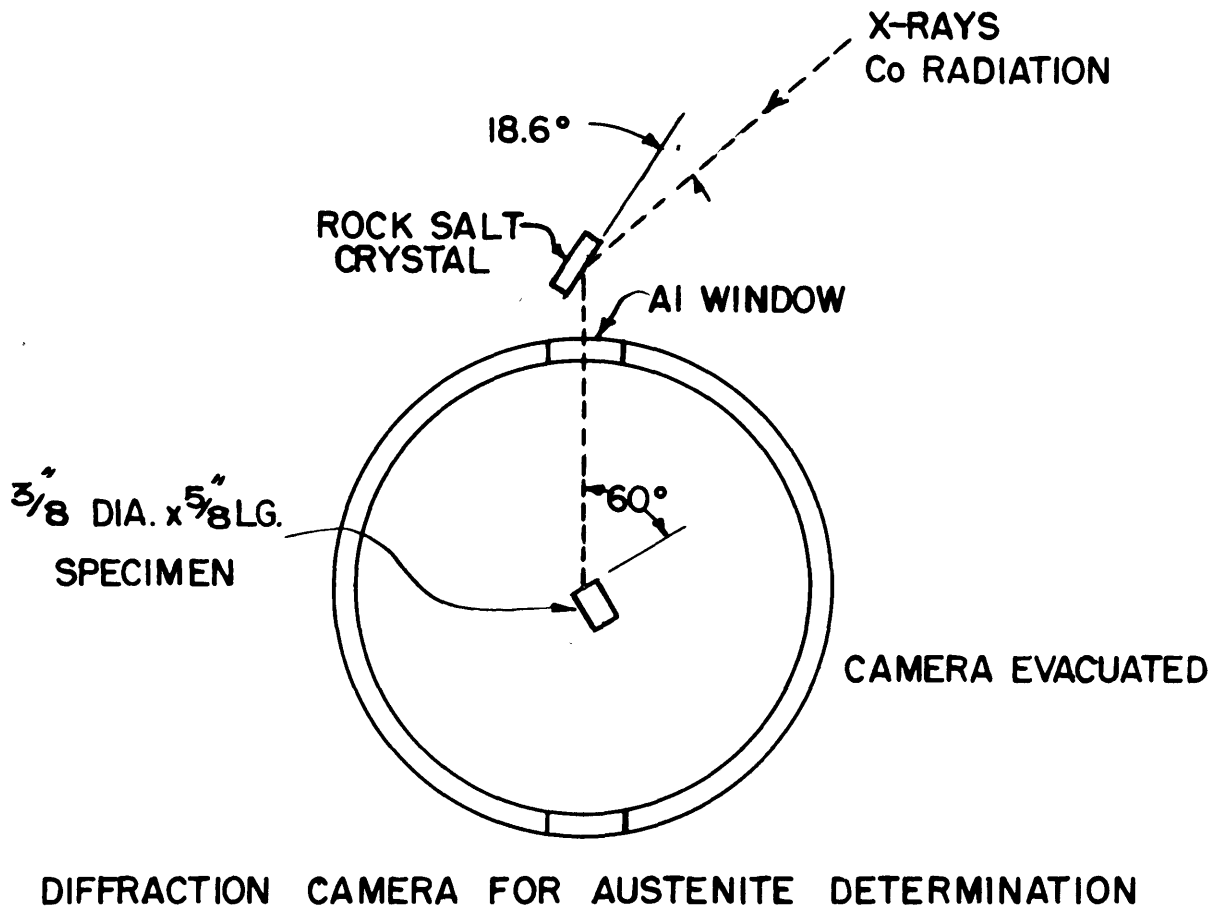


Figure 15. Arrangement of diffraction camera to obtain monochromatic radiation on a flat sample.

times were about 24 hours and the central reproduction in Figure 16 shows the diffraction pattern obtained by this method for the K steel water quenched from 1450° F (790° C).

The x-ray patterns were recorded on Eastman No-Screen film, and all films were processed so as to produce a linear blackening vs. intensity curve up to a blackening of 1.5. In practice, however, the maximum blackening used was approximately 1.2. These films were then microphotometered in a Kipp and Zonen recording microphotometer with the light intensity adjusted to provide the greatest possible vertical enlargement of the lines, and the central trace of Figure 17 shows the microphotometer record of the corresponding film of Figure 16. This densitometer trace was then converted to a blackening curve and the areas under each peak calculated by Simpson's rule in the manner described by Fitzwilliam<sup>(24)</sup>.

Most of the factors for the value of R in equation (3) have been tabulated by Taylor<sup>(23)</sup>. The volume of the unit cell was calculated in each case from the known parameters of austenite and martensite for this carbon content<sup>(15)</sup>. Since the CoK $\alpha$  radiation (1.7872 kX units) is very close to the absorption edge of iron (1.7394 kX units) a rather large correction must be made in the listed atomic scattering factors for dispersion. This correction has been tabulated by H $\ddot{o}$ nl<sup>(25)</sup> and takes the

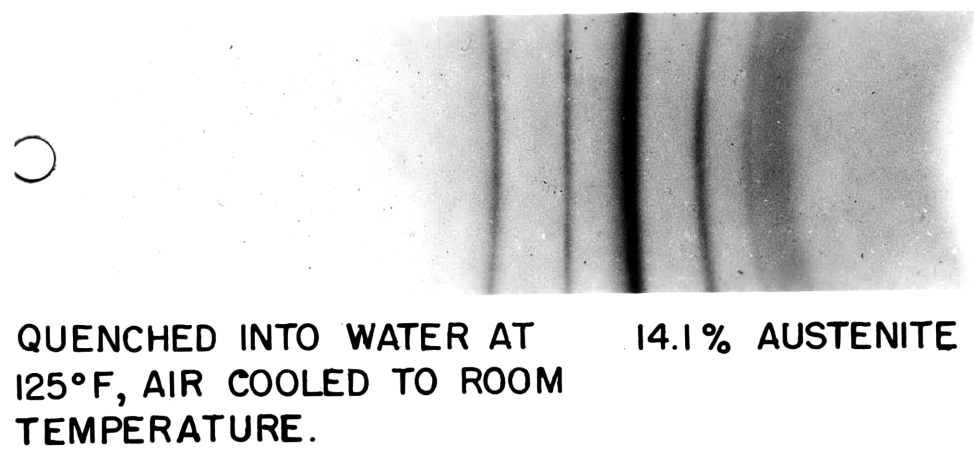
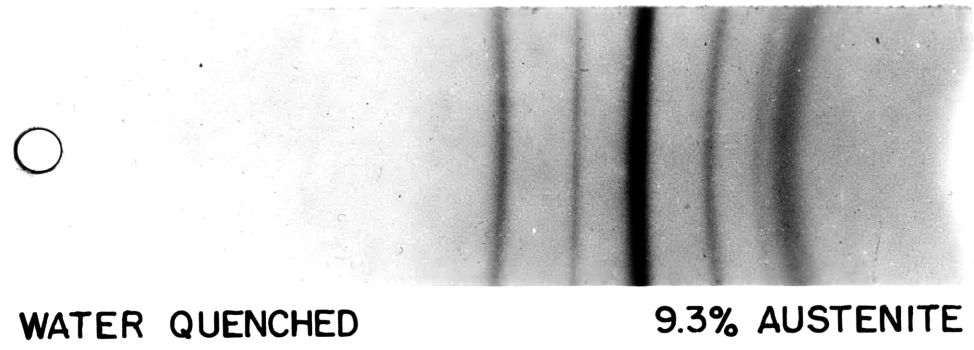
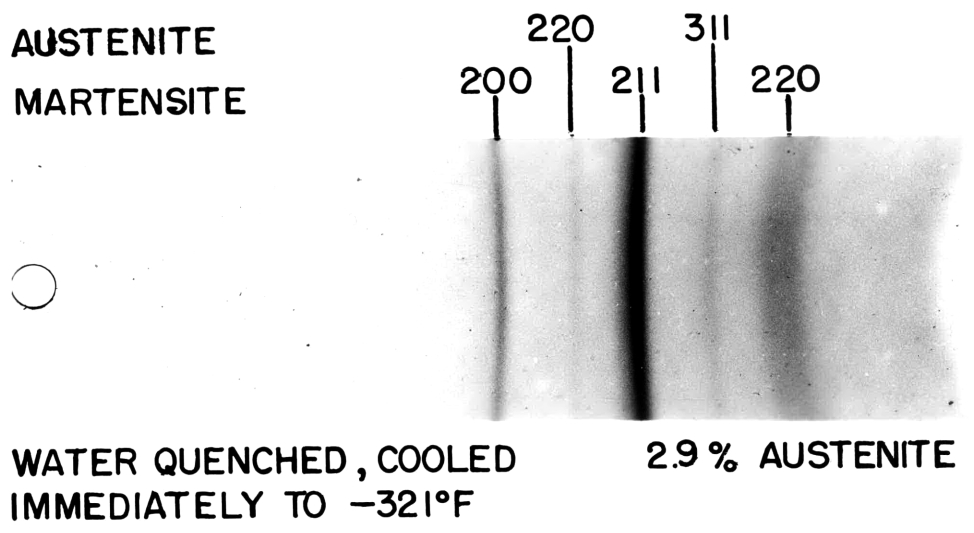


Figure 16. X-ray diffraction patterns obtained with CoK monochromatic radiation showing austenite and martensite lines.

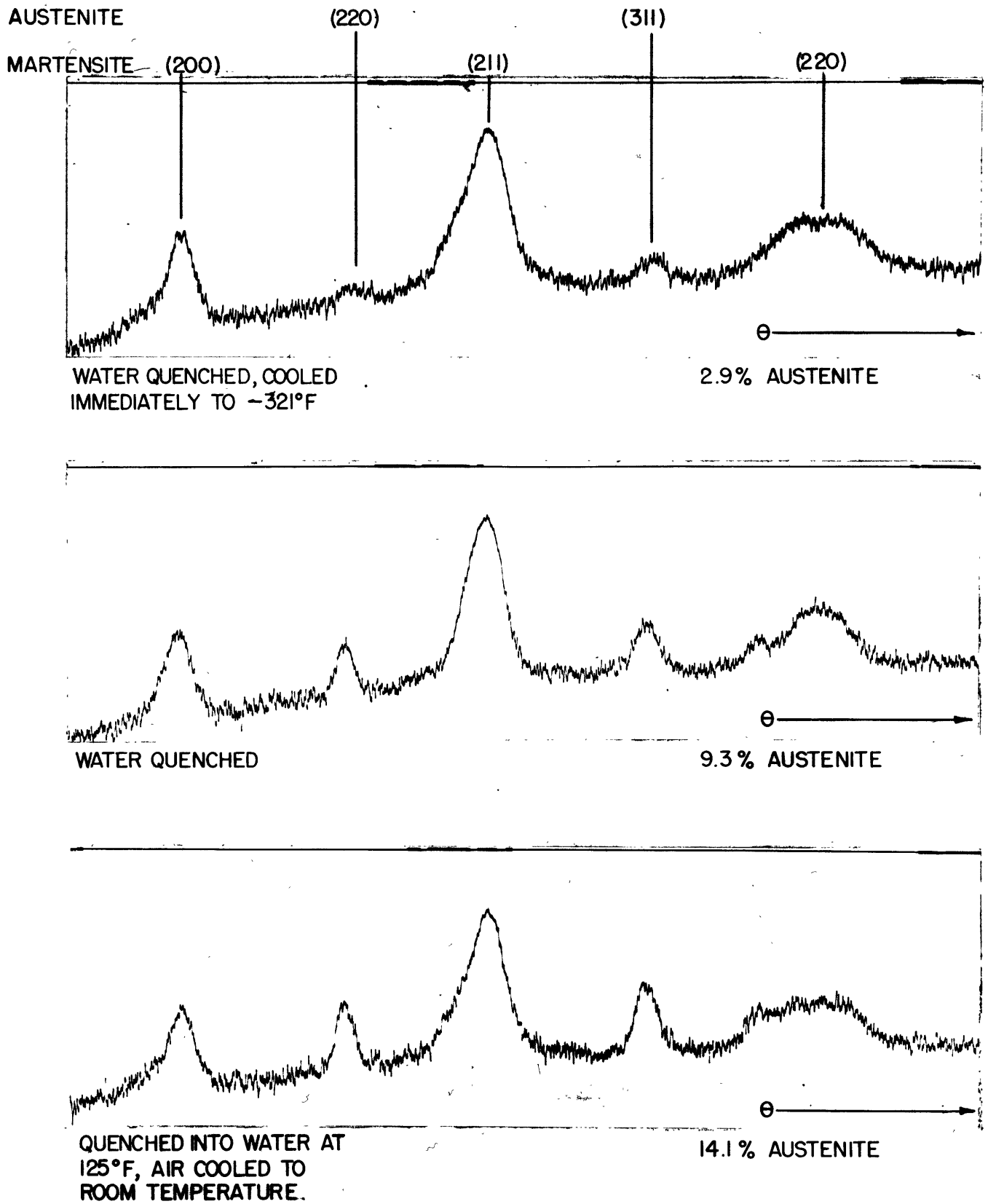


Figure 17. Microphotometer traces of diffraction patterns shown in Figure 16.

form:

$$(5) \quad f = f_0 - \Delta f$$

where  $f$  = effective atomic scattering factor

$f_0$  = calculated atomic scattering factors for the case where the irradiating wavelength is not close to an absorption edge of the sample

$\Delta f$  = decrement of the atomic scattering factor due to interaction with the K electrons

For the case of  $\text{CoK}\alpha$  radiation on iron,  $\Delta f = 4.0$  units. Since the camera was too small and the lines too diffuse to allow resolution of the martensite doublet for most of the lines, the doublets were lumped together as if they were effectively body centered cubic lines for the martensite and the structure factor as well as the multiplicity were calculated on this basis.

The Debye-Waller temperature factor was calculated from the Debye temperature for iron taken as  $420^\circ \text{K}$ <sup>(26)</sup>. In the Lorenz and polarization factor, account was taken of the fact that a beam of x-rays monochromated by a rock salt crystal is not completely unpolarized and the (L.P.) factor was calculated from

$$(6) \quad (\text{L.P.}) = \frac{1 + \cos^2 2\theta_c \cos^2 2\theta}{\sin\theta \sin 2\theta}$$

where  $\theta_c$  = Bragg angle for the monochromating crystal. The values of each of these factors are listed for austenite and martensite in Table II.



TABLE II

X-ray Constants for Austenite and Martensite Lines

CoK $\alpha$  radiation (1.7872 kX units) crystal monochromated.

Martensite: body centered tetragonal

$$a_0 = 2.852 \qquad v_a = 24.2 \text{ (kX)}^3$$

$$c_0 = 2.975$$

<u>Line</u>	<u><math>\theta^\circ</math></u>	<u>f (eff.)</u>	<u>F</u>	<u>n</u>	<u>L.P.</u>	<u><math>e^{-2M}</math></u>	<u>R</u>
(200) (002)	38.60	10.4	20.8	6	1.70	.920	6.91
(211) (112)	49.90	8.8	17.6	24	1.35	.875	15.05
(220) (022)	61.90	7.6	15.2	12	1.65	.835	6.54

Austenite: face centered cubic

$$a_0 = 3.597 \qquad v_y = 46.4 \text{ (kX)}^3$$

(220)	44.68	9.4	37.6	12	1.40	.890	9.80
(311)	55.18	8.2	32.8	24	1.42	.860	14.75

The integrated intensities in arbitrary units for each of the lines for a sample of K steel (1.07 carbon) exposed 30 hours after quenching are listed in Table III. On plotting the values of  $V_{\alpha} \cdot A(\theta)$  for the martensite lines, Figure 18, it is evident that the shape of the absorption correction is the same as that predicted by the calculated curve for a flat sample in Figure 14. Similarly the values of  $V_{\gamma} \cdot A(\theta)$  for the austenite points lie on a curve considerably lower than that for the martensite. From Figure 18 it is evident that the  $(220)\gamma$  must be multiplied by 9.7 to bring it up to the martensite curve and the  $(311)\gamma$  by 9.2. On averaging, the ratio  $\frac{\text{martensite}}{\text{austenite}} = 9.5$ .

If the entire volume of the sample were composed of austenite and martensite the percentage of austenite could be computed readily. Undissolved carbides are, however, plainly visible under the microscope. These carbides contribute diffracted energy to neither the martensite nor the austenite lines so that:

$$(7) \quad V_{\alpha} + V_{\gamma} = (100 - \text{volume percent of carbides})$$

These carbides were measured by a lineal analysis under the microscope and this sample was found to contain 2.6 percent by volume.

Therefore:

$$(8) \quad \frac{\alpha}{\gamma} = 9.5$$

$$\alpha + \gamma = 97.4$$

and  $\gamma = 9.3$  percent by volume.

TABLE III

Integrated Intensities for Austenite Determination

K Steel (1.07 C) - 1450° F water quenched

2.6 percent carbides

	<u>Line</u>	<u>Integrated Intensity P'</u>	<u>V•A(θ)</u>	$\frac{\alpha}{\gamma}$	<u>Volume Percent</u>
Martensite	(200)	4.849	0.702		
	(211)	19.431	1.295		
	(220)	9.591	1.470		
Austenite	(220)	1.095	0.112	9.7	
	(311)	2.318	0.163	9.2	
			Ave.	9.5	9.3

$$\frac{\alpha}{\gamma} = 9.5$$

$$\alpha + \gamma = 100 - 2.6 = 97.4$$

$$\gamma = 9.3$$

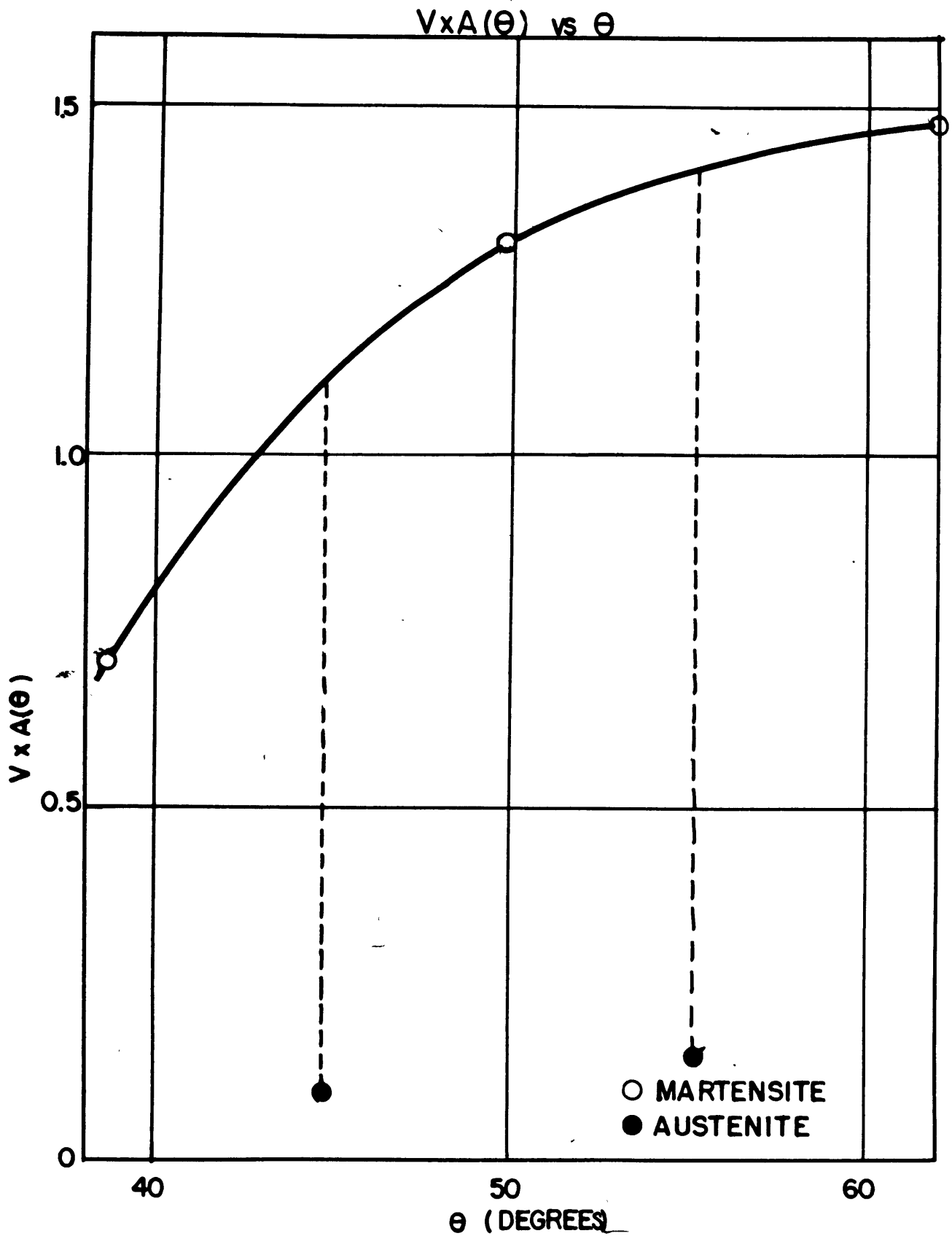


Figure 18. The variation of  $V \cdot A(\theta)$  with diffraction angle obtained for K steel (1.07 C) austenitized at 1450° F (790° C) and quenched into water. The lower points are calculated from the austenite lines and the constant ratio needed to bring the lower points on to the upper curve gives the volume ratio of martensite to austenite.

This correction for the volume of carbides is small and lies within the limit of accuracy of the determination. Whereas the microscope has been used here for the carbide correction, it is only responsible for a small correction on the total volume. No direct calibration with observed austenite contents is necessary, and the undissolved carbides can be determined on the actual sample under observation. The carbide volume is usually a function of the austenitizing temperature only and appreciable errors in the carbide count will influence the austenite results only slightly.

The carbide volume can also be checked from the  $M_s$  point determination. If we assume for the plain carbon steel (1.07 carbon) that the undissolved carbides are present as  $Fe_3C$ , on subtraction of the carbon in the 2.6 percent carbides from the total carbon, it would seem that 0.90 percent carbon is in solution. The  $M_s$  point for such a steel has been given as about  $400^\circ F$  ( $205^\circ C$ ) by Klier and Troiano<sup>(27)</sup> and this checks exactly with the  $M_s$  point observed here for these quenching conditions. For the ball-bearing steel (1.6 carbon, 1.5 chromium, 0.20 vanadium) oil-quenched from  $1550^\circ F$  ( $845^\circ C$ ) the undissolved carbides were found to be 4 percent by volume by lineal analysis. Performing a similar calculation from the measured  $M_s$  point it is found that this steel behaves effectively as if 0.84 percent carbon and 0.5 percent chromium were in solution.

To check on the reproducibility of the austenite determination, another exposure was made on the same sample immediately afterwards. This result and the results on several other samples treated identically are shown in Table IV. The error in the determination was estimated to be +5 percent of the amount of retained austenite, or +0.30 percent austenite, whichever is the greater. The sensitivity of the method is quite high since the exposure time can be increased to bring out even very weak austenite lines. Figures 16 and 17 illustrate the x-ray patterns and microphotometer traces for cases where the austenite contents are as low as 2.9 percent and as high as 14.5 percent. It should be possible to detect austenite contents as small as one-half percent with the exposure conditions used here.

It is also interesting to note in Figure 17 that the austenite lines become relatively sharper as the austenite content increases, and that at low austenite contents the lines are quite broad. This effect is due to either fine particle size or distortion and contributes to the error caused by using peak intensities alone as a criterion of austenite content.

#### D. Extinction and Absorption Effects

Before this method could be accepted with confidence several other factors had to be considered. Equation (2) is applicable only in the absence of extinction. Primary extinction is caused by the cancellation in energy due to a  $180^\circ$  phase shift as the

TABLE IV

Effect of Room Temperature Aging on Retained Austenite Contents

---

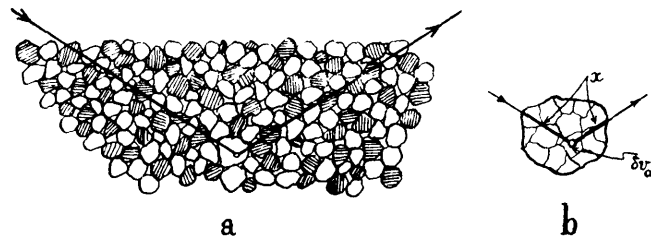
K Steel (1.07 C) - 1450° F, quenched into water at 68° F.

<u>Sample</u>	<u>Time After Quench (Hours)</u>	<u>% Retained Austenite</u>	<u>% Martensite</u>	<u>% Carbides</u>
1	30	9.5	89.1	2.6
1	54	9.5	88.9	2.6
2	72	9.4	89.0	2.6
3	240	9.0	89.4	2.6
4	480	9.1	89.3	2.6
5	6000	8.8	89.6	2.6

primary beam proceeds through a given set of planes in a single crystal. As the crystal becomes smaller the extinction decreases, but the particle size in this case is not small enough to justify the assumption that extinction is absent. There is, however, considerable distortion in both the austenite and martensite crystals and it has been shown<sup>(28)</sup> that plastic deformation practically eliminates extinction, especially for the weaker reflections. In addition, extinction has its greatest effect on the very strong reflections,  $(111)\gamma$  and  $(110)\alpha$ , which are not used in this determination. It seems reasonable to assume, therefore, that the extinction effects are negligible here.

Equation (2) is also limited to the case where the particle size is so small that the absorption in the individual particle produces a negligible reduction of intensity of the transmitted beam. Unfortunately, although this effect is quite troublesome, it has generally been overlooked. This phenomenon is termed microabsorption and has recently been treated theoretically by Brindley<sup>(29)</sup>, Taylor<sup>(30)</sup> and Brentano<sup>(31)</sup>. Following the reasoning of Brindley, a given crystal A, in a mixture of A and B crystals, Figure 19, is considered as it is irradiated by x-rays. The path of the incident beam to the crystal and of the diffracted beam from the crystal may be considered as a statistical average of A and B according to the average composition of the sample. To this part of the path an average absorption coefficient  $\bar{\mu}$  calculated from the composition in the usual fashion may be used,





X-ray reflection from mixed medium grade powders ( $0.01 < \mu D < 0.1$ ). (a) shows a two-component powder. (b) shows reflection from a volume-element,  $\delta v_a$  of a crystal in a polycrystalline particle;  $x$  is the path of the radiation in the particle.

Figure 19. Diffraction of x-rays by a given grain in a mass of crystallites. (After Brindley<sup>(19)</sup>).

and it is this macroabsorption coefficient which appears in the usual absorption correction such as the one given by equation (4). In this case the absorption coefficients of A and B appear only as part of an average for the absorption of the entire sample. For a diffraction line of A however, part of the path, as shown in Figure 19 must lie completely within A. Similarly, for the diffraction lines of B part of the path must lie completely within B. If the absorption coefficient for A is very much larger than that for B, or if the particle size of A is very much larger than that of B, a larger part of the energy will be lost by absorption in A, and the particle with the smaller absorption will be disproportionately accentuated on the pattern. Such an effect may seem trivial, but a large number of particles must diffract to produce an observable diffraction line, and this factor can become the most important single cause of error in a quantitative determination by x-rays.

Fitzwilliam<sup>(24)</sup> demonstrated this effect by irradiating powder compacts of known composition and particle size with x-rays of different wavelengths. Table V taken from his data shows the startling errors which may be obtained, and it is evident that microabsorption correction ( $\tau$ ) must be applied here. This correction should be some function of the absorption coefficient and the particle size for each constituent and it appears in the intensity equation as:

$$(9) \quad P_A^i = \text{const} \cdot N_o^2 F^2 e^{-2M} m \text{ (L.P.) } V_A \cdot \tau_A \cdot A(\theta)$$

TABLE V\*

The Microabsorption Effect

Sample I - 40.0 Fe, 60.0 Ni (Wt. percent) -- <200 mesh, >325 mesh

$\lambda$	Observed Composition		True Mass Ratio	Observed Mass Ratio	K		
	Fe	Ni			Observed	Brentano Theory	Brindley Theory
0.709	42.6	57.4	1.500	1.346	0.90	0.80	0.60
1.539	12.3	87.7	1.500	7.123	4.75	5.38	>34
1.787	42.7	57.3	1.500	1.344	0.90	0.73	0.42

Sample II - 49.9 Cu, 50.1 Al (Wt. percent) -- <200 mesh, >325 mesh

	Cu	Al					
0.709	29.3	70.7	1.004	2.412	2.40	1.92	5.28
1.539	36.2	63.8	1.004	1.764	1.76	2.10	3.88
1.787	32.2	67.8	1.004	2.106	2.10	2.60	6.91

Linear Absorption Coefficients

$\lambda$	Al	Cu	Fe	Ni
.709	14.3	444	302	422
1.539	131	470	2550	438
1.787	195	711	466	669

\* After Fitzwilliam<sup>(24)</sup>

Similarly in the intensity equation for B a factor  $\tau_B$  will appear and the ratio  $\frac{P_A}{P_B}$  will be in error by a factor  $K = \frac{\tau_A}{\tau_B}$ . If  $K = 1$ , there is no microabsorption factor, and the farther  $K$  is from unity the greater is the correction.

The form which the microabsorption coefficient,  $\tau$ , should take is not quite clear at present. Bridnley and Taylor have derived the equation for this correction as:

$$(10) \quad \tau_A = \frac{1}{V_a} \int_0^{V_a} e^{-(\mu_A - \bar{\mu})x} dV_a$$

where  $dV_a$  = volume element of crystal A correctly oriented to reflect radiation

$\bar{\mu}$  = mean absorption coefficient of the solid material forming the powder specimen

$\mu_A$  = linear absorption coefficient of substance A

$x$  = path length of the radiation in the particle of A

The values of  $\tau$  have been tabulated by Brindley<sup>(29)</sup> for various values of  $(\mu_A - \bar{\mu}) \cdot r$  ( $r$  = radius of the particle), and the values of  $K$  predicted by this theory are shown for Fitzwilliams's data in Table V. It is evident from a comparison with the experimental data that the value of  $K$  is always in the right direction, but that it overestimates the effect.

Considering the same problem in a somewhat different fashion, Brentano<sup>(31)</sup> calculated the value of  $K$  for a series of cube crystal-

lites diffracting in the back reflection direction. He obtained the correction in the form:

$$(11) \quad K = \frac{\mu_B}{\mu_A} \frac{1 - e^{-2\mu_A \cdot Z_A}}{1 - e^{-2\mu_B \cdot Z_B}}$$

where  $Z =$  cube edge dimension

Values of K by the Brentano theory are also shown in Table V and it is seen that these values agree much more closely with the experimental data, and could be used to estimate an approximate value for the correction factor K.

For the martensitic steels considered here, the largest particle of either constituent can be no greater than the original austenite grain size and the smallest could be estimated as being about a tenth of that value. Estimating the austenite grain size from the fracture grain size, which was ASTM No. 9 for most of the cases investigated here, the mean grain radius may be taken as about  $0.90 \times 10^{-3}$  cm<sup>(32)</sup>. Because of the difference in density the austenite has a lower absorption coefficient than the martensite but the factor  $(\mu_A - \bar{\mu})$  is only about 15. Using either the Brindley theory, which overestimates the effect, or the Brentano theory, which seems to be about right, the value of K is unity, despite the generous assumptions which have been made with respect to particle size. This is quite fortunate since it eliminates a troublesome correction and the results for the quantitative determination of the austenite-martensite system may be regarded with greater confidence.

### E. Results of Austenite Determinations

Table VI lists the austenite contents for the K steel (1.07 carbon) as a function of the quenching conditions. Each determination is the average of at least two determinations. These values are somewhat higher than the corresponding values shown by Fletcher<sup>(15)</sup> and a surprisingly large amount of austenite is present even after immediate refrigeration to liquid nitrogen temperature. Although previous data had indicated that this treatment left no residual austenite, the dimensional changes discussed previously had indicated that some austenite must be present even after immediate cooling with liquid nitrogen, and the transformation of all of the austenite by subcooling alone seems to become impossible in this case.

Of interest also is the significant increase in retained austenite as the quenching bath is raised to as low a temperature as 125° F (50° C). During some commercial quenching practices, the work is removed from the quench before it has reached room temperature, and this in effect approximates a quench into lukewarm water. Such a quench can result in appreciably higher retained austenite.

Similarly, Table VII indicates the retained austenite contents for the ball-bearing steel (T steel, 1.0 carbon, 1.5 chromium, 0.20 vanadium) as a function of quenching conditions. Here again, the austenite content rises somewhat as the temperature of the quenching bath rises, and on quenching above the  $M_s$

TABLE VI

Retained Austenite Contents

---

K Steel (1.07 C) - Austenitized at 1450° F for 30 minutes

(2.6 percent Carbides)

<u>Treatment</u>	<u>Hardness Rockwell C</u>	<u>% Retained Austenite*</u>
Water quenched to 68° F	67.0	9.0
Water quenched to 125° F, air cooled to room temperature	65.9	14.1
Quenched into iced brine at 25° F	67.2	8.5
Water quenched to 68° F, refrig- erated immediately to -321° F	68.0	2.9

\*10 days after heat treatment

TABLE VII

## Retained Austenite Contents

<u>Treatment</u>	<u>Hardness Rockwell C</u>	<u>% Retained Austenite*</u>
T Steel (1.0 C, 1.5 Cr, 0.20 V)		
<u>Austenitized 1550° F for 30 minutes (4.0% Carbides)</u>		
Oil quenched to 68° F, air cooled to room temperature	66.5	7.0
Oil quenched to 125° F, air cooled to room temperature	64.9	9.0
Oil quenched to 250° F, air cooled to room temperature	64.4	9.5
Quenched into molten salt at 450° F, air cooled to room temperature	64.0	10.6
Oil quenched to 68° F, refrigerated immediately to -321° F	67.0	2.0
<u>Austenitized 1450° F for 30 minutes</u>		
Quenched into water at 68° F	65.5	3.1
Quenched into water at 68° F, refrig- erated immediately to -321° F	65.6	0.5

\*10 days after heat treatment



point ( $420^{\circ}$  F for this steel when austenitized at  $1550^{\circ}$  F) as in martempering, it is seen that about 10 percent of austenite is retained.

A check of the x-ray method against the line counting method in the regions where the microscope is applicable is summarized in Table VIII. Samples of the ball-bearing steel were quenched into oil at  $68^{\circ}$  F ( $20^{\circ}$  C) after austenitizing for 30 minutes at  $1550$ ,  $1650$ , and  $1750^{\circ}$  F ( $845$ ,  $900$ , and  $955^{\circ}$  C). Austenite contents were determined by x-ray, the martensite was then darkened for 10 seconds at  $610^{\circ}$  F ( $320^{\circ}$  C) and the austenite determined by lineal analysis. At the higher austenitizing temperatures the structure was coarse enough to give some confidence in the visual determination and Table VIII shows that both methods checked reasonably well for the higher austenite contents. When samples were quenched from  $1550^{\circ}$  F ( $845^{\circ}$  C), however, no austenite was visible under the microscope, but the x-ray method indicated 7.0 percent present.

In the chromium steel (T steel) the rate of cooling through the martensite region has a very marked effect on the amount of retained austenite, and Table IX shows that as the rate of cooling through the region of martensite formation is increased, the percentage of retained austenite is decreased. A specimen quenched from  $1550^{\circ}$  F ( $845^{\circ}$  C) into oil contains 7.0 percent austenite, compared to 5.8 percent for a water quenched specimen. This effect of cooling rate below the  $M_s$  point was shown in another

TABLE VIII

Comparison at X-ray Determination vs. Lineal Analysis

T Steel (1.0 C, 1.5 Cr, 0.20 V)

<u>Treatment</u>	<u>% Carbides</u>	<u>% Retained Austenite</u>	
		<u>Lineal Analysis</u>	<u>X-ray</u>
Austenitized 1550° F, 30 minutes, oil quenched	4.0	0	7.0±0.4
Austenitized 1650° F, 30 minutes, oil quenched	2.6	14.1±2.0	14.0±0.8
Austenitized 1750° F, 30 minutes, oil quenched	0.2	18.0±2.0	20.0±1.0

TABLE IX

Effect of Quenching Conditions on Retained Austenite Content

T Steel (1.0 C, 1.5 Cr, 0.20 V) - austenitized 1550° F, 30 minutes

<u>Treatment</u>	<u>Austenite Content* Volume Percent</u>
Quenched into oil at 68° F	7.0
Quenched into water at 68° F	5.8
Quenched into iced brine at 23° F	4.9
Quenched into iced brine at 23° F, refrigerated immediately to -321° F	0.7
Quenched into molten salt at 450° F, air cooled to room temperature	10.6
Quenched into molten salt at 450° F, oil quenched to room temperature	6.2
Quenched into molten salt at 450° F, water quenched to room temperature	6.1
Quenched into molten salt at 450° F, quenched into liquid N <sub>2</sub> at -321° F	0.9

\*10 days after heat treatment

way by quenching specimens into molten salt at 450° F (230° C), which is above the  $M_s$  temperature, and then air cooling, oil quenching, and water quenching to 68° F (20° C). The data for this series in Table IX again indicate that an increase in cooling rate below the  $M_s$  point reduces the austenite content. This effect of cooling rate through the martensite range is probably due to the very rapid stabilization of austenite towards transformation on cooling which occurs during aging at and slightly above room temperature. A similar effect has been observed by Fletcher and Cohen<sup>(16)</sup> who found that aging of retained austenite at room temperature progressively stabilized it against further transformation on subcooling.

It is also interesting to note that even a quench into liquid nitrogen at -321° F (-195° C) from above the  $M_s$  temperature was still unable to transform all of the austenite into martensite. About 0.9 percent retained austenite remained after this treatment even though the cooling had been continuous from the  $M_s$  temperature to -321° F (-195° C) without any interruption at room temperature. It seems almost impossible to completely transform all of the retained austenite in a specimen of this size (3/8 inch diameter, 5/8 inch long) by merely cooling through the martensite range, and the temperature at which martensite is completely transformed on cooling, that is the  $M_f$  point, becomes rather difficult to define without some reference to stabilization phenomena.

#### F. Effect of Tempering on Austenite Determinations

As a mixture of austenite and martensite is tempered, two effects occur simultaneously. The austenite decomposes, in a fashion shown in greater detail by the precision length measurements, and the martensite tempers. With the decomposition of the austenite, the intensity of the austenite line decreases, but at the same time, as the transition precipitate forms during the tempering, iron atoms are tied up within the transition precipitate lattice and can no longer contribute to the martensite line. The observed ratio of the austenite and martensite integrated intensities will depend, therefore, on the amount of precipitation which has taken place, as well as on the austenite content itself.

From  $M_s$  point data and from microscopic observations on the volume percentages of undissolved carbides present, the ball-bearing steel (1.0 C, 1.5 Cr, 0.20 V) has 0.84 percent carbon in solution after an oil quench from 1550° F (845° C), and the plain carbon steel (1.07 carbon), has 0.90 percent carbon in solution after an oil quench from 1450° F (790° C). If these steels are tempered at 300° F (150° C), later data will show that 0.30 percent carbon is precipitated from the martensite lattice for the plain carbon steel (K steel) and 0.15 percent carbon by the ball-bearing steel (T steel). Kurdjumov<sup>(33)</sup> indicates that about 0.45 percent carbon should be precipitated, but his data is derived

from axial ratio determinations on martensite formed from a single crystal of austenite containing 1.4 percent carbon and would be expected to apply only approximately to this case.

This transition precipitate is definitely known from magnetic measurements not to be  $\text{Fe}_3\text{C}$ , yet if it were, 4.5 percent of  $\text{Fe}_3\text{C}$  by volume would be formed for the K steel (using the 0.30 percent precipitated carbon figure). There has been some evidence<sup>(34), (35)</sup> to support an average composition of  $\text{Fe}_6\text{C}$  for the precipitate, and on this basis it seems reasonable to assume, therefore, that about 10 percent of the volume will be occupied by the transition precipitate for the K steel (1.07 carbon) and about 5 percent for the T steel (1.0 carbon, 1.5 chromium, 0.20 vanadium) after tempering at 300° F (150° C). There is some doubt if the correction should be applied in this way since it is questionable whether all of the iron atoms in the initially formed transition precipitate will move far enough out of the iron lattice so that none will diffract with the martensite, and this correction is probably only a first approximation. Table X shows the effect of this correction to the martensite lines and the differences caused by the correction are practically all within the limit of accuracy for the x-ray determination. The differences between tempered and non-tempered specimens check qualitatively, however, with the decompositions of austenite observed later by length measurements. (See Table XIV).

TABLE X

Effect of Tempering on Austenite Determinations

T Steel (1.0 C, 1.5 Cr, 0.20 V)

<u>Treatment</u>	<u>% Retained Austenite</u>	
	<u>Uncorrected</u>	<u>Corrected for Tempering of Martensite</u>
1550° F, oil quenched, tempered 300° F, 30 minutes	7.4	6.8
1550° F, oil quenched, tempered 300° F, 1 hour	7.2	6.7
1550° F, oil quenched, tempered 300° F, 5 hours	<u>7.3</u>	<u>7.0</u>
Average	7.3	6.8
1550° F, oil quenched, tempered 68° F, 240 hours	7.0	
1150° F, oil quenched, tempered 68° F, 6700 hours	6.7	
1550° F, oil quenched, tempered 200° F, 6700 hours	6.2	

K Steel (1.07 C)

1450° F, water quenched, tempered 68° F, 240 hours	9.0	
1450° F, water quenched, tempered 68° F, 6000 hours	8.8	
1450° F, water quenched, tempered 200° F, 6000 hours	6.2	
1450° F, water quenched, tempered 300° F, 1 hour	9.3	8.4

At tempering temperatures below 250° F (120° C) the tempering correction on the martensite lines is negligible and Tables IV and X show that some austenite decomposes isothermally on tempering at temperatures as low as 68° F (20° C). This isothermal decomposition of austenite is determined more accurately later by precision length measurements.



## V. THE DECOMPOSITION OF MARTENSITE

---

Previous investigations on the decomposition of martensite (7),(34) have been handicapped by the inability to quantitatively account for the effects caused by retained austenite, which was always present. By a combination of the quantitative x-ray determinations of austenite and the precision length measurements it was possible in the study, however, to subtract out the changes caused by the austenite and to observe each reaction separately. In addition, these methods were sensitive enough not only to show the fine detail involved in the first stage of tempering but also to detect minute amounts of the isothermal transformation of austenite proceeding at room temperature.

If we consider a steel containing only austenite and martensite, then the total change in length observed may be considered as the sum of the contraction caused by the decomposition of the martensite and the expansion caused by the transformation of the austenite. For two mixtures containing different percentages of each constituent this may be expressed algebraically:

$$(12) \quad \Delta L_1 = m_1 M + a_1 A$$

$$\Delta L_2 = m_2 M + a_2 A$$

where  $m_1$  = volume percent of martensite in Mixture 1  
at time = 0.

$m_2$  = volume percent of martensite in Mixture 2  
at time = 0.

$a_1$  = volume percent of austenite in Mixture 1  
at time = 0.

$a_2$  = volume percent of austenite in Mixture 2  
at time = 0.

$\Delta L_1$  = unit change in length of Mixture 1 up to  
time = t.

$\Delta L_2$  = unit change in length of Mixture 2 up to  
time = t.

M = unit change in length caused by partial de-  
composition in 1 percent of martensite up  
to time = t.

A = unit change in length caused by partial  
transformation in 1 percent of austenite  
up to time = t.

It is not difficult to show that:

$$(13) \quad \Delta L_1 - \frac{a_1}{a_2} \Delta L_2 = M \left( m_1 - \frac{a_1}{a_2} m_2 \right)$$

This formulation assumes that the decomposition of one percent of martensite or austenite has the same kinetics in each mixture.

As an example, for the ball-bearing steel (T steel) oil quenched to 68° F (20° C) and refrigerated immediately to -321° F (-195° C) in liquid nitrogen, x-ray and lineal analysis has shown that such a

steel contains 2 percent retained austenite, 4 percent carbides, and 94 percent martensite by volume. Its isothermal dimensional behavior is shown in Figure 3. Similarly, if this same steel is merely oil quenched to 68° F (20° C) and not refrigerated, its analysis will be 7 percent retained austenite, 4 percent carbides, and 89 percent martensite. The dimensional changes on tempering for this steel are shown in Figure 2. Therefore,

$$\begin{array}{lcl} m_1 = 94.0 & m_2 = 89.0 & \\ a_1 = 2.0 & a_2 = 7.0 & \frac{a_1}{a_2} = 0.286 \end{array}$$

If from each curve in Figure 3, 0.286 of the corresponding ordinate in Figure 2 is subtracted, the difference will be the contraction caused by 68.6 percent of martensite (94 - 0.286 x 89.0). Proportionately, the contraction due to 100 percent martensite may be constructed for each aging temperature and these curves are plotted in Figure 20. Similarly, in Figure 21 the contractions for 100 percent martensite in the plain carbon tool steel (1.07 carbon) on aging at various temperatures were obtained by a suitable combination of Figures 7 and 8 and the x-ray determinations of austenite for these treatments.

Not only can the contraction of 100 percent martensite be obtained from these curves but also the expansion caused by the isothermal decomposition of the retained austenite in each specimen. For example, if 89 percent of the martensite contraction curves in Figure 20 are subtracted from the corresponding curves in Figure 2, (i.e. for the oil quenched ball-bearing steel with

Figure 20. Relative changes in length on aging 100 percent martensite of a ball-bearing steel austenitized for 30 minutes at 1550° F (845° C) and quenched into oil.

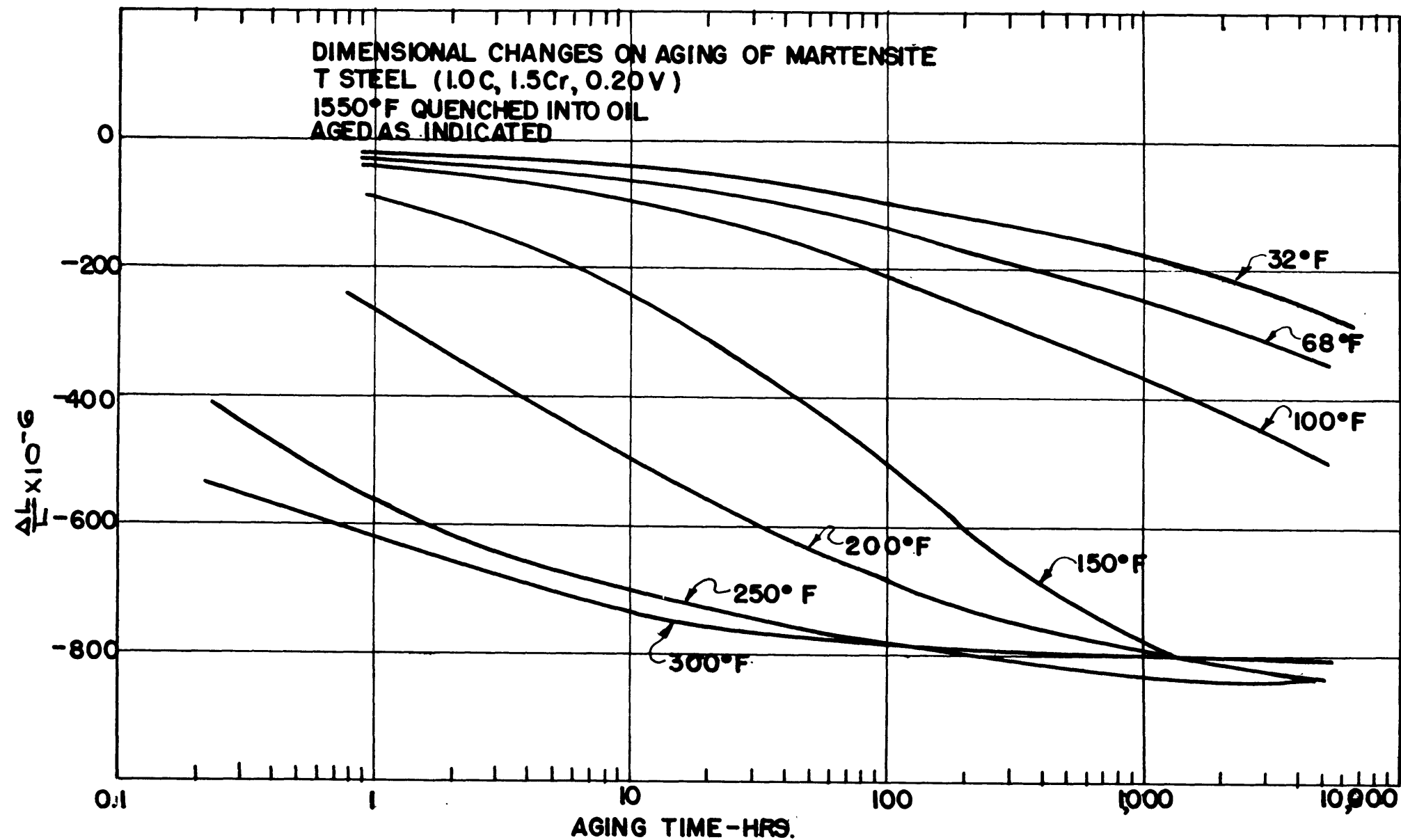
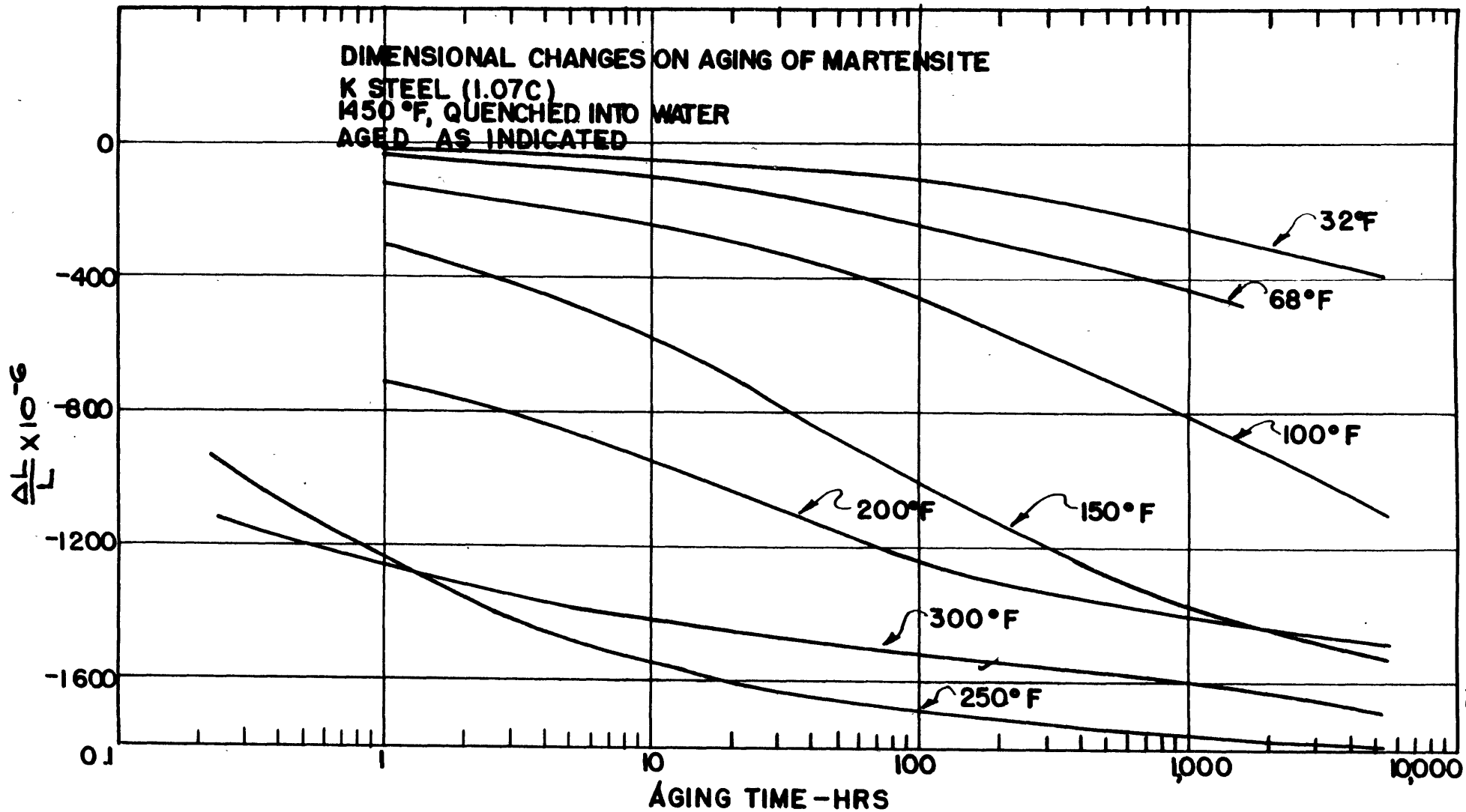


Figure 21. Relative changes in length on aging 100 percent martensite of a plain carbon tool steel austenitized for 30 minutes at 1450° F (790° C) and quenched into water.



7 percent austenite and 89 percent martensite) the net expansion caused by the decomposition of 7 percent of retained austenite will be obtained. These calculations were also made for each combination of austenite and martensite in both steels and the results will be presented later in the discussion of isothermal austenite decomposition.

In making these subtractions two assumptions have been made. It was first assumed that the subcooling had no effect on the subsequent rate of martensite contraction. This point was checked by refrigerating quenched specimens very rapidly and also rather slowly with liquid nitrogen and then observing their dimensional changes on aging at room temperature. If the refrigeration had had any effect on the subsequent martensite decomposition the specimens would have contracted at different rates on room temperature aging, but all samples contracted at exactly the same rate with no apparent relation to the rate of subcooling. It was therefore safe to assume that refrigeration had no effect on the rate of martensite contraction.

The second assumption implied that the condition of the austenite in both steels was identical and that it would decompose at the same relative rate in each case. This is probably not precisely true. Stress undoubtedly plays an important part in the austenite transformation, and stress conditions in the refrigerated sample were probably somewhat different than in the other. There is also an active mass effect for the larger amount of austenite balanced against a stabilization towards isothermal trans-

formation which is known to occur on tempering<sup>(18)</sup>. Since a correction for the presence of only about 2 percent of austenite had to be made for the refrigerated steel, the error in this correction would in the worst case be relatively small and would probably make little difference in the final curves. In addition, the corrections were obtained from two steels which had austenite contents within a few percent of each other so that conditions in each steel were probably similar.

From the contraction curves for 100 percent martensite in Figures 20 and 21 several qualitative trends can be drawn directly. The reaction starts immediately with no apparent incubation period, and if the reaction curves are plotted on a linear scale, it is seen that the rate of reaction seems to be a maximum at the beginning. That a precipitation accompanies the martensite decomposition is apparent in Tables XI and XII where the hardness values for both steels are tabulated after various combinations of tempering and quenching treatments. It is interesting to note that this reaction is quite similar to the usual precipitation hardening phenomena observed in non-ferrous alloys. The maximum hardening occurs at low aging temperatures during the early stages of formation of the transition precipitate and softening commences as disregistry with the matrix lattice and stress relief sets in and the agglomeration of the precipitate starts. This hardening is not caused by the isothermal decomposition of retained austenite, for a comparison of the refrigerated and non-refrigerated steels

TABLE XI

Effect of Tempering on Hardness

T Steel (1.0 C, 1.5 Cr, 0.20 V)  
Austenitized 1550° F, quenched as indicated

Hours at Temperature	1	10	100	1000	3000
Aging Temperature °F	<u>Rockwell C</u>				

Quenched into oil at 68° F

32	66.8	67.1	67.0	67.3	66.7
68	66.9	67.0	67.1	67.5	67.7
100	67.0	67.3	67.4	67.4	66.9
150	67.1	67.4	66.8	65.7	65.3
200	66.9	66.7	65.5	64.2	63.6
250	65.7	64.5	63.8	61.4	60.7
300	64.0	62.6	61.1	60.3	60.3

Quenched into oil at 68° F, refrigerated immediately to -321° F

32	67.2	67.2	67.2	67.6	67.3
68	67.2	67.2	67.4	68.2	68.5
100	67.6	67.6	67.8	67.2	66.6
150	68.2	68.3	67.6	66.2	66.4
200	68.0	67.3	66.3	64.5	65.3
250	66.1	65.2	64.1	62.1	61.1
300	63.7	62.4	61.0	60.0	60.0

Quenched into oil at 125° F, air cooled to 68° F

32	64.8	65.0	65.3	65.4	65.2
68	65.2	65.5	65.6	65.8	66.1
100	65.1	65.4	65.8	65.3	64.6
150	65.1	65.3	65.2	64.2	64.1
200	65.0	64.7	64.1	62.2	61.8
250	64.2	63.6	62.9	61.2	58.9
300	64.0	62.7	61.3	60.3	57.6

Quenched into oil at 250° F, air cooled to 68° F

32	65.6	65.9	66.0	66.0	-
68	64.8	65.3	65.7	65.6	65.5
100	64.8	65.1	65.3	65.4	65.4
150	65.8	65.6	65.4	64.8	64.4
200	64.8	64.1	63.7	62.3	62.1
250	64.2	63.1	62.0	59.1	58.9
300	63.2	61.7	60.0	58.5	58.0

Quenched into molten salt at 450° F, air cooled to 68° F

32	62.5	62.8	62.8	63.0	
68	62.7	62.7	63.0	63.9	
100	64.9	65.0	65.2	65.0	
150	64.3	64.9	64.7	64.5	
200	63.8	63.6	63.4	62.9	
250	64.5	64.4	63.6	61.9	
300	64.4	63.3	62.6	61.0	



TABLE XII

Effect of Tempering on Hardness

K Steel (1.07 C) - Austenitized 1450° F, quenched as indicated

Hours at Temperature	1	10	100	1000	2000
Aging Temperature °F	<u>Rockwell C</u>				
<u>Quenched into brine iced at 23° F</u>					
32	67.1	67.6	67.9	68.3	68.0
68	67.1	67.8	67.9	68.9	68.1
100	67.5	68.3	68.8	69.0	68.6
150	68.2	69.0	68.7	68.2	67.0
200	68.5	68.1	67.2	65.7	65.0
250	67.9	67.0	66.1	64.0	63.0
300	67.1	65.9	63.8	62.7	62.0

Quenched into water at 68° F

32	66.8	67.0	67.7	68.3	67.7
68	66.8	67.3	67.5	68.5	69.2
100	66.8	67.6	67.7	68.2	-
150	67.5	68.4	67.8	67.1	66.9
200	68.4	67.3	66.9	65.0	64.7
250	68.4	67.6	65.4	63.2	62.6
300	67.0	64.5	62.5	62.5	62.2

Quenched into water at 68° F, refrigerated immediately to -321° F

32	67.6	67.6	67.7	68.3	68.8
68	67.6	67.7	68.0	69.4	68.4
100	67.7	68.3	68.7	69.4	64.9
150	68.6	69.0	68.5	68.3	68.0
200	69.0	68.6	67.0	65.9	65.2
250	68.6	67.6	66.5	64.0	62.5
300	67.3	65.4	64.2	63.5	62.3

Quenched into water at 125° F, air cooled to 68° F

32	66.1	66.3	66.4	66.6	66.7
68	66.5	66.6	66.9	67.5	67.3
100	66.6	66.8	67.9	66.9	66.9
150	66.9	67.7	67.2	66.7	65.6
200	67.3	66.8	66.6	64.8	64.0
250	65.8	64.6	64.2	62.2	60.0
300	65.1	63.0	63.0	62.4	60.0

aged at 68° F (20° C) shows that the refrigerated steels underwent greater hardening on aging, and these steels contained considerably less retained austenite than the non-refrigerated steels quenched in the same fashion.

At 250 and 300° F (120 and 150° C), Figures 20 and 21 also show that the initial reaction rate of martensite contraction is very high but that it slows up considerably as time progresses and reaches a plateau which delineates the end of the first stage of tempering. By the time this plateau has been reached, softening is already well advanced because of the depletion of carbon from the martensite lattice and the overaging of the transition precipitate. The surprising trend, however, is the fact that the total shrinkage at the plateau does not increase as the aging temperature increases, but actually seems to be inversely proportional to the aging temperature. This is most evident in the ball-bearing steel, Figure 20, where more total shrinkage can occur at 150° F (66° C) than at 300° F (150° C). Since the shrinkage measured here accompanies a rejection of carbon from the martensite lattice, the inverse relationship of the first stage total shrinkage to the temperature must indicate that the solubility of carbon in the martensite lattice increases with increasing temperature up to 300° F (150° C) and that the transition precipitate is in metastable equilibrium with greater percentages of carbon in the martensite lattice as the temperature rises. Such an assumption for the increasing solubility of carbon in martensite is not inconsistent with the

most recent measurements of Kurdjumov and Lyssak<sup>(53)</sup> on the axial ratio of martensite as a function of tempering temperature. They show that the axial ratios increase slightly or remain practically constant on tempering up to 300° F (150° C) for one hour. With the much more sensitive method available here, the indications are that the transition precipitate must be in balance with slightly increasing percentages of carbon in the martensite lattice as the temperature rises, up to 300° F (150° C).

One might be tempted to explain the increase in solubility of carbon in martensite with increasing temperature on the basis of a change in stable particle size. However, the stable particle size would increase with temperature and a decreasing solubility should be obtained with increasing temperature, whereas an increasing solubility is actually observed. In addition, the transition precipitate which is formed is more voluminous than its decomposition products and the plateau in the martensite contraction curves indicates that very little cementite is formed on aging up to temperatures of 300° F (150° C). The decomposition of transition precipitate to  $Fe_3C$  is therefore also unable to explain the sequence of the contraction arrests, since such a reaction would cause an effect in the reverse direction. It seems reasonable to conclude therefore, that the solubility of carbon in martensite must increase slightly as the temperature rises to 350° F (150° C).

To consider the kinetics of the martensite decomposition it might first be assumed that the precipitation proceeds by a process of nucleation and growth and therefore follows the Mehl and Johnson equation<sup>(36)</sup>. In differential form for the simple case where the rates of nucleation and growth are not functions of time this may be written as:

$$(14) \quad \frac{-dc}{dt} = K_1 ct^3$$

where  $c$  = concentration of carbon remaining in solution in the lattice at the time  $t$

$K_1$  = rate constant which includes the rates of nucleation and growth.

The rate constant,  $K_1$ , is of course a function of temperature and would be expected to follow an activation type of equation for its dependence on temperature. This equation has been applied to the recrystallization of aluminum<sup>(37)</sup> although Cook and Richards<sup>(38)</sup> had to use a lower power of  $t$  to fit their data on the recrystallization of copper. Avrami<sup>(39)</sup> has also derived similar but more general expressions for the kinetics of phase change. In general, these reactions have a measurable incubation period at the start of the process where both the rates of nucleation and growth are low, and equation (14) indicates that at  $t = 0$ , the rate will be zero.

The striking difference between the recrystallization phenomena and the precipitation reaction observed here is that there is no incubation period in the martensite decomposition, and that the rate

at the beginning of the reaction is a maximum. A simple first order reaction which follows the equation

$$(15) \quad \frac{-dc}{dt} = K_1 c$$

has these characteristics, but when the data were fitted to this equation, it was evident that even this equation did not provide for a sufficiently rapid reaction at the beginning.

Neither of these equations takes any account of the effect of stress on the reaction. From the very nature of the austenite-martensite transformation it would be expected that freshly formed martensite is under considerable stress. This stress would promote the precipitation reaction and thereby tend to wipe out any period of incubation at the beginning. Stress relief occurs, however, during aging and the effect of stress would diminish steadily as the aging proceeded. The rate of stress relief on steel castings has been recently studied by Rominski and Taylor<sup>(40)</sup> who observed the relaxation rates of steel as a function of time at various temperatures. Their results may be expressed by the equation:

$$(16) \quad \frac{-d\sigma}{dt} = \frac{K_2}{t^S}$$

where  $\sigma$  = stress

$S$  = plasticity index

The plasticity index,  $S$ , increases with temperature, indicating that stress relief would proceed faster at higher temperatures. An anal-

agous relationship was also found by Hargreaves<sup>(41)</sup> who studied the variation of the recovered Brinell diameter for plastically deformed materials as a function of loading time. Hargreaves also found that the value of S increased with cold work and considered the plasticity index as a measured of the rate of self annealing of the material.

Since the rate of martensite decomposition would be expected to diminish as stress relief proceeded, the reaction rate would, therefore, be expected to have the form:

$$(17) \quad -\frac{dc}{dt} = K_1 K_2 \frac{c}{t^S}$$

The plasticity index, S, is a function of temperature and might be expected to follow the activation form:

$$(18) \quad S = B e^{-\frac{E}{RT}}$$

where

B = constant

E = activation energy for stress relief

R = gas constant = 1.998 cal/mol

T = temperature, °K

Similarly, the rate constant K, which includes the rates of nucleation and growth would also be temperature dependent and follow the form:

$$(19) \quad K_1 = A e^{-\frac{Q}{RT}}$$

where            A = constant  
                   Q = activation energy for the precipitation reaction  
                   T = temperature, °K

Equation (17) may now be rewritten:

$$(20) \quad \frac{-dc}{dt} = K(T) \cdot \frac{c}{tS(T)}$$

and the activation energy for K(T) can also be considered as that for nucleation and growth taking place under these conditions.

Since both the height and base dimension of the martensite lattice vary linearly with the carbon content<sup>(33)</sup> it is reasonable to assume that the volume of the unit cell decreases proportionately as the carbon is rejected from the lattice, and since relative changes in length are directly proportional to volume changes, the differential equation for the rate of relative change in length may be written:

$$(21) \quad \frac{dy}{dt} = K(T) \cdot \frac{(a-y)}{tS(T)}$$

where            y = contraction which has occurred up to time, t  
                   a = total contraction at the end of the reaction

This may be integrated for the isothermal case to:

$$(22) \quad y = a \left( 1 - e^{-Kt(1-S)} \right)$$

or

$$(23) \quad \log \log \frac{a}{a-y} = (1-S) \log t + \log \frac{K}{2.3}$$

Before equation (23) can be evaluated, however, the end point of the reaction, that is the value of "a", must be determined. If the steel were to be tempered completely to cementite and ferrite, specific volume data on a steel containing 1.02 percent carbon indicate that a total shrinkage of  $\frac{\Delta L}{L} = 6000 \times 10^{-6}$  could be expected<sup>(10)</sup>. This same data also indicated that the end of the first stage of tempering obtained by tempering at a temperature of about 300° F (150° C) was about 30 percent of the total contraction. The reaction considered here, which is the precipitation of the transition precipitate, ends with the first stage of tempering, and it was found that the shrinkage value for the end of this first step was quite consistent with the plateau reached at 300° F for the plain carbon tool steel (1.07 carbon) in Figure 21. A value of  $a = 1700 \times 10^{-6}$  was chosen, however, as best fitting the data. In keeping with the concept of increasing solubility of carbon in the martensite lattice up to 300° F (150° C), the value of "a" would be expected to decrease as the temperature increased. The ideal solution law could have been used to calculate the variation of "a" with temperature, but since the solution is far from ideal and very super-saturated, the value of "a" was simply assumed to be inversely proportional to temperature. The value of "a" was chosen to fit the plateau at the higher temperatures where the reaction approached completion and then extrapolated to fit the lower temperatures where the reaction was still in its initial stages. The variation of "a" with temperature was quite small in comparison with the total contraction and the values which were chosen are listed in Table XIII.



TABLE XIII

Constants of Rate Equation for Martensite Decomposition

$$\frac{dy}{dt} = \frac{K(T) \cdot (a-y)}{t^S(T)}$$

Tempering Temperature		a	S	K	% Carbon in Solution at end of First Stage of Tempering
$O_F$	$\frac{1}{T} \times 10^{-3}$	$\frac{\Delta L}{L} \times 10^{-6}$			

K Steel (1.07 C) - austenitized 1450° F 30 minutes

32	3.67	2240	.63	0.0090	.57
68	3.31	2160	.65	0.0215	.58
100	3.21	2100	.68	0.0590	.59
150	2.95	2000	.70	0.163	.60
200	2.74	1900	.84	0.477	.61
250	2.54	1800	.84	1.270	.63
300	2.37	1700	.89	1.390	.64

T Steel (1.0 C, 1.5 Cr, 0.20 V) - austenitized 1550° F 30 minutes

32	3.67	1035	.64	.0185	.70
68	3.31	1000	.69	.0319	.70
100	3.21	980	.71	.0635	.70
150	2.95	940	.71	.167	.71
200	2.74	900	.79	.482	.71
250	2.54	860	.84	1.100	.72
300	2.37	820	.88	1.530	.72

Heats of Activation for Rate Constants

$$\ln K = \ln A - \frac{Q}{RT}$$

$$\ln S = \ln B - \frac{E}{RT}$$

Steel	<u>Q</u> cal/mol	<u>E</u> cal/mol
K	9050	380
T	<u>7480</u>	<u>495</u>
Average	8300	Average 440

With the end point of the reaction determined, it was possible to verify the proposed kinetics by evaluating equation (23). If values for  $\log \log \frac{a}{a-y}$  are plotted as a function of  $\log t$  at a given temperature, a straight line should be obtained with a slope of  $(1 - S)$  and an intercept of  $\log \frac{K}{2.3}$  at  $\log t = 0$ . Figure 22 shows the data for the plain carbon steel (K steel) plotted in this form and it is evident that equation (23) fits quite well. A family of straight lines is obtained as tempering is carried out at various temperatures, and the values for the rate constant,  $K$ , and the plasticity index,  $S$ , are listed in Table XIII. The variation of these constants with temperature is indicated in Figure 23 and it is seen that they follow the activation energy form of equations (18) and (19) reasonably well.

An exactly similar procedure was followed for the ball-bearing steel (1.0 carbon, 1.5 chromium, 0.20 vanadium) except that values of "a" for the end of the first stage of tempering about one-half as great as the corresponding ones for the plain carbon steel had to be chosen. That the first stage was completed was evident from the shape of the curves in Figure 20 where well-defined plateaus had been reached in much the same manner as for the plain carbon steel. A comparison of the hardness values in Tables XI and XII for the two steels indicated that the precipitation reaction in each had followed the same general pattern, except that the end of the first stage of tempering in the chromium steel was accompanied by about half the the precipitation of carbon that was necessary in the plain carbon steel.

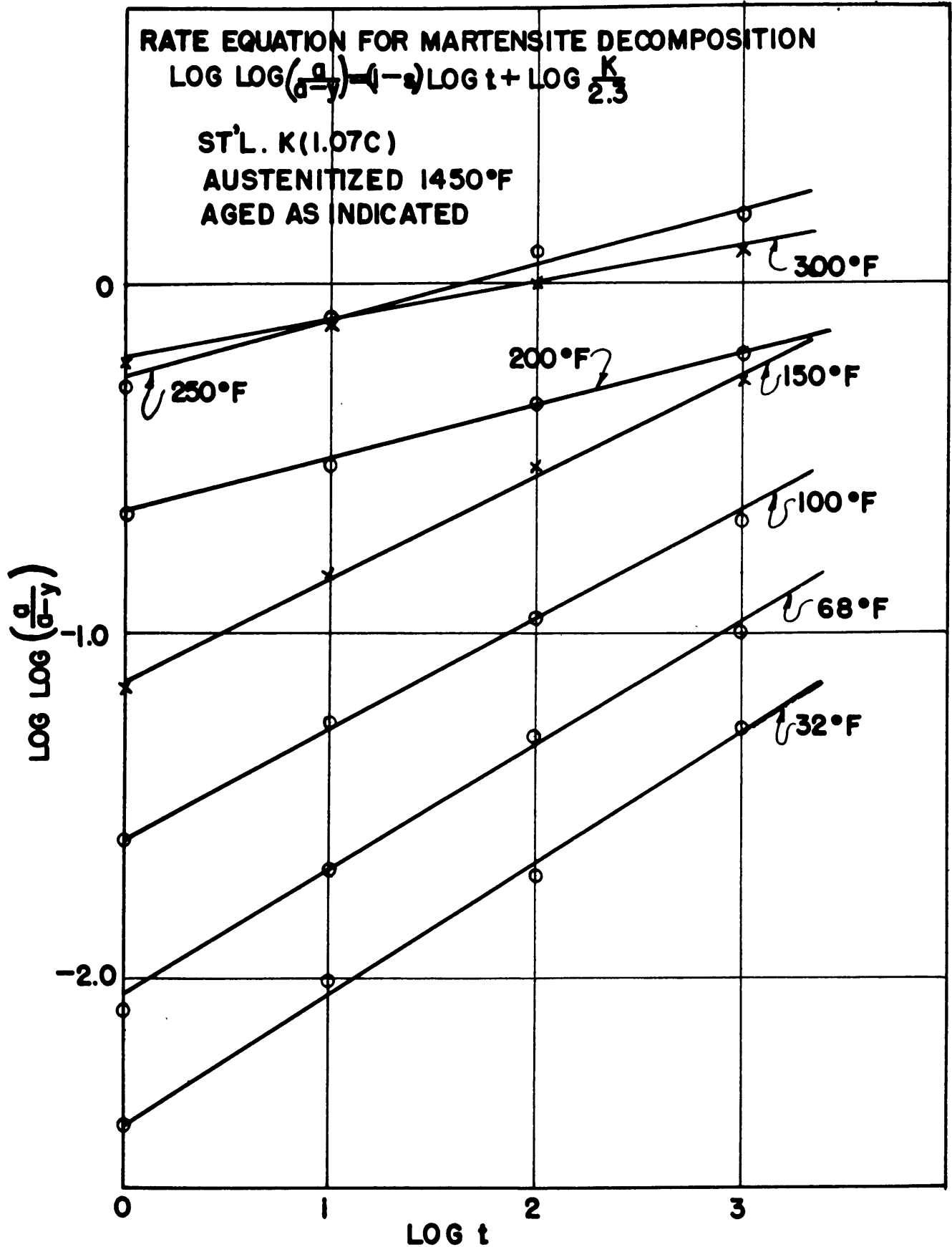


Figure 22. Rate equation for martensite decomposition in a plain carbon tool steel at temperatures from 32 to 300° F (0 to 150° C).

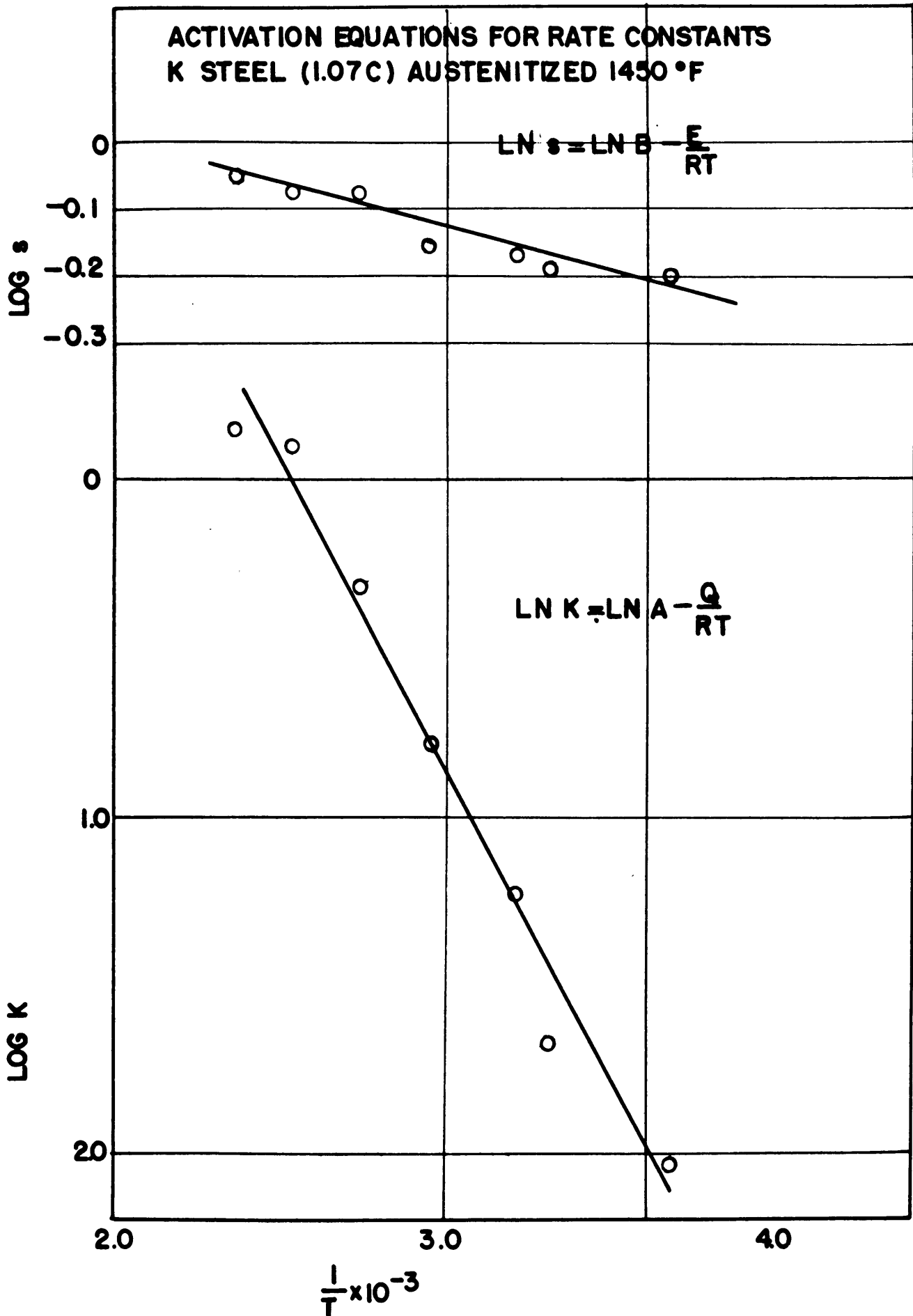


Figure 23. Activation equations for rate constants of martensite decomposition in a plain carbon tool steel.

From the  $M_s$  temperatures measured for these steels it was previously shown that the plain carbon steel behaved as if 0.90 percent carbon were in solution, and the ball-bearing steel as if 0.85 percent carbon and 0.50 percent chromium were in solution in the martensite under the hardening conditions used here. From these values, and the values of "a" chosen for the end of the first stage of tempering, the percentage of carbon remaining in solution at the completion of the first stage of tempering may be calculated if the value of  $6000 \times 10^{-6}$  is taken as the total change which occurs if the carbon were completely converted to cementite. Since this calculation does not take into account the difference in density between the transition precipitate and  $Fe_3C$  it must be considered as only approximate. These solubilities of carbon in martensite are listed in Table XIII and it is evident that the sensitivity of the precision length determinations is great enough to detect a rather small variation in solubility with temperature. The chromium bearing steel is able to retain about 0.10 percent carbon more in solution than the plain carbon steel and this can be attributed to an increase of the solubility of carbon in martensite as the chromium content increases. Less precipitation of transition product and a smaller increase in hardness should be evident on aging martensite of the chromium steel. This is verified in Tables XI and XII, where on comparing the effect of aging at  $68^\circ F$  ( $20^\circ C$ ), for example, it is seen that the ball-bearing steel (T steel) undergoes a smaller increase in hardness than the plain carbon steel (K steel).

The values for the rate constant,  $K$ , and plasticity index,  $S$ , are also listed in Table XIII for the ball-bearing steel. Both steels have practically the same constants and the same heats of activation for the precipitation and for stress relief. These heats of activation are tabulated for each steel in Table XIII. If we consider that the precipitation is controlled by the diffusion of carbon in martensite, then the heat of activation for the diffusion constant cannot be greater than the value of  $Q$ , the heat of activation for the precipitation reaction. An average value for this activation energy for the diffusion of carbon in martensite is about 8300 cal/mol, from Table XIII, and it is interesting to note that this is about half of the value of 18,000 cal/mol calculated by Polder<sup>(42)</sup> for the heat of activation for the diffusion of carbon in ferrite. From the close similarity of the ferrite and martensite lattices, the diffusion of carbon in the interstitial positions should be opposed by about the same potential barrier, but the high stress level in the martensite seems to have reduced this potential barrier somewhat.

## VI. THE ISOTHERMAL DECOMPOSITION OF RETAINED AUSTENITE

---

Considerable data were now also available on the transformation of retained austenite. This information was derived from three sources:

- a) relative changes in length immediately after the quench measured on the quenching dilatometer
- b) isothermal decomposition measured by subtracting the appropriate precision dimensional curves
- c) quantitative austenite determinations by x-ray.

From the quenching dilatometer curves in Figures 12 and 13, it is evident that the length continues to increase and the austenite continues to transform even after room temperature is reached. The temperature measurement was such that it indicated when the last portion of the specimen had reached room temperature, so that it seems safe to assume the transformation observed was truly isothermal and not caused by any transient cooling effects. Martensite contracts during and immediately after the quench, and from equation (23) and the constants in Table XIII the contraction for each steel during the first 1.5 hours at room temperature after the quench can be evaluated. The calculated unit contraction for the first 1.5 hours is only  $50 \times 10^{-6}$  for the plain carbon steel and  $30 \times 10^{-6}$  for the ball-bearing steel. Since these values are small in comparison with the expansions observed immediately after the quench, they may be neglected, and the observed

expansion may then be evaluated directly in terms of percentage of austenite transformed. The transformation of 1 percent of austenite into martensite at room temperature would cause a relative expansion of  $140 \times 10^{-6}$ , and this figure was used to convert expansions observed at room temperature into percentages of austenite transformed.

In the determination of the contraction curves for 100 percent martensite, the relative expansions caused by the isothermal decomposition of austenite was obtained by subtracting the dimensional curves for two states of heat treatment resulting in different and known amounts of austenite. These net expansions were quite small at low temperatures, seldom exceeding the equivalent of 1 percent of austenite even after several thousand hours at 68° F (20° C), but they seemed to be merely the trailing-off of the larger expansions observed immediately after the quench in the quenching dilatometer. A quantitative x-ray determination was usually made at about 240 hours after the quench, where the transformation rate of the austenite was known to be small, and from the changes in length, the absolute austenite contents could be calculated back to the first instant where the specimen had come to room temperature. Since both the dimensional and dilatometer specimens were of the same size, there was little uncertainty in reproducing the rates of cooling and in the direct combination of the data from both types of measurement.



The isothermal decomposition of retained austenite at 68° F (20° C) has been tabulated in Table XIV as a function of time after the quench, and of the interrupting temperature for both steels. These data are also plotted in Figures 24 and 25, and it is seen that the rate of isothermal transformation of austenite at room temperature diminishes rapidly on aging, but that even after several months at room temperature the reaction is still proceeding measurably. The dilatometer curves in Figures 12 and 13 show no discontinuity in the expansion when room temperature is reached and the cooling has stopped. It seems reasonable to conclude, therefore, that the formation of martensite does not stop completely when the cooling stops, and that the observed isothermal decomposition of austenite is merely a residual effect of the main austenite-martensite reaction which started on cooling below the  $M_s$  point. From Figures 24 and 25 it is seen that as much as 3 or 4 percent of austenite may transform isothermally into martensite depending on the composition and on the quenching conditions. This isothermally formed martensite probably consists of plates that were about to form as the cooling stopped and merely continued their formation even after cooling had ceased.

It is interesting to note that the austenite content of the T steel (1.0 carbon, 1.5 chromium, 0.20 vanadium) immediately after the quench is increased if the temperature of the quenching bath is raised even slightly above room temperature. Continuing to raise this interrupting temperature above the  $M_s$  point has no additional

TABLE XIV

Isothermal Decomposition of Austenite at 68° F

T Steel (1.0 C, 1.5 Cr, 0.20 V), 1550° F, 30 minutes - quenched as indicated

Time After Quench-hours	% Retained Austenite			
	Oil quenched to 68° F	Oil quenched to 125° F*	Oil quenched to 250° F*	Salt quenched to 450° F*
0	11.2	14.3	14.3	14.4
0.1	10.5	14.1	13.9	14.0
0.5	9.6	12.9	13.4	13.3
1.0	9.1	12.2	13.2	13.2
1.5	8.3	11.5	13.0	13.0
2.5	8.2	11.0	12.4	12.6
11.5	7.9	10.4	11.6	12.4
100	7.5	9.7	10.5	11.6
1000	7.0	9.0	9.5	10.6
2000			9.3	
3000		8.8		
5000	6.9			

K Steel (1.07 C), 1450° F, 30 minutes, quenched as indicated

	Water quenched to 68° F	Water quenched to 125° F*
	0	11.2
0.1	11.1	17.1
0.5	10.7	16.2
1.0	10.3	15.6
1.5	10.3	15.6
2.5	10.2	15.3
11.5	10.0	15.0
100	9.7	14.5
1000	9.3	14.1
3000		14.0
5000	9.2	

\*Air cooled to 68° F.

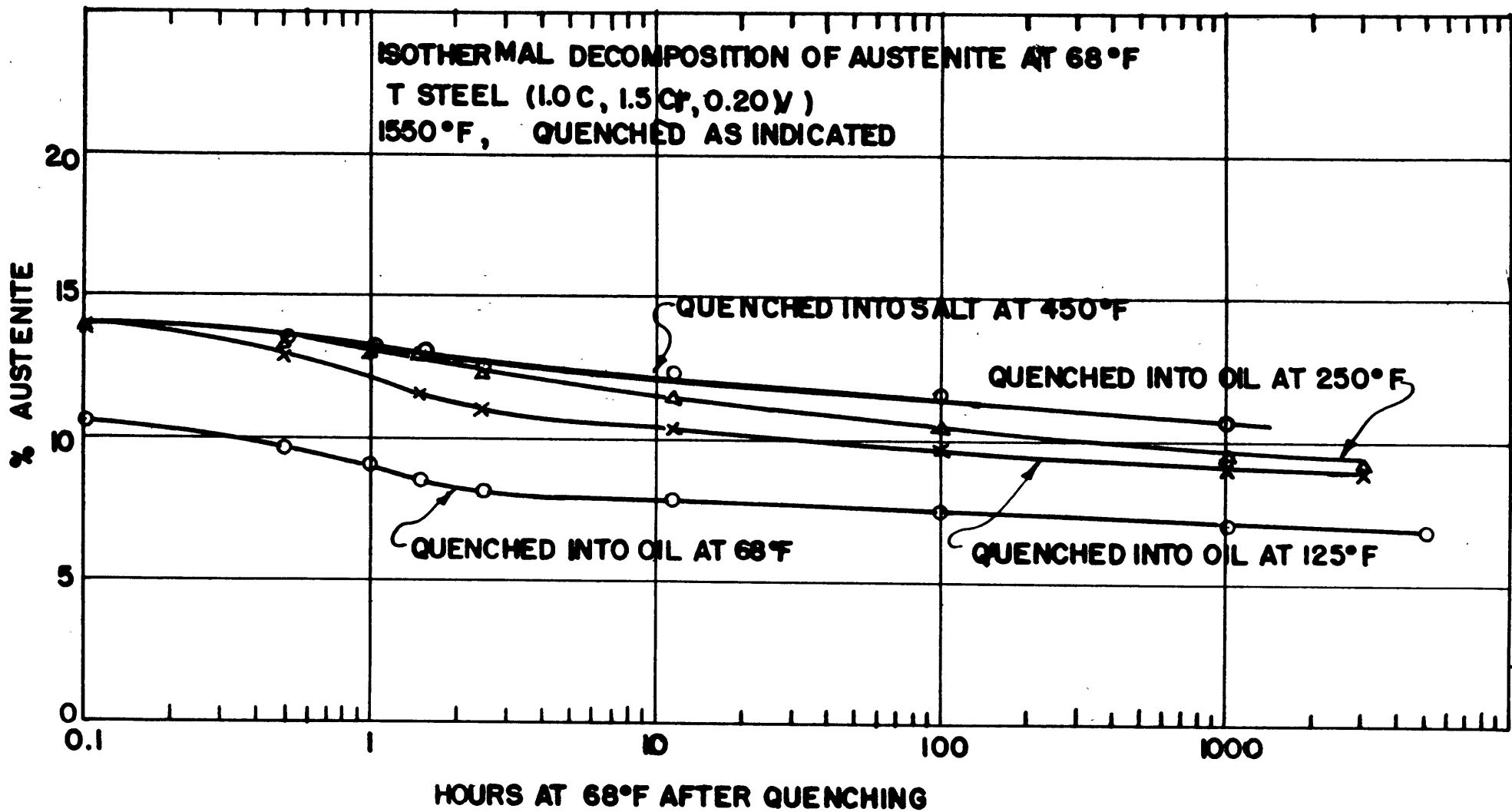


Figure 24. Isothermal decomposition of austenite at 68° F (20° C) for a ball-bearing steel.

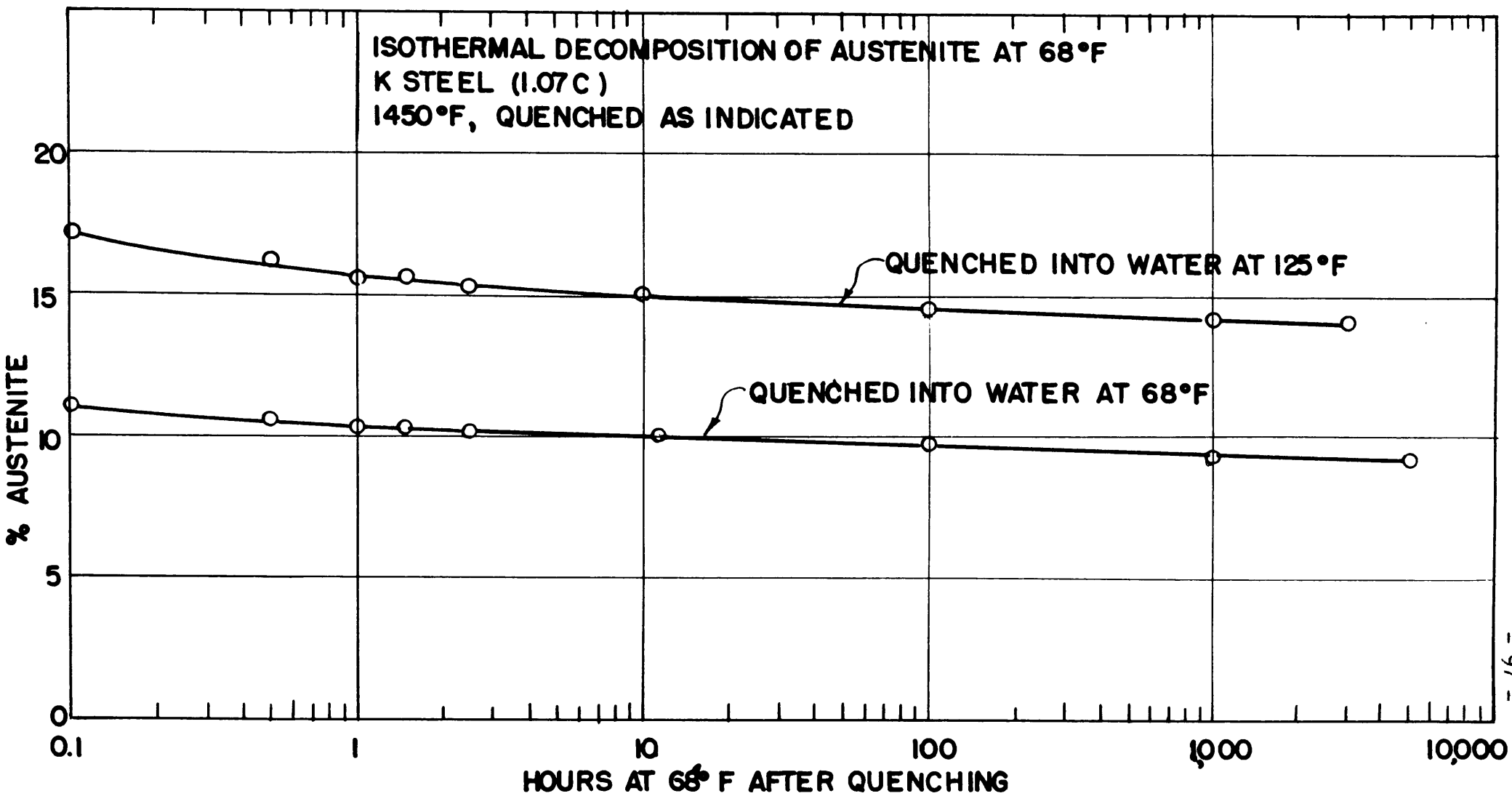


Figure 25. Isothermal decomposition of austenite at 68° F (20° C) for a plain carbon tool steel.

effect on the amount of retained austenite but the austenite has different stability depending on the interrupting temperature. In the water quenched K steel (1.07 carbon) a slight increase in the temperature of the quenching bath raised the retained austenite content appreciably at the end of the quench and in addition rendered the austenite considerably more unstable. This emphasizes the need for precautions in controlling the quenching conditions in commercial heat treatment.

If most of the residual isothermal transformation of retained austenite into martensite takes place within the first 1.5 hours at room temperature after the quench, then little additional transformation could be expected by tempering at higher temperatures until the isothermal decomposition of austenite into bainite started. Tables XV and XVI confirm this by showing that the isothermal transformation of austenite is practically the same at all tempering temperatures up to 250° F (120° C), where the bainite transformation begins on prolonged aging. At 300° F (150° C) the bainite reaction is considerably faster and more austenite transforms. It should be noted in Tables XV and XVI that time is calculated as commencing after the first 1.5 hours at room temperature, so that the value for zero time is shown as the austenite content at 1.5 hours taken from Table XIV, and the same at zero time for all of the tempering temperatures. To convert the length changes from the dimensional curves into percentages of austenite for the tempering temperatures above 68° F (20° C) it was assumed that the decomposition product of austenite would have the same specific volume as

TABLE XV

Decomposition of Austenite on Tempering

T steel (1.0 C, 1.5 Cr, 0.20 V)  
Austenitized 1550° F, 30 minutes, quenched as indicated and kept  
1.5 hours at 68° F before tempering.

<u>Hours</u>	<u>Tempering Temperature °F</u>						
	<u>32</u>	<u>68</u>	<u>100</u>	<u>150</u>	<u>200</u>	<u>250</u>	<u>300</u>
<u>% Retained Austenite</u>							
<u>Oil Quenched to 68° F</u>							
0	8.3	8.3*	8.3	8.3	8.3	8.3	8.3
1	8.1	8.2	8.1	7.8	7.8	7.7	7.6
10	7.7	7.9	7.9	7.5	7.5	7.6	7.4
100	7.2	7.5	7.6	7.3	7.4	7.6	6.9
1000	6.7	7.0	7.3	7.1	7.2	6.8	5.0
3000	6.4	6.9	7.2	7.1	7.1	6.2	3.9
<u>Oil quenched to 125° F, air cooled to 68° F</u>							
0	11.5	11.5*	11.5	11.5	11.5	11.5	11.5
1	11.1	11.0	11.0	10.5	10.5	10.4	9.7
10	10.6	10.4	10.4	9.7	9.8	9.4	9.3
100	9.8	9.7	9.7	9.0	9.1	9.1	8.6
1000	9.3	9.0	9.0	8.7	8.7	8.7	6.6
3000	8.9	8.8	8.7	8.5	8.5	8.2	5.3
<u>Oil quenched to 250° F, air cooled to 68° F</u>							
0	13.0	13.0*	13.0	13.0	13.0	13.0	13.0
1	12.2	12.4	12.3	11.6	11.7	10.2	10.9
10	11.5	11.6	11.6	10.3	10.4	9.7	10.0
100	10.6	10.5	10.5	8.9	8.9	9.6	9.2
1000	9.7	9.5	9.7	7.9	8.0	8.8	6.6
2000	9.6	9.3	9.5	7.7	7.8	8.3	5.3
<u>Salt Quenched to 450° F, air cooled to 68° F</u>							
0	13.0	13.0*	13.0	13.0	13.0	13.0	13.0
1	12.5	12.6	12.6	11.8	11.8	10.6	10.1
10	11.9	12.4	12.6	10.4	10.4	9.7	8.2
100	10.9	11.6	11.6	8.8	8.8	7.5	7.3
1000	10.1	10.6	10.7	7.1	7.1	6.2	3.5

\*Austenite contents shown in this table for zero time at 68° F are actually the values for 1.5 hours at 68° F. The true values for zero time at 68° F are shown in Table XIV.

TABLE XVI

Decomposition of Austenite on Tempering

K Steel (1.07 C)  
 Austenitized 1450° F, 30 minutes, quenched as indicated and kept  
 1.5 hours at 68° F before tempering

Hours	Tempering Temperature ° F						
	32	68	100	150	200	250	300
<u>% Retained Austenite</u>							
<u>Water Quenched to 68° F</u>							
0	10.3	10.3*	10.3	10.3	10.3	10.3	10.3
1	10.2	10.2	10.0	9.6	9.7	9.5	9.6
10	10.0	10.0	9.8	9.4	9.7	9.5	9.5
100	9.8	9.7	9.6	9.1	9.7	8.9	7.6
1000	9.5	9.3	9.3	8.7	9.2	7.8	2.8
3000	9.0	9.2	9.1	8.7	8.9	6.5	1.6
<u>Water Quenched to 125° F, Air Cooled to 68° F</u>							
0	15.6	15.6*	15.6	15.6	15.6	15.6	15.6
1	15.4	15.3	15.0	14.8	14.7	13.6	13.8
10	15.1	15.0	14.6	14.6	14.7	13.1	13.2
100	14.6	14.5	14.2	14.0	14.7	12.1	12.2
1000	14.0	14.1	13.7	13.4	14.3	10.3	6.6
3000	13.7	14.0	13.4	13.3	13.8	8.8	6.0

\*Austenite contents shown in this table for zero time at 68° F are actually the values for 1.5 hours at 68° F. The true values for zero time at 68° F are shown in Table XIV.

the martensite tempered at the same temperature. The actual conversion figures used here are listed in Table XVII and were obtained from specific volume data<sup>(10),(11)</sup>.

The combined data from the quenching dilatometer and dimensional measurements indicate that the isothermal decomposition of austenite proceeds by a two-step process. In Figures 26 and 27 selected data from Tables XIV, XV, and XVI are plotted to show the effects of aging on the isothermal decomposition of austenite. Each specimen was aged at 68° F (20° C) for 1.5 hours immediately after the quench, and the isothermal austenite-martensite reaction is shown as a residual effect of the main hardening reaction. If these specimens are now tempered, Figures 26 and 27 show that this isothermal decomposition into martensite continues for some time even at temperatures up to 300° F (150° C) until the bainite decomposition begins after prolonged aging at 250 and 300° F (120 and 150° C). Retained austenite decomposes isothermally, therefore, first into martensite and then at higher temperatures into bainite.

This isothermal decomposition of austenite immediately after the quench suggests that the Greninger-Troiano technique for the study of the austenite-martensite reaction may contain an inherent error because of this reaction. In this method, specimens are quenched into hot baths and immediately darkened at some elevated tempering temperature. Although the darkening times are short, the temperatures may be quite high, and if 3 or 4 percent of austenite can transform isothermally into martensite at room temperature, perhaps an equivalent



TABLE XVII

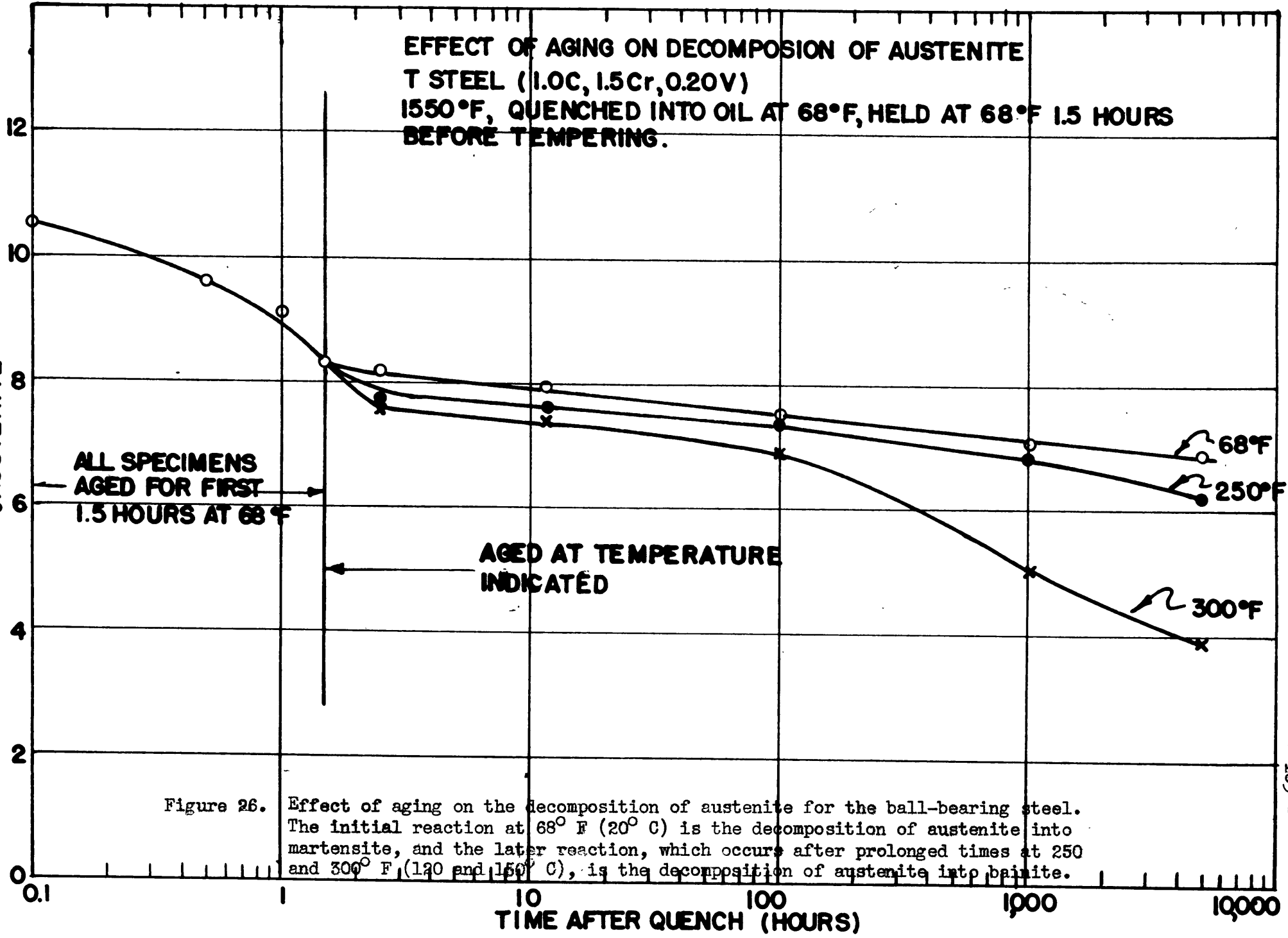
Relative Change in Length Caused by Decomposition  
of 1 Percent of Austenite at Various Temperatures

---

<u>Decomposition Temperature</u> <u>°F</u>	<u><math>\frac{\Delta L}{L} \times 10^{-6}</math></u>
32	140
68	140
100	140
150	137
200	132
250	123
300	114

**EFFECT OF AGING ON DECOMPOSITION OF AUSTENITE  
T STEEL (1.0C, 1.5Cr, 0.20V)  
1550°F, QUENCHED INTO OIL AT 68°F, HELD AT 68°F 1.5 HOURS  
BEFORE TEMPERING.**

**%AUSTENITE**



**ALL SPECIMENS  
AGED FOR FIRST  
1.5 HOURS AT 68°F**

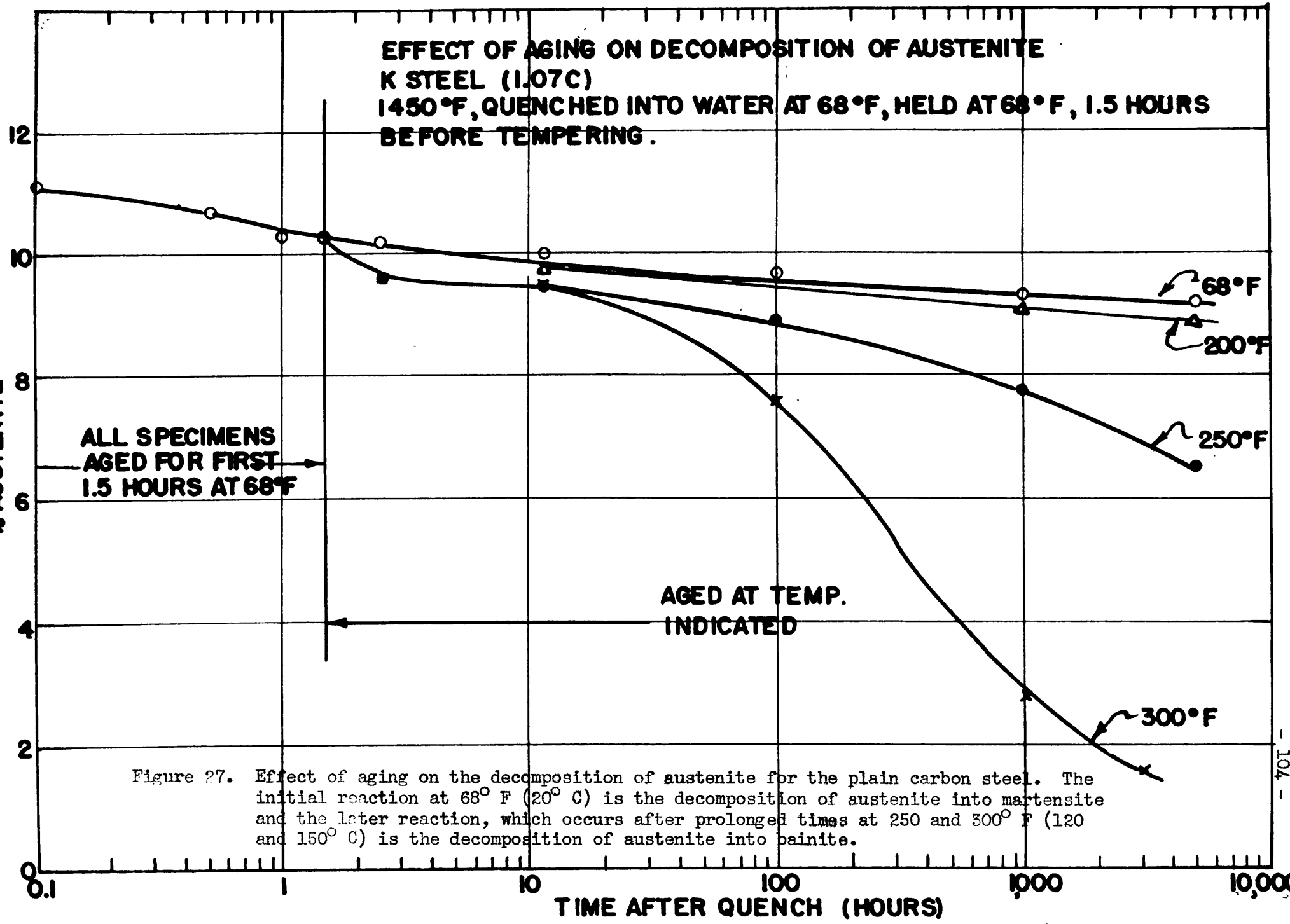
**AGED AT TEMPERATURE  
INDICATED**

**68°F**  
**250°F**  
**300°F**

Figure 26. Effect of aging on the decomposition of austenite for the ball-bearing steel. The initial reaction at 68° F (20° C) is the decomposition of austenite into martensite, and the later reaction, which occurs after prolonged times at 250 and 300° F, (120 and 150° C), is the decomposition of austenite into bainite.

**EFFECT OF AGING ON DECOMPOSITION OF AUSTENITE  
K STEEL (1.07C)  
1450°F, QUENCHED INTO WATER AT 68°F, HELD AT 68°F, 1.5 HOURS  
BEFORE TEMPERING.**

**% AUSTENITE**



**ALL SPECIMENS  
AGED FOR FIRST  
1.5 HOURS AT 68°F**

**AGED AT TEMP.  
INDICATED**

Figure 27. Effect of aging on the decomposition of austenite for the plain carbon steel. The initial reaction at 68° F (20° C) is the decomposition of austenite into martensite and the later reaction, which occurs after prolonged times at 250 and 300° F (120 and 150° C) is the decomposition of austenite into bainite.

amount can transform at the higher darkening temperatures, so that somewhat less austenite will be observed than was actually present after the quench.

It is difficult to express quantitatively the kinetics of the isothermal decomposition of austenite into martensite since it is merely the after-effect of the main austenite-martensite reaction which occurred on cooling, and it would depend greatly on the conditions under which the main reaction took place. When a quantitative treatment is developed, however, it should be able to account for 3 or 4 percent more austenite transforming into martensite when the cooling is stopped.

This work on the isothermal austenite and martensite reactions in gage steels emphasizes that the dimensional stability of these steels is a function of the amount of martensite and of the condition and quantity of the retained austenite present. The contraction of the martensite is quite predictable and seems to be a function only of the tempering which it has received. Retained austenite decomposition, however, causes an expansion which depends not only on the amount, but also on the conditions under which the austenite was left, and this process seems to be inseparable from the main hardening reaction. The austenite decomposition is, therefore, very sensitive to the method of quenching, and each austenite condition responds in a different manner to tempering. For this reason, the quenching operation becomes of utmost importance in gage manufacture, since slight deviations from a standard practice can cause large differences in austenite stability which are not corrected by tempering and which thereby produce an erratic dimensional behavior later.

## VII. CONCLUSIONS

---

From a combination of the results of quantitative x-ray analysis, quenching dilatometer observations, and precision length determinations, the following conclusions may be drawn concerning some of the reactions occurring in martensitic steels.

1. A normally hardened ball-bearing or plain carbon tool steel contains 7 - 9 percent of retained austenite after quenching and remaining at room temperature for several days.
2. Continued cooling below room temperature is unable to transform austenite completely to martensite and even continuous cooling from the  $M_s$  point to liquid nitrogen temperatures leaves about 1 percent of retained austenite.
3. The rate of cooling through the martensite region influences the quantity of retained austenite, and if the cooling is retarded by an interrupted quench, the amount of retained austenite is increased.
4. During the first stage of tempering, the martensite decomposition proceeds by the rejection of a transition precipitate at an increasing rate with increasing temperatures until the end of the first stage is reached. At this point the rejection of carbon from the martensite lattice almost ceases before the formation of cementite begins.
5. The solubility of carbon in martensite at the end of the first stage of tempering increases slightly with increasing temperature up to 300° F (150° C), and the ball-

bearing steel can dissolve about 0.10 percent carbon more than the plain carbon steel because of the presence of chromium in solution.

6. The decomposition of martensite seems to proceed by a process of nucleation and growth of the transition precipitate accelerated by the stresses present in the martensite lattice. The kinetics of the process may be represented by the rate equation:

$$\frac{-dc}{dt} = K(T) \cdot \frac{c}{tS(T)}$$

7. The heat of activation for the diffusion of carbon in martensite has been determined as approximately 8300 cal/mol. This indicates that the potential barrier opposing the diffusion of carbon in martensite is about half as great as barrier opposing the diffusion of carbon in ferrite, and the difference is probably due to the highly stressed condition of the martensite lattice.
8. The austenite-martensite reaction does not stop completely when the cooling stops, but 3 or 4 percent more of austenite may transform isothermally into martensite at room temperature. This isothermal transformation proceeds rather rapidly during the first 1.5 hours after the quench, but it continues at a diminishing rate for several months. As retained austenite is tempered at higher temperatures, the decomposition of austenite into bainite

becomes evident after prolonged aging times at 250 and 300° F (120 and 150° C), but this bainite decomposition (i.e. the second stage of tempering) is quite distinguishable from the earlier isothermal decomposition into martensite.

REFERENCES

---

1. Annual Reports of the National Physical Laboratory, 1922, 1927, 1928, 1929, 1930, 1931, 1932 and 1933.
2. H. J. French: "Artificial Seasoning of Steel", American Machinist, Vol. 55, 768 (1921); Chem. and Met. Eng., Vol. 25, 155 (1921); Scientific American, Vol. 3, 80 (1921).
3. F. H. Rolt: Gauges and Fine Measurements, MacMillan and Company, London, 2 vols., 366 and 357 pp (1929).
4. T. Matsushita: "On the Slow Contraction of Hardened Carbon Steels", Proc. Physico-Mathematical Society of Japan, Vol. 9, 312 (1917-18).
5. S. Steinberg and W. Subow: "Aging of Hardened Carbon Steels", Stahl und Eisen, Vol. 51, 911 (1931); Metallurgist, Vol. 7, 131 (1931).
6. W. P. Boyle: "Aging Tools and Gages", Steel, Vol. 109, 71 (September 22, 1941).
7. H. Scott: "Dimensional Changes Accompanying the Phenomena of Tempering and Aging Tool Steels", Trans. A.S.S.T., Vol. 9, 277 (1926).
8. A. R. Troiano and A. B. Greninger: "The Martensitic Transformation", Metal Progress, Vol. 50, 303 (1946).
9. R. T. Howard: "The Kinetics of the Austenite-Martensite Reaction", ScD Thesis, Metallurgy Department, M.I.T. (June 1947).
10. S. G. Fletcher and M. Cohen: "The Effect of Carbon on the Tempering of Steel", Trans. A.S.M., Vol. 32, 333-357 (1944).



11. D. P. Antia, S. G. Fletcher, and M. Cohen: "Structural Changes During the Tempering of High Carbon Steel", Trans. A.S.M., Vol. 32, 290-324 (1944).
12. M. Cohen: "Tempering of Tool Steels", Metal Progress, Vol. 51, 781-788 (May 1947) and 962-968 (June 1947).
13. S. Epstein: The Alloys of Iron and Carbon, Vol. I - Constitution, McGraw-Hill Book Company, 210-234 (1936).
14. H. Carpenter and J. M. Robertson: Metals, Vol. II, 928-941, Oxford University Press, (1939).
15. S. G. Fletcher: "The Tempering of Plain Carbon Steels", ScD Thesis, Metallurgy Department, M.I.T. (June 1947).
16. S. G. Fletcher and M. Cohen: "The Dimensional Stability of Steel. Part I - Subatmospheric Transformation of Retained Austenite", Trans. A.S.M., Vol. 34, 216-236 (1945).
17. S. G. Fletcher, B. L. Averbach, and M. Cohen: "The Dimensional Stability of Steel. Part II - Further Experiments on Subatmospheric Transformation", Trans. A.S.M. (1947).
18. B. L. Averbach, M. Cohen, and S. G. Fletcher: "The Dimensional Stability of Steel. Part III - Decomposition of Martensite and Austenite at Room Temperature". Trans. A.S.M. (1947).
19. A. B. Greninger and A. R. Troiano: "Kinetics of the Austenite to Martensite Transformation in Steel", A.S.M. Trans., Vol. 28, 537 (1940).
20. R. A. Flinn, E. Cook, and J. A. Fellows: "A Quantitative Study of Austenite Transformation", Trans. A.S.M., Vol. 31, 41 (1943).

21. A. B. Greninger: "The Martensite Thermal Arrest in Iron-Carbon Alloys and Plain Carbon Steels", Trans. A.S.M., Vol. 30, 1 (1942).
22. F. S. Gardner, M. Cohen, and D. P. Antia: "Quantitative Determination of Retained Austenite by X-rays", Trans. A.I.M.E., Iron and Steel Division, Vol. 154, 306-317 (1943).
23. A. Taylor: An Introduction to X-ray Metallography, John Wiley and Sons, Inc. (1945).
24. J. W. Fitzwilliam: "X-ray Study of Order in Binary Systems", PhD Thesis, Physics Department, M.I.T., June 1947.
25. A. H. Compton and S. K. Allison: X-rays in Theory and Experiment, D. Van Nostrand Company, 298-315 (1935).
26. N. F. Mott and H. Jones: The Theory of the Properties of Metals and Alloys, Oxford University Press, 1-15 (1936).
27. E. P. Klier and A. R. Troiano: "Ar" in Chromium Steels", Trans. A.I.M.E., Vol. 162, 175 (1945).
28. B. E. Warren and B. L. Averbach: "Measurements on the Effect of Cold Work with a Geiger Counter Spectrometer", A.S.X.R.E.D., June 1947.
29. G. W. Brindley: "The Effect of Grain or Particle Size on X-ray Reflections from Mixed Powders and Alloys Considered in Relation to the Quantitative Determination of Crystalline Substances by X-ray Methods", Phil. Mag., Series 7, Vol. 36, 347-369 (1945).

30. A. Taylor: "On the Application of the Micro-Absorption Factor to Problems of Lattice Distortion and the Nature of Anti-Phase Domains", *Phil. Mag.*, Series 7, Vol. 35, 404-414 (1944).  
A. Taylor: "The Influence of Crystal Size on the Absorption Factor as Applied to Debye-Scherrer Diffraction Patterns", *Phil. Mag.*, Series 7, Vol. 35, 315-229 (1944).
31. J. C. M. Brentano: "The Quantitative Measurement of the Intensity of X-ray Reflections from Crystalline Powders", *Proc. Phys. Soc. (London)*, Vol. 47, 932-947 (1935).
32. E. C. Bain and J. R. Vilella: "Austenitic Grain Size in Steel", *Metals Handbook*, A.S.M., 754 - 769 (1939).
33. G. Kurdjumov and L. Lyssak: "The Application of Single Crystals to the Study of Tempered Martensite", *I. Iron & Steel Inst.*, Vol. 156, Part 1, 29-36 (May 1947).
34. W. Fraenkel and E. Heymann: "Zur Kinetik der Anlass Vorgänge im Stahl", *Zeit. An. Chemie*, Vol. 134, 137 (1924).
35. H. Lipson and N. J. Petch: "The Crystal Structure of Cementite, Fe<sub>3</sub>C". *J. Iron and Steel Inst.*, Vol. 148, 95 (No. II 1940).
36. W. A. Johnson and R. F. Mehl: "Reaction Kinetics in Processes of Nucleation and Growth", *Trans. A.I.M.E.*, Vol. 135, 416 (1939).
37. W. A. Anderson and R. F. Mehl: "Recrystallization of Aluminum in Terms of the Rate of Nucleation and Growth". *Trans. A.I.M.E.*, Vol. 161, 140 (1945).
38. M. Cook and T. L. Richards: "Observations on the Rate and Mechanism of Recrystallization in Copper", *J. Inst. Metals*, Vol. 73, 1 (September 1946).

39. M. Avrami: "Granulation, Phase Change, and Microstructure",  
J. Chem. Physics, Vol. 9, 177 (1941).
40. E. A. Rominski and H. F. Taylor: "Stress Relief and the  
Steel Casting", Trans. A.F.A., Vol. 51, 709 (1943).
41. F. Hargreaves: "The Ball Hardness and the Cold Working of  
Soft Metals and Eutectics", J. Inst. Metals, Vol. 39, 301  
(1928).
42. D. Polder: "Theory of the Elastic After-Effect and the Dif-  
fusion of Carbon in Alpha Iron", Philips Research Reports,  
Vol. 1, No. 1, 1 (October 1945).

## IX. BIOGRAPHICAL NOTE

---

The author was born in Rochester, New York on August 12, 1919, attended public schools there, and received the degree of B.Met. Eng. in 1940 and M.Met.Eng. in 1942 from Rensselaer Polytechnic Institute at Troy, New York. Until 1943 he was a research fellow at Rensselaer, and from 1943 to 1945 he was Chief Metallurgist of the U. S. Radiator Corporation.

In 1945 he was associated with the General Electric Company as a metallurgist and in November 1945 he entered M. I. T. as the Sheffield Fellow to study the dimensional stability of steel. In 1947 he was appointed an Assistant Professor of Metallurgy at M. I. T.